# 7 Settlement Analysis

## 7.1 INTRODUCTION

Foundations on soft clay are liable to undergo excessive settlement and prediction of this settlement is an important aspect of foundation design. A part of this settlement, known as the immediate settlement, is a result of undrained shear deformation of the soil and takes place during loading. A major part of the settlement, however, occurs due to volume change of the clay caused by the dissipation of excess pore pressure developed from imposed loads. This is a gradual process and is known as *primary consolidation*. In addition, there may be settlement due to secondary consolidation caused by volume change of the clay apparently under constant effective stress. Except in clays which exhibit high secondary effect, settlement analysis usually involves an evaluation of the immediate and primary consolidation settlement only.

Soft clays, in general, are normally consolidated and their behaviour differs somewhat from overconsolidated clays and clay shales. A survey of case records of settlement of shallow foundations on clay (Simons and Som 1970) reveals that structures founded on N.C. clays, in general, experience more settlement than those founded on overconsolidated clay. This is only to be expected because the main effect of overconsolidation is to reduce the compressibility of the clay. However, it is more important, that for normally consolidated clay, only 15–20% of the total settlement occurs during construction, whereas for overconsolidated clays, as much as 50–60% of the total settlement may occur during construction. This shows the importance of consolidation on the settlement of foundations on clay and evaluation of this settlement becomes a major part of the settlement analysis.

### 7.1.1 Definitions

Figure 7.1 shows the development of net pressure and the associated settlement of a foundation on clay during different stages of construction. Before application of the building load, there is usually an excavation down to the foundation level during which there is a heave of the subsoil. The magnitude of this heave is generally small, unless the excavation is deep and is kept open for a long time. After excavation, the foundation load is gradually applied and there comes a time when the applied pressure on the soil equals the pressure

released by excavation and the net foundation pressure becomes zero. The corresponding settlement due to the restoration of the excavation load may be assumed to be equal to the prior heave. Any further increase of load is a net increase in foundation pressure and the associated settlement is the net settlement of the foundation.

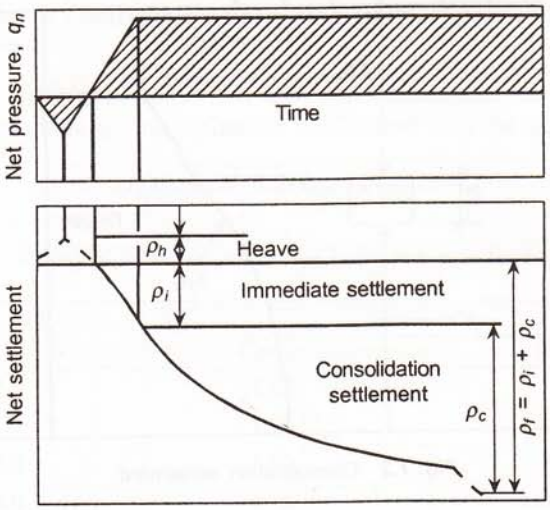


**Fig. 7.1** Time–settlement relationship of foundations on clay.

When the construction is complete and the total building load has been applied, the immediate settlement, $\rho_i$ has already occurred. If the construction is rapid this settlement is a result of shear deformation of the clay. For a saturated clay, this occurs essentially under the condition of zero volume strain. Any consolidation settlement at this stage is small.

After the construction is over, the clay undergoes consolidation and the settlement gradually increases with time until, theoretically, after infinite time, the consolidation is complete. The total consolidation settlement, $\rho_c$ is then added to the immediate settlement, $\rho_i$, to give the final settlement, $\rho_f$ of the foundation. Therefore,

$$\rho_f = \rho_i + \rho_c \tag{7.1}$$

## 7.1.2 Methods of Settlement Analysis

The principle of effective stress and Terzaghi's theory of one-dimensional consolidation have been the essential basis for settlement analysis of foundations founded on clay. The earliest method of settlement analysis for a foundation placed on a layer of clay is shown in Fig. 7.2. The settlement is given by the equation,

$$\rho_c = \int_0^z m_v \, \Delta\sigma_z \, dz \tag{7.2}$$

where,

$q_n$ is the net foundation pressure,
$B$ is a width of the foundation,
$E$ is the Young's modulus of the clay,
$\nu$ is the Poisson's ratio, and
$I_\rho$ is the influence coefficient whose magnitude depends on the geometry of the foundation.

The values of $I_\rho$ for different values of $L/B$ for rectangular foundations are given in Table 7.1. For rigid foundations, the influence coefficient may be taken as:

$$(I_\rho)_{\text{RIGID}} = 0.8(I_\rho)_{\text{CENTRE}} \tag{7.4}$$

**Table 7.1** Values of influence coefficient $I_\rho$ for rectangle foundation, $L \times B$

| $m = L/B$ | *Values of $I_\rho$* | |
|---|---|---|
| | *Centre* | *Corner* |
| 1.0 | 1.12 | |
| 1.5 | 1.36 | |
| 2.0 | 1.52 | |
| 3.0 | 1.78 | |
| 4.0 | 1.96 | 1/2 centre values |
| 5.0 | 2.10 | |
| 6.0 | 2.24 | |
| 7.0 | 2.32 | |
| 8.0 | 2.42 | |
| 9.0 | 2.50 | |
| 10.0 | 2.53 | |
| Circle: Dia B | 1.00 | 0.64 |

Because of sample disturbance, values of $E$ obtained from laboratory triaxial compression tests are often unreliable. It is preferable to obtain $E$ values from plate load tests made in the field or from established empirical relations of $E$ and the undrained shear strength, $c_u$, of the clay. Butler (1974) gives $E/c_u$ ratio of 400 for overconsolidated London clay while Bjerrum (1973) gives the $c_u/p$ ratios in the range of 500 to 1500 for normally consolidated clays, based on measurement of undrained shear strength of the clay by the vane shear test.

For foundations placed at some depth beneath the ground surface, a 'depth correction' may be applied to the settlement calculated by Eq. (7.3) (Fox 1948). The depth correction depends on the depth to width ratio and length to width ratio of the foundation. Values of the depth correction, given in Fig. 7.3, are defined as

$$\text{Depth correction factor} = \frac{\text{settlement of foundation at depth } D}{\text{settlement of corresponding surface foundation}}$$

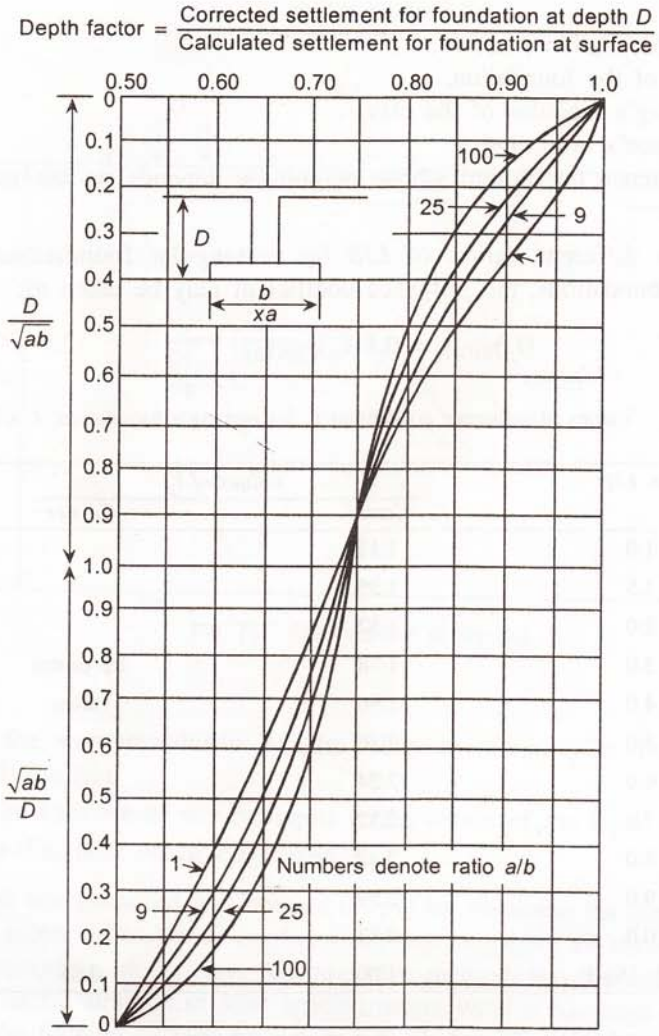


**Fig. 7.3** Depth correction factor.

## Consolidation settlement

While Eq. (7.3) still remains the most widely used expression for calculating the immediate settlement, the method of obtaining the consolidation settlement has undergone some changes. Skempton and Bjerrum (1957) recognized that there was lateral deformation in the clay during load application and that the consolidation settlement should be a function of the excess pore pressure set up by the applied load. Therefore, taking account of the shear stresses, a modified expression for the total settlement was given as,

$$\rho_f = \rho_i + \mu\rho_{oed} \tag{7.5}$$

where

$\mu$ is the pore pressure correction factor which depends on the pore pressure parameter $A$ and the geometry of the foundation and

$\rho_{oed}$ is the consolidation settlement obtained by the direct application of the oedometer test results (Eq. (7.2)).

The values of pore pressure correction factor as given by Skempton and Bjerrum (1957) are given in Fig. 7.4.

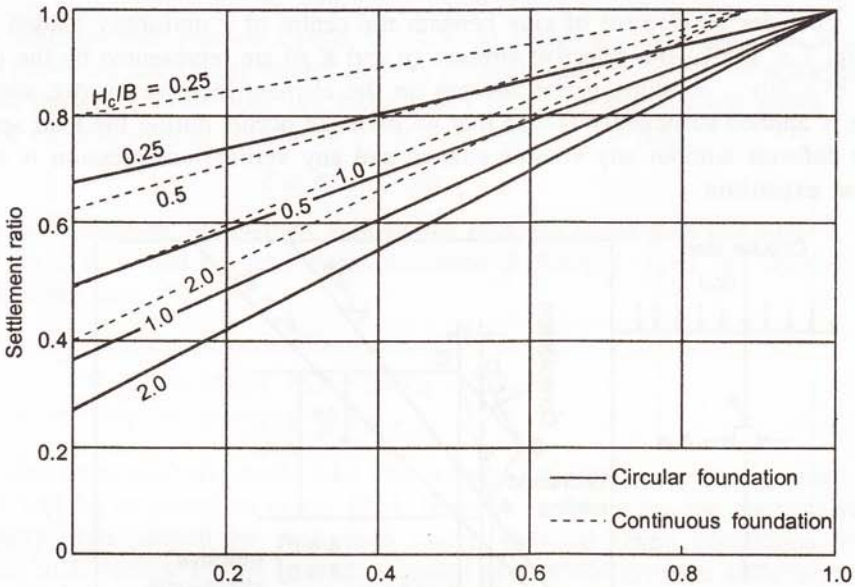


**Fig. 7.4** Pore pressure correction factor for foundations on clay (after Skempton and Bjerrum 1957).

For routine design, the following values of the pore pressure correction factor may be used:

| | | |
|---|---|---|
| Normally consolidation clay | : | 1.0–0.7 |
| Overconsolidated clay | : | 0.7–0.5 |
| Heavily overconsolidated clay | : | 0.5–0.3 |

## 7.2 STRESS-PATH

It is well-recognized that the deformation of an element of soil is a function not only of magnitude of the applied stresses but also of the manner of their application. In other words, a knowledge of the magnitude of stress increase is not, in itself, sufficient to indicate precisely how a soil element is going to deform. To obtain a more complete picture, we have also to know how the applied stresses change, at what rate and in what relation to one another (Som 1968).

A stress-path is essentially a curve drawn through points on a plot of stress changes. It shows the relationship between the components of stresses at various stages in moving from one stress point to another. In the present study, however, consideration is given only to cases where by virtue of symmetry, the intermediate and minor principal stresses are equal and where the vertical and horizontal stresses are the principal stresses, for example, in the laboratory triaxial test or along the centre line beneath a loaded circular area. In its natural condition, before any load is applied, an element of soil is in a $K_o$ state of stresses ($K_o$ = coefficient of earth pressure at rest). Depending on whether the soil is normally consolidated or overconsolidated the horizontal stress in-situ may be smaller or greater than the vertical stress.

Let us consider an element of clay beneath the centre of a uniformly loaded circle, as shown in Fig. 7.5. The in-situ effective stresses ($p$ and $K_o p$) are represented by the point 'A'. Due to the foundation pressure, $q$, the stresses on the element increase by $\Delta\sigma_v$ and $\Delta\sigma_{h1}$. If the pressure is applied sufficiently fast so that no drainage occurs during the load application, the element deforms without any volume change and any vertical compression is associated with a lateral expansion.

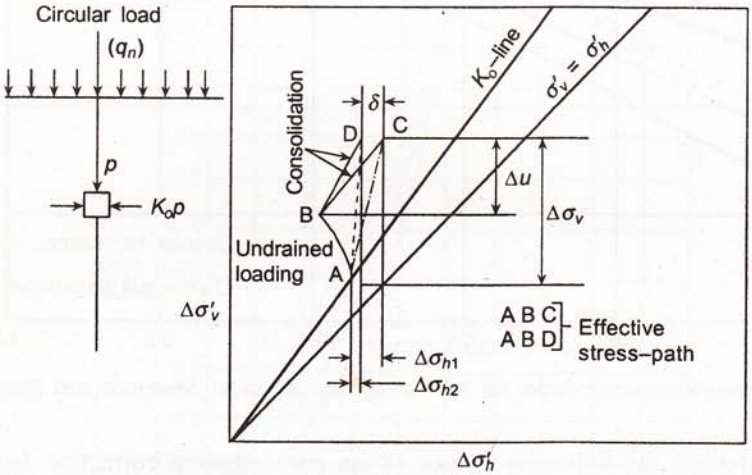


**Fig. 7.5** Stress–path of an element of soil beneath foundation in the field.

Now, the increase of stresses $\Delta\sigma_v$ and $\Delta\sigma_{h1}$, which are the increase in principal stresses in this instance, will set up an excess pore–water pressure in the element according to the equation,

$$\Delta u = B\,[\Delta\sigma_{h1} + A\,(\Delta\sigma_v - \Delta\sigma_{h1}) \tag{7.6}$$

where $A$ and $B$ are Skempton's pore-pressure parameters (Skempton, 1954).

If the clay is saturated, as all clays below the water table are, $B = 1$. Then,

$$\Delta u = \Delta\sigma_{h1} + A\,(\Delta\sigma_v - \Delta\sigma_{h1}) \tag{7.7}$$

Therefore, immediately after the load application, the effective stresses become:

$$\left.\begin{aligned} \sigma'_v o &= p + \Delta\sigma_v - \Delta u \\ \sigma'_h o &= K_o p + \Delta\sigma_{h1} - \Delta u \end{aligned}\right\} \tag{7.8}$$

Since for most clays, the value of $A$ is positive in the range of stresses normally encountered in practice, the excess pore-pressure $\Delta u$ is greater than $\Delta\sigma_{h1}$. So while the effective vertical stress increases on load application, the effective horizontal stress decreases and the stress point moves from 'A' to 'B'. The vertical strain during loading, that is, the immediate settlement, is, therefore, a function of the stress-path AB.

The element now begins to consolidate. At the early stages of consolidation, the increase in effective horizontal stress is only a recompression until the original value $k_o p$ is restored. Beyond this point, any further increase of horizontal stress is a net increase while there is a net increase in vertical stress during the entire process of consolidation.

Now during load application, in undrained condition, a saturated clay behaves as an incompressible medium with Poisson's ratio, $\nu = 0.5$. As the excess pore-pressures dissipate, Poisson's ratio decreases and finally attains its fully drained value at the end of consolidation. This change in Poisson's ratio does not have much effect on the vertical stress but the horizontal stress decreases by an amount $\delta$ to its new value $K_o p + \Delta\sigma_{h2}$, i.e.,

$$\delta = \Delta\sigma_{h1} - \Delta\sigma_{h2} \tag{7.9}$$

So during consolidation, the element follows the effective stress path BD while it would have moved from B to C had the total stress remained unchanged. After full consolidation, therefore, the stresses are:

$$\left.\begin{aligned} \sigma'_{vf} &= \Delta\sigma_v \\ \sigma'_{hf} &= K_o p + (\Delta\sigma_{h1} - \delta) \\ &= K_o p + \Delta\sigma_{h2} \end{aligned}\right\} \tag{7.10}$$

An ideal settlement analysis should take into account the complete pattern of stresses an element of soil will be subjected to in the field. In order to determine the relevant vertical strains, laboratory tests should be performed under identical stress conditions and an integration of all such vertical strains beneath a loaded area would give the settlement of the foundation (Lambe 1964, Davis and Poulos 1967).

The methods most widely used in practice, however, are the ones based on the oedometer test. Figure 7.6 summarizes all these methods indicating the effective stress-paths associated with each of them. In plotting the stress-path AF in Fig. 7.6, it has been assumed that an undisturbed sample when subjected to the in-situ vertical stress also restores the in-situ horizontal stress so that subsequent stress-path for loading starts from the point A.

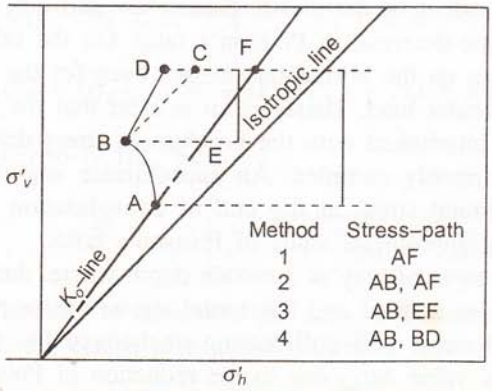


**Fig. 7.6** Methods of settlement analysis and implied stress–path.

Method 1, described by Skempton and McDonald (1955) as the conventional method, was first proposed by Terzaghi (1929) and later used by Taylor (1948). It assumes that all settlement occurs from one-dimensional compression and that the excess pore-pressure is equal to the increase in vertical stress. Therefore, the corresponding stress–path is AF.

Method 2 recognizes that the soil undergoes shear deformation during undrained loading (path AB), and this causes the immediate settlement, but still assumes that the excess pore-pressure, which should be a function of the induced shear stress, is equal to the vertical stress increment. Consolidation settlement, therefore, occurs along the stress–path AF. This inconsistency in Method 2 has been overcome by Skempton and Bjerrum (1957) in Method 3. Here, the immediate settlement is a function of the stress–path AB while the consolidation settlement occurs along the path EF. The latter, therefore, is only a part of the total strain along the path AF depending on the magnitude of the excess pore-pressure set up during loading.

While the method of Skempton and Bjerrum introduces for the first time, the concept of stress-path in settlement analysis, the assumption is still implicit that during consolidation all strain is one-dimensional which requires the horizontal stresses to adjust accordingly. Therefore, there is a discrepancy between the field stress–path BD and the path EF used in the analysis. The condition of no lateral strain may be approximately true in cases like that of a loaded area which is very large compared to the thickness of the clay layer. But in the majority of field problems, this condition may be far from true. Moreover, while computing the immediate settlement, Method 3 obviously accepts that the clay undergoes lateral deformation during loading (with constant volume, there would be no settlement otherwise) but this is neglected in estimating the consolidation settlement. Consequently, of course, the effect of the horizontal stress is completely ignored except in determining the excess pore–water pressure.

### 7.2.1 Stresses During Loading and Consolidation in the Field

It is evident that during load application in the field, most of the deformation takes place under condition of no volume change, implying a value of Poisson's ratio of the soil equal to 0.5. As the excess pore-pressures dissipate, Poisson's ratio also decreases and finally drops to its fully drained value. It is known that for an isotropic homogeneous elastic medium, the vertical stresses are independent of the elastic parameters and are, therefore, unlikely to be significantly affected by this decrease in Poisson's ratio. On the other hand, Poisson's ratio has a considerable influence on the horizontal stresses even for the Boussinesq case beneath the centre of a uniform circular load. Therefore, it is clear that the problem of consolidation in the field is very much interlinked with the problem of stress distribution, whose rigorous analytical treatment is extremely complex. An approximate analysis may be made on the assumption that the horizontal stress at the end of consolidation will be the same as the Boussinesq stresses for the appropriate value of Poisson's ratio.

If we consider an element of clay at a certain depth where, during load application, $\Delta\sigma_v$ and $\Delta\sigma_{h1}$ are the increase in vertical and horizontal stresses respectively then, at the end of consolidation, the vertical stress will still remain unchanged but the horizontal stress will have decreased to the new value $\Delta\sigma_{h2}$ due to the reduction of Poisson's ratio.

So, the changes in effective stress during consolidation are given as

Horizontal: $$[\Delta\sigma_h]_c = \Delta u - \delta \tag{7.11}$$

Vertical: $$[\Delta\sigma_v]_c = \Delta u$$

where $\delta = \Delta\sigma_{h1} - \Delta\sigma_{h2}$.

The ratio of the effective stress changes during consolidation, $K'$ is then given by

$$K' = \frac{[\Delta\sigma_h]_c}{[\Delta\sigma_v]_c} = 1 - \frac{\delta}{\Delta u} \tag{7.12}$$

Now, for the Boussinesq problem, the general expressions for stresses beneath the centre of a uniform circular load (diameter $2b$ and load intensity, $q$) are (Wu 1966),

$$\left.\begin{aligned} \sigma_z &= q\left[1 - \frac{(z/b)^3}{(1 + z^2/b^2)^{3/2}}\right] \\ \sigma_h &= \frac{q}{2}\left[(1 + 2\nu) - \frac{2(1 + \nu)(z/b)}{(1 + z^2/b^2)} + \frac{(z/b)^3}{(1 + z^3/b^3)^{3/2}}\right] \end{aligned}\right\} \tag{7.13}$$

which can be more conveniently written as,

$$\sigma_z = q(1 - \eta^3)$$

$$\sigma_h = \frac{q}{2}[(1 + 2\nu) - 2(1 + \nu)\eta + \eta^3] \tag{7.14}$$

where,

$$\eta = \frac{z/b}{(1 + z^2/b^2)^{1/2}} \tag{7.15}$$

Using these expressions,

$$\left.\begin{aligned} \Delta\sigma_v &= (\sigma_v)_{\nu=1/2} = q(1 - \eta^3) \\ \Delta\sigma_{h1} &= (\sigma_h)_{\nu=1/2} = \frac{q}{2}[2 - 3\eta + \eta^3] \\ \Delta\sigma_{h2} &= (\sigma_h)_{\nu=\nu'} = \frac{q}{2}[(1 + 2\nu') - 2(1 + \nu')\eta + \eta^3] \end{aligned}\right\} \tag{7.16}$$

Combining Eqs. (7.13) to (7.16), we have

$$K' = 1 - \left[\frac{1 - 2\nu}{1 + \eta(1 + \eta)(3A - 1)}\right] \tag{7.17}$$

Eq. (7.17) can then be used to determine the ratio of the stress increase during consolidation at any depth beneath the centre of a uniform circular load.

### 7.2.2 Influence of Stress-path on the Drained Deformation of Clay

It has been shown in the foregoing that the stress changes that occur in the field during consolidation are primarily dependent on the drained Poisson's ratio and the pore pressure parameter $A$ of the soil. Therefore, it is of considerable practical significance to study the influence of stress-path, such as BD (see Fig. 7.5) on the axial and volumetric strain during consolidation. Experimental investigation with undisturbed London clay (Som, 1968), normally consolidated Kaolinite (Das and Som et al., 1975) and undisturbed Calcutta clay (Guha, 1979) show that the stress increment ratio during consolidation has important effect on the deformation characteristics of the soil. Two things need to be considered here:

(a) the influence of stress increment ratio on the volumetric strain of the soil and
(b) the influence of stress increment ratio on the strain ratio (that is, axial strain/volumetric strain) of the soil.

There is conflicting evidence on the effect of stress ratio on the volumetric compressibility of clay. Some investigators have found that the volumetric compressibility is independent of the stress increment ratio and can be expressed as function of vertical effective stress only (Som, 1968). This means that the results of one-dimensional consolidation tests would be applicable irrespective of the changes in lateral pressure during consolidation. Others have found that the volumetric compressibility is not independent of the lateral pressure and can best be expressed as functions of mean effective stress during consolidation (Das, 1975). It seems that the appropriate relationship has to be determined for the particular soil under investigation.

The major effect of lateral stresses during consolidation is, however, manifested in the axial strain associated with volumetric deformation. Figure 7.7 shows some typical results of stress-path controlled triaxial tests on different clays. The results are plotted as relationships between the stress increment ratio, $K'$ and the strain ratio, $\lambda$ during consolidation or drained deformation. It is to be noted that one-dimensional consolidation implies a strain ratio, $\lambda = 1.0$ and that occurs at a particular stress increment ratio only. For any other stress ratio, the strain ratio would also the difference and assumption of one-dimensional strain (i.e. $\varepsilon_1/\varepsilon_v = 1.0$) would lead to significant error in settlement analysis.

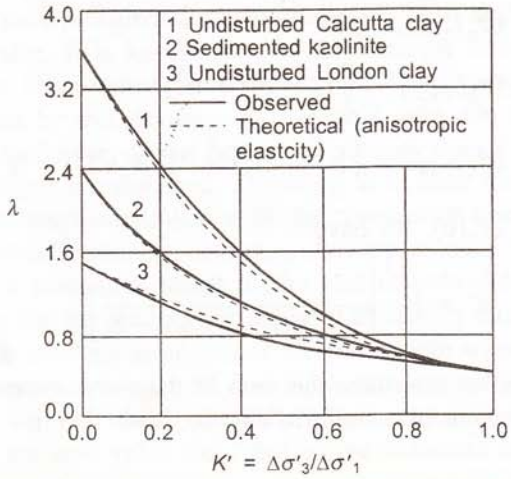


**Fig. 7.7** Strain ratio, $\lambda$ versus stress increment ratio, $K'$ for drained deformation.

The relationships shown in Fig. 7.7 can best be determined from stress controlled triaxial tests. However, Som (1968), Simons and Som (1969) have demonstrated that this relationship can also be established theoretically from consideration of anisotropic elasticity as:

$$\frac{\varepsilon_1}{\varepsilon_v} = \frac{1 - 2\eta v_2' K'}{(1 - 2v_3') + 2\eta(1 - v_1' - v_2')K'} \tag{7.18}$$

where,

$v_1'$ = effect of one horizontal strain in the other horizontal strain;

$v_2'$ = effect of horizontal strain on vertical strain;

$v_3'$ = effect of vertical strain on horizontal strain;

$\eta$ = ratio of vertical drained deformation modulus to the horizontal drained deformation modulus.

Equation (7.18) can also be expressed as

$$\frac{\varepsilon_1}{\varepsilon_v} = \frac{1 - 2\eta v_2' K'}{(1 - 2v_3')[K'/K_o - 1] - 2\eta v_2' K'} \tag{7.19}$$

The parameters $v_3'$ and $\eta v_2'$ can be determined from two tests with different values of $K'$ and measuring $\varepsilon_1/\varepsilon_v$ in each case. The most convenient values of $K'$ to choose are 0 and 1.0, that is, those from the standard drained compression test and the isotropic consolidation test.

### 7.2.3 Settlement Analysis by Stress-path Method

The methods of settlement analysis in current use have been described earlier. These methods have given satisfactory results in many field problems, particularly where the condition of zero lateral strain is satisfied. However, more often than not appreciable lateral deformation occurs in the field and the currently used methods of settlement analysis become inadequate to predict the settlement. A method of settlement prediction by the stress-path method has, therefore, been introduced for the case of axi-symmetric loading (Simons and Som, 1969, Som et al., 1975).

#### Immediate settlement

The common practice in estimating the immediate (elastic) settlement of foundation on clay is to assume the soil to be a homogeneous, isotropic, elastic medium, thus, permitting the application of Boussinesq analysis. However, in practice, the elastic modulus, $E$ of the soil varies with depth as a consequence not only of the inherent non-homogeneity of the soil but also of varying applied stress levels at different depths. Stress–strain relationship of soft clay is essentially non-linear and the deformation modulus varies considerably with the stress level. While it is possible to make theoretical analysis of undrained deformation using the finite element technique and taking the non-linear stress versus strain behaviour of the soil into consideration, they are not yet available in readily usable form. A simple expression for immediate settlement following the stress-path method may be given as,

$$\rho_i = \int_0^z \frac{\Delta\sigma_v - \Delta\sigma_h}{E(z)} \tag{7.20}$$

where $\Delta\sigma_v$ and $\Delta\sigma_h$ are the increase in total vertical and horizontal stresses at any depth respectively and $E(z)$ is the corresponding deformation modulus, taking due account of the vertical and horizontal effective stresses prior to and at the end of loading.

It has been shown by many investigators that the stresses in the subsoil due to a foundation loading are not significantly dependent upon the variation of $E$ (Huang 1968, Som 1968). Therefore, in the absence of more rigorous analysis, the Boussinesq stresses may be used in evaluating the settlement by Eq. (7.21), the integration being done numerically by dividing the compressible stratum into a number of layers and taking the appropriate value of $E$ for the layer into account.

**Consolidation settlement**

In the conventional method, the consolidation settlement is given by,

$$\rho_c = \int_0^z (m_v)_1 \Delta\sigma_z \, dz \tag{7.21}$$

where $(m_v)_1$ is the coefficient of volume compressibility determined from standard consolidation test and $\Delta\sigma_z$ is the increase of vertical pressure at the centre of layer,
Following the Skempton and Bjerrum (1957) method, the settlement is,

$$\rho_c = \mu \int_0^z (m_v)_1 \Delta\sigma_z \, dz \tag{7.22}$$

where $\mu$, the pore-pressure correction factor, is a function of the soil type and the geometry of the foundation, (refer Fig. 7.4).

For the stress-path method, the settlement is given by,

$$\rho_c' = \int_0^z \lambda (m_v)_3 \Delta u \, dz \tag{7.23}$$

$$= \lambda \rho_c$$

where,

$\Delta u$ = increase of pore–water pressure under undrained loading which dissipates during the consolidation.

$(m_v)_3$ = coefficient of volume compressibility for three-dimensional strain.

$\lambda$ = the ratio of vertical strain to volumetric strain which is a function of the stress increment ratio during consolidation.

If Eq. (7.23) is to be applied in settlement analysis, $K'$ during consolidation needs to be known in order to determine the value of $\lambda$. Accurate determination of $K'$ for actual foundation may be difficult because it depends on many factors such as Poisson's ratio,

pressure parameter $A$, stress–strain relationship of the soil, and so on. As an approximation, however, its value can be determined from Eq. (7.17), for a footing of diameter $2a$. According to Eq. (7.17),

$$K' = 1 - \left[\frac{1 - 2\nu}{1 + \eta(1 + \eta)(3A - 1)}\right]$$

where,

$$\eta = \frac{z}{a}\left(1 + \frac{z^2}{a^2}\right)^{-1/2},$$

$\nu$ = Poisson's ratio

$A$ = Skempton's pore-pressure parameter

Knowing the value of $K'$, $\lambda$ can be obtained from experimental relationships as shown in Fig. 7.7. The value of $(m_v)_3$ should, of course, be obtained from appropriate stress-path test, but, for practical purposes, can be determined from properly conducted oedometer test. Then, $(m_v)_3$ may be taken as approximately equal to $(m_v)_1$, the oedometer compressibility in terms of vertical effective stress.

It may be noted here that evaluation of the $K'$ versus $\lambda$ relationship for any problem requires determination of Poisson's ratio and pore-pressure parameter, $A$ of the soil. But for most soils, Poisson's ratio varies between 0.1 and 0.3 and pore-pressure parameter, $A$ between 0 and 1. Accordingly, $K'$ varies within a narrow range of 0.6–0.9 and $\lambda$ in the range 0.5–0.8. It would, therefore, be convenient to select a value of $\lambda$ within this range for most practical problems (Som, 1968).

## 7.3 RATE OF SETTLEMENT

The rate of settlement of foundations on clay is generally determined from Terzaghi's theory of one-dimensional consolidation although field-consolidation is often three-dimensional (See Chapter 1, Section 1.9.5).

According to this, the excess pore-pressure at any point at depth $z$ within a soil mass after a time from load application, is governed by the equation

$$C_v \frac{\delta^2 u}{\delta z^2} = \frac{\delta u}{\delta t} \tag{7.24}$$

where, $u$ is the excess pore-pressure and

$C_v$ coefficient of consolidation.

The degree of consolidation at any time, $t$ (defined as the percentage dissipation of pore-pressure) may be obtained by solving Eq. (7.24) for appropriate boundary conditions. Table 7.2 gives the relationship between time factor, $T_v = C_v t/H^2$ and degree of consolidation, $U$ for different boundary conditions.

**Table 7.2** $U$ versus $T_v$ relationship ($T_v = C_v t/H^2$)

| $U$% | $(u_1/u_2) = 0$ | 0.5 | 1.0 | 5.0 | $T_v$ |
|---|---|---|---|---|---|
| 0 | 0 | 0 | 0 | 0 | 0 |
| 20 | 0.01 | 0.05 | 0.031 | 0.014 | 0.01 |
| 40 | 0.21 | 0.17 | 0.126 | 0.081 | 0.049 |
| 60 | 0.39 | 0.31 | 0.287 | 0.195 | 0.155 |
| 80 | 0.64 | 0.58 | 0.567 | 0.460 | 0.420 |
| 100 | ∞ | ∞ | ∞ | ∞ | ∞ |

For double drainage (any distribution of pressure, that is, $u_1/u_2$ = any value), take $H$ = 1/2 times thickness of clay and $T_v$ values for $(u_1/u_2) = 1$.

## 7.4 FOUNDATION ON SAND

Foundations on sand do not present the same degree of problem with regard to settlement as foundations on clay. Firstly, except for loose sand, settlement is usually small and secondly, because of high permeability the settlement is usually over during the period of construction. In this case, there is no time dependent settlement similar to the consolidation settlement in clayey soils, although large foundations may undergo minor settlement caused by fluctuations of load due to wind, machinery vibrations, and storage loads.

Prediction of settlement of foundations on sand is, by and lange, empirical although elastic theory has sometimes been used. The common methods used for this purpose are:

### 7.4.1 Elastic Theory

The problem is similar to calculation of immediate settlement of foundations on clay as given in Eq. (7.3). For a homogeneous, isotropic, elastic medium

$$\delta = \frac{q_n B}{E}(1 - \nu)^2 I_\rho \tag{7.25}$$

where the different terms have the same meaning as in Eq. (7.3). However, it is to be considered that because of volume change during load application, Poisson's ratio, $\nu$ can no longer be taken as 0.5. The value of $E$ and $\nu$ should be determined from the laboratory triaxial tests for the appropriate relative density and confining pressure. The Poisson's ratio normally varies between 0.15 for coarse sand to 0.3 for fine to silty sand. The value of $E$ can also be determined from the standard penetration resistance of the soil (refer Chapter 2, Table 2.7).

Elastic theory, however, gives only a very approximate estimate of settlement, because the assumption of homogeneity would be far from reality.

### 7.4.2 Semi-empirical Method (Buisman, 1948)

Buisman (1948) has given an empirical method of estimating the settlement of foundations on sand by numerical integration of the strains occurring in different strata, as shown in Fig. 7.8. Accordingly,

$$\delta = \sum \frac{2.3p_o}{E} \log_{10} \frac{p_o + \Delta p}{p_o} \, dz \tag{7.26}$$

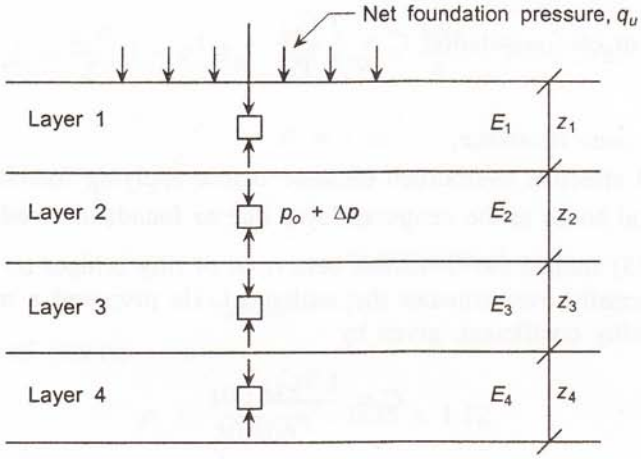


**Fig. 7.8** Settlement calculation for foundations on sand (after Buisman, 1948).

where,

$p_o$ = initial effective overburden pressure before loading,
$\Delta p$ = increase of vertical stress at the centre of layer due to foundation loading, and
$E$ = modulus of elasticity.

The sand layer is subdivided into a number of sublayers and the $E$ values are taken from empirical relationship for the average $N$ value for the layer, as described in Section 2.7.1 (Chapter 2).

## 7.4.3 Plate Load Test

Terzaghi and Peck (1948) gave an empirical relationship between the settlement, $S_p$ of a loaded plate of diameter, $D_p$ for a given intensity of pressure and the settlement, $S_f$ of a foundation of diameter, $D_f$ at the same pressure. Bjerrum and Eggestad (1963) modified this relationship as follows:

$$\frac{S_f}{S_p} = \frac{4}{(1 + D_p/D_f)^2} \tag{7.27}$$

The use of this equation is based on the assumption that the density of the soil within the zone affected by the foundation loading is similar to that beneath the test plate. This may be approximately true if the plate diameter is of the same size as the foundation, but for large foundations, there is likely to be considerable difference in density.

## 7.4.4 Static Cone Test

If $C_{kd}$ is the point resistance measured by the static cone test, the settlement of the foundation is given by the empirical relationship (Beer and Martens 1957),

$$\delta = \frac{2.3H}{C} \sum \log \frac{p_o + \Delta p}{p_o} \tag{7.28}$$

where, coefficient of compressibility, $C = \frac{3}{2} \frac{C_{kd}}{p_o}$

where,

$C_{kd}$ = static cone resistance,

$p_o$ = initial effective overburden pressure before applying foundation loading, and

$\Delta p$ = vertical stress at the centre of layer due to foundation loading.

De Beer (1965) studied the settlement behaviour of fifty bridges on sand and concluded that Eq. (7.28) normally overestimates the settlement. He proposed a modified relationship for the compressibility coefficient, given by

$$C = \frac{1.9 C_{kd}}{p_o} \tag{7.29}$$

The cone penetration data are plotted with depth and the soil is divided into a number of layers and each layer is assigned an average $C_{kd}$ value for obtaining the coefficient of compressibility.

**Example 7.1**

Figure 7.9 shows an isolated column in a building frame with a column grid of 4 m × 4 m which carries a vertical load of 400 kN and is supported on a footing, 2 m × 2 m, placed 1 m below G. L. The subsoil consists of 5 m of firm desiccated silty clay ($c_u$ = 50 kN/m$^2$, $C_c/1 + e_0$ = 0.06) followed by medium sand ($N$ = 20). Calculate the settlement of the footing.

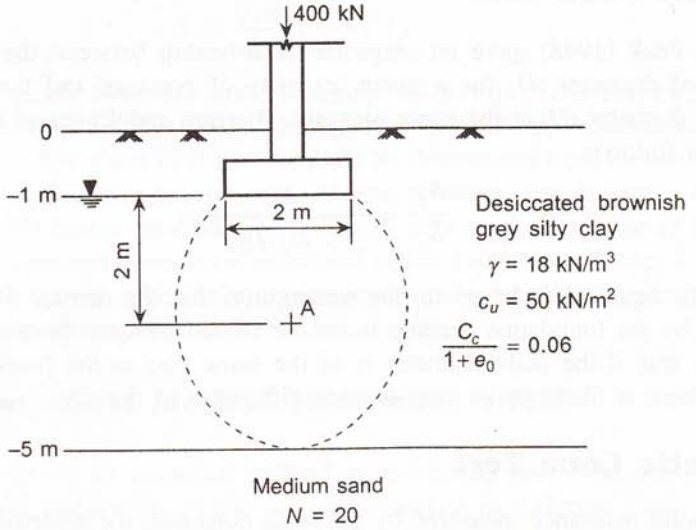


**Fig. 7.9** Isolated footing on clay.

***Solution***

(a) *Immediate settlement*

$$\rho_i = \frac{q_n B}{E}(1 - \nu^2) I_\rho \quad \text{and} \quad q_n = \frac{400}{4} = 100 \text{ kN/m}^2$$

Also,

$$B = 2 \text{ m}$$
$$\nu = 0.5$$
$$E = 600\, c_u$$
$$= 30{,}000 \text{ kN/m}^2$$
$$(I_\rho)_{\text{centre}} = 1.12$$

∴ At the centre of footing,

$$\rho_i = \frac{100 \times 2}{30{,}000} \times 0.75 \times 1.12$$

$$= 0.0056 \text{ m} = 5.6 \text{ mm}$$

$$\frac{L}{B} = 1.0 \quad \text{and} \quad \frac{D_f}{B} = 0.5$$

⇒ depth correction, $\alpha = 0.86$

∴ $(\rho_i)_{\text{corr}} = 0.86 \times 5.6 = 4.8$ mm

(b) *Consolidation settlement*

Take influence zone extending to twice the width of footing, that is, 4 m, below footing. Consider single layer within the zone of influence.

$$\therefore \quad \rho_{\text{oed}} = \frac{C_c}{1 + e_0} H \log \frac{p_0 + \Delta p}{p_0}$$

At A: $p_0 = 1 \times 18 + 8 \times 2 = 34 \text{ kN/m}^2$

$\Delta p = 0.34 \times 100 = 34 \text{ kN/m}^2$

$$\therefore \quad \rho_{\text{oed}} = 0.06 \times 4 \times \log \frac{34 + 34}{34}$$

$$= 0.072 \text{ m} = 72 \text{ mm}$$

Depth correction, $\alpha = 0.86$

∴ $(\rho_{\text{oed}})_{\text{corr}} = 0.86 \times 72 = 62$ mm

*Skempton and Bjerrum's method*

$$\rho_c = \mu(\rho_{\text{oed}})_{\text{corr}}$$

Pore-pressure correction factor, $\mu = 0.7$ (refer Fig. 7.4)

$$\rho_c = 0.7 \times 62 = 43.4 \text{ mm}$$

$\therefore$ Final settlement $= 4.8 + 43.4$
$= 48.2$ mm

*Stress-path method*

$$\rho'_c = \lambda \rho_c$$

From Eq. (7.17),

$$K' = 1 - \left[\frac{1 - 2\nu}{1 + \eta(1 + \eta)(3A - 1)}\right]$$

Substituting $\nu = 0.3$ and $A = 0.7$,

$$K' = 1 - \left[\frac{1 - 2 \times 0.3}{1 + 0.3(1.3)(3 \times 0.7 - 1)}\right]$$

$$= 0.84$$

From Fig. 7.7, for undisturbed Calcutta soil

$$\lambda = 0.6$$

$$\therefore \quad \rho'_c = 0.6 \times 43.4 = 26 \text{ mm}$$

$$\therefore \quad \rho_f = 4.8 + 26 = 30.8 \text{ mm}$$

**Example 7.2**

A raft foundation, 8 m × 12 m in plan is to be placed 2 m below G. L. in the subsoil shown in Fig. 7.10. The net foundation pressure is 50 kN/m$^2$. Calculate the total settlement of the foundation

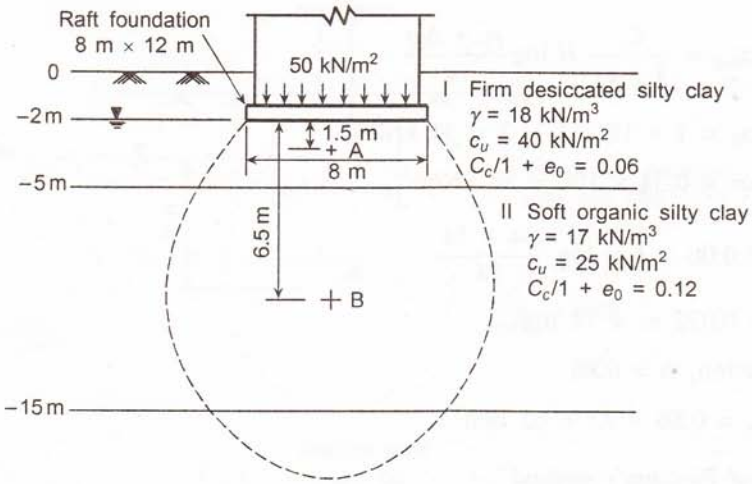


**Fig. 7.10** Raft foundation on clay.

Take influence zone extending to twice the width of foundation, that is, 16 m below foundation. Neglect the effect of settlement due to sand layer.

***Solution***

(a) *Immediate settlement*

$$\rho_i = \frac{q_n B}{E}(1 - \nu^2) I_\rho$$

For the given problem,

$$q_n = 50 \text{ kN/m}^2$$
$$B = 8 \text{ m}$$
$$\nu = 0.5$$

$I_\rho$ (for $L/B = 12/8 = 1.5$) = 1.36 (refer Table 7.1)

for, Stratum I: $E_1 = 600 \times 40 = 24{,}000 \text{ kN/m}^2$

Stratum II: $E_2 = 600 \times 25 = 15{,}000 \text{ kN/m}^2$

Weighted average, $E$

$$E = \frac{24{,}000 \times 3 + 15{,}000 \times 10}{13}$$
$$= 17{,}000 \text{ kN/m}^2$$

$$\therefore \quad \rho_i = \frac{50 \times 8}{17{,}000} \times 0.75 \times 1.36$$
$$= 0.024 \text{ m} = 24 \text{ mm}$$

Depth correction = 1.0

Rigidity correction = 0.8 (Considering raft with interconnected beams providing rigidity to the foundation)

$$\therefore \quad (\rho_i)_{\text{corr}} = 0.8 \times 24 = 19 \text{ mm}$$

(b) *Consolidation settlement*

$$\rho_{\text{oed}} = \sum \frac{C_c}{1 + e_0} H \log \frac{p_o + \Delta p}{p_o}$$

At A, $p_o = 18 \times 2 + 8 \times 1.5 = 48 \text{ kN/m}^2$

$\Delta p = 0.82 \times 50 = 41 \text{ kN/m}^2$

At B, $p_o = 18 \times 2 + 8 \times 3 + 7 \times 5 = 95 \text{ kN/m}^2$

$\Delta p = 0.42 \times 50 = 21 \text{ kN/m}^2$

$$\therefore \quad \rho_{\text{oed}} = 0.06 \times 3 \times \log \frac{48 + 41}{48} + 0.12 \times 10 \log \frac{95 + 21}{95}$$
$$= 0.048 + 0.104$$
$$= 0.152 \text{ m} = 152 \text{ mm}$$

Using, depth correction = 1.0
Rigidity correction = 0.8

$$\therefore \quad (\rho_{oed})_{corr} = 0.8 \times 152 = 121 \text{ mm}$$

*Skempton and Bjerrum method*

$$\rho_c = \mu(\rho_{oed})_{corr}$$

Take $\mu = 0.8$ (settlement being predominantly in soft normally consolidated soil of stratum II)

$$\therefore \quad \rho_c = 0.8 \times 121 = 97 \text{ mm}$$

$$\therefore \quad \rho_f = 19 + 97 = 116 \text{ mm}$$

*Stress-path method*

$$\rho'_c = \lambda \rho_c$$

From Eq. (7.17)

$$K' = 1 - \left[\frac{1 - 2\nu}{1 + \eta(1 + \eta)(3A - 1)}\right]$$

Substituting $\nu = 0.3$ and $A = 0.8$

$$K' = 1 - \left[\frac{1 - 2 \times 0.3}{1 + 0.3(1.3)(3 \times 0.8 - 1)}\right]$$

$$= 0.84$$

From Fig. 7.7,

$$\lambda = 0.6$$

$$\therefore \quad \rho'_c = 0.6 \times 97 = 58 \text{ mm}$$

$$\therefore \quad \rho_f = 19 + 58 = 77 \text{ mm}$$

**Example 7.3**

A 5 m × 5 m foundation is placed 1 m below G. L. in the stratified sandy deposit as depicted in Fig. 7.11. Calculate the settlement of the foundation.

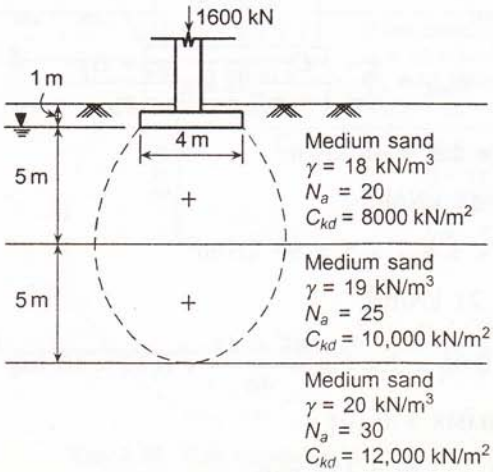


**Fig. 7.11** Foundation on sand.

***Solution***

Net foundation pressure,

$$q_n = \frac{1600}{4 \times 4} = 100 \text{ kN/m}^2$$

(a) *Elastic theory*

$$\delta = \frac{q_n B}{E}(1 - \nu^2) I_\rho$$

Also,

$q_n = 100 \text{ kN/m}^2$
$B = 4 \text{ m}$
$\nu = 0.3$ (assumed)
$I_\rho = 1.12$
$E = C_1 + C_2 N$ (Take average $N$ value of the two layers having almost equal depth within the influence zone)
$= 39 + 4.5 \times 22.5$
$= 140 \text{ kg/cm}^2$
$= 14{,}000 \text{ kN/m}^2$

$$\therefore \quad \delta = \frac{100 \times 4}{14{,}000} \times 0.91 \times 1.12$$
$$= 0.029 \text{ m}$$
$$= 29 \text{ mm}$$

$$\frac{L}{B} = 1 \quad \text{and} \quad \frac{D_f}{B} = 0.25$$

$\therefore$ Depth correction, $\alpha = 0.97$

(b) *Buisman (1948) method*

Consider two layers within the influence zone

$$\delta = \sum \frac{2.3 p_o}{E} \log_{10} \frac{p_o + \Delta p}{p_o} dz$$

At A, $p_o = 1 \times 18 + 2.5 \times 9 = 40.5 \text{ kN/m}^2$
$\Delta p = 0.56 \times 100 = 56 \text{ kN/m}^2$
$E_1 = 39 + 4.5 \times 20 = 129 \text{ kg/cm}^2 = 12{,}900 \text{ kN/m}^2$

At B, $p_o = 1 \times 18 + 5.0 \times 8 + 2.5 \times 9 = 80.5 \text{ kN/m}^2$
$\Delta p = 0.11 \times 100 = 11 \text{ kN/m}^2$
$E_1 = 39 + 4.5 \times 25 = 151.5 \text{ kg/cm}^2 = 15{,}150 \text{ kN/m}^2$

$$\therefore \quad \delta = \frac{2.3 \times 40.5}{12{,}900} \times 5 \log_{10} \frac{40.5 + 56}{40.5} + \frac{2.3 \times 80.5}{15{,}150} \times 5 \log_{10} \frac{80.5 + 11}{80.5}$$

$$= 0.012 + 0.0034 = 0.0154 \text{ m} = 15.4 \text{ mm}$$

Depth correction = 0.97

$\therefore \quad (\delta)_{corr} = 0.97 \times 15.4 = 15 \text{ mm}$

(c) *Beer and Martens (1957)*

$$\delta = \frac{2.3H}{C} \log_{10} \frac{p_o + \Delta p}{p_o}.$$

***Layer 1:***

$H = 5$ m; $p_o = 40.5$ kN/m$^2$; $\Delta p = 56$ kN/m$^2$

$$\therefore \quad C = \frac{1.9 C_{kd}}{p_o}$$

$$= \frac{1.9 \times 8000}{40.5} = 375$$

***Layer 2:***

$H = 5$ m; $p_o = 80.5$ kN/m$^2$; $\Delta p = 11$ kN/m$^2$

$$\therefore \quad C = \frac{1.9 \times 10{,}000}{80.5} = 236$$

$$\therefore \quad \delta = \frac{2.3 \times 5}{12{,}900} \times 5 \log_{10} \frac{40.5 + 56}{40.5} + \frac{2.3 \times 5}{15{,}150} \times 5 \log_{10} \frac{80.5 + 11}{80.5}$$

$$= 0.017 + 0.002 = 0.019 \text{ m} = 19 \text{ mm}$$

Depth correction = 0.97

$\therefore \quad (\delta)_{corr} = 19 \times 0.97 \approx 18 \text{ mm}$

**Example 7.4**

The results of a plate load test on a sandy stratum are shown in Fig. 7.12. The size of the plate used is 30 cm × 30 cm. Determine the size of a square footing for a column carrying a load of 1800 kN with a maximum permissible settlement of 50 mm.

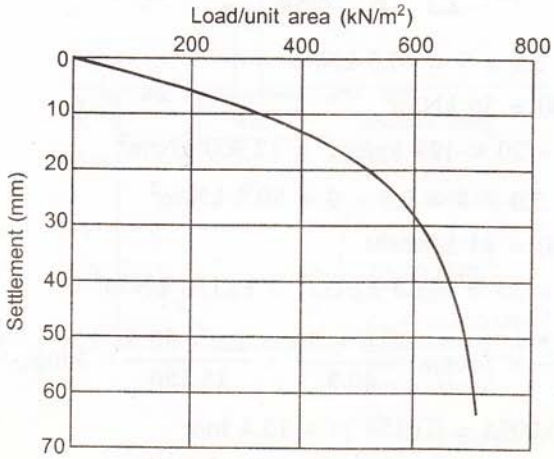


**Fig. 7.12** Plate load test data.

***Solution***

The problem has to be solved by trial and error.

*First trial*

Size of footing = 3 m × 3 m

$$q_n = 1800/9 = 200 \text{ kN/m}^2$$

From Eq. (7.27)
$$\frac{S_f}{S_p} = \frac{4}{\left(1 + \frac{D_p}{D_f}\right)^2}$$

$$\therefore \quad S_p = \frac{S_f}{4}\left(1 + \frac{D_p}{D_f}\right)^2$$

$$= \frac{50}{4}\left(1 + \frac{300}{3000}\right)^2$$

$$= 15 \text{ mm}$$

∴ Allowable pressure (From curve) = 440 kN/m$^2$

*Second trial*

Size of footing = 2 m × 2 m

$$q_n = \frac{1800}{2 \times 2} = 450 \text{ kN/m}^2$$

Again, $S_p = \frac{50}{4}\left(1 + \frac{300}{2000}\right)^2$

$$= 16.5 \text{ mm}$$

∴ Allowable pressure = 480 kN/m$^2$

## REFERENCES

Bjerrum, L. (1964), *Relasjon Mellom Malte og Beregnede Setninger a v Byggverk pa Leire og Sand*, N.G.F. Foredraget, 1964. Norwegian Geotechnical Institute, Oslo 92 pp.

Bjerrum L. (1963), *Discussion on Section 6. European Conference S.M.F.E.*, Wiesbaden, Vol. 2, pp. 135–137.

Butler, F.G. (1974), *General Report and State-of-the-Art Review*, Session 3: Heavily Overconsolidated Clays, Proceedings of Conference on Settlement of Structures, Cambridge.

Das, S.C. (1975), *Predicted and Measured Values of Stress and Displacements Downloading and Construction under Circular Footings Resting on Saturated Clay Medium*, Ph.D. Thesis, Jadavpur University, Calcutta.

Das, S.C. and N.N. Som (1976), *Settlement of Footings on Soft Clay*, Proc. Symp. on Foundations and Excavation in Weak Soil, Calcutta, Vol. 1.

Davis, E.H. and H.G. Poulos (1968), The Use of Elastic Theory for Settlement Prediction under Three-dimensional Conditions, *Geotechnique*, Vol. 18.

De Beer, E.E. (1965), *Bearing Capacity and Settlement of Shallow Foundations on Sand*, Proc. Symposium on Bearing Capacity and Settlement of Foundations, Duke University, pp. 15–33.

De Beer, E. and A. Martens (1957), *Method of Computation of an Upper Limit for the Influence of Heterogeneity of Sand Layers in Settlement of Bridges*, 4th I.C.S.M.F.E., London, Vol. 1, pp. 275–281.

Fox, E.N. (1948), *The Mean Elastic Settlement of Uniformly Loaded Area at a Depth below Ground Surface*, 2nd I.C.S.M.F.E., Rotterdam, Vol. 1, p. 129.

Guha, S. (1979), *Effect of Initial and Incremental Strain Ratios or Drained Deformation of Calcutta Soil*, MCE Thesis, Jadavpur University, Calcutta.

Ladd, C.C. (1969), *The Prediction of in-situ Stress–Strain Behaviour of Soft Saturated Clays during Undrained Shear*, Bolkesj $\phi$ Symposium on Shear Strength and Consolidation of Normally Consolidated Clays, Norwegian Geotechnical Institute, Oslo, pp.14–19.

Lambe, T.W. (1964), Methods of Estimating Settlement, *Journal of Soil Mechanics and Foundation Division*, A.S.C.E., 90, No. SM5, pp. 43–67.

Raymond, G.P., D.L. Townsend, and M.J. Lojkasek (1971), The Effect of Sampling on the Undrained Soil Properties of a Leda Soil, *Canadian Geotechnical Journal*, Vol. 8, pp. 546–557.

Simons, N.E. (1957), *Settlement Studies on Two Structures in Norway*, 4th I.C.S.M.F.E., London, Vol. 1, pp. 431–436.

Simons, N.E. and N.N. Som (1970), *Settlement of Structures on Clay with Particular Emphasis on London Clay*, Construction Industry Research and Information Association Report 22, p. 51.

Skempton, A.W. (1954), The Pore-pressure Coefficients A and B, *Geotechnique*, Vol. 4, pp. 143–147.

Skempton, A.W., R.B. Peck, and D.H. McDonald (1955), *Settlement Analyses of Six Structures in Chicago and London*, Proc. I.C.E., Part 1, Vol. 4, No. 4, p. 525.

Skempton, A.W. and L. Bjerrum (1957), A Contribution to the Settlement Analysis of Foundations on Clay, *Geotechnique*, Vol. 7, No. 4, pp. 168–178.

Som, N.N. (1968), *The Effect of Stress Path on the Deformation and Consolidation of London Clay*, Ph.D. Thesis, University of London.

Som, N.N. (1975), *Regional Deposits: Contribution for Panel Discussion*, Proc. 5th Asian Regional Conf. in SMFE, Vol. 2, p. 20.

Taylor, D.W. (1948), *Fundamentals of Soil Mechanics*, John Wiley and Sons, Inc, New York.

Terzaghi, K. (1943), *Theoretical Soil Mechanics*, John Wiley and Sons Ltd., p. 510.

Terzaghi, K. and R.B. Peck (1948), *Soil Mechanics in Engineering Practice*, 1st ed., Wiley, New York.

# 8 Footings and Raft Design

## 8.1 INTRODUCTION

Footings and rafts are the common shallow foundations wherein the subsoil immediately beneath the ground surface is required to support the foundation load. The superstructure load from a building is transmitted to the ground through columns and load-bearing walls and suitable structural members are to be provided to transfer the load into the subsoil. These structural members which are placed at some depth beneath the ground surface serve to 'spread' the load from high stress intensity of the superstructure material (concrete, steel, or brick) to the low allowable stresses in the soil mass.

The different types footings and rafts have been illustrated in Chapter 4. They are generally made of reinforced concrete. The reinforcements are provided to resist the bending moment on the footing caused by the upward soil reaction either in one direction as in the case of strip footings or in two directions as in case of isolated or combined footings, refer Fig. 8.1. The section of the footings may be sloped to economize on the volume of concrete. Heavily loaded structural steel columns are sometimes provided with grillage foundations.

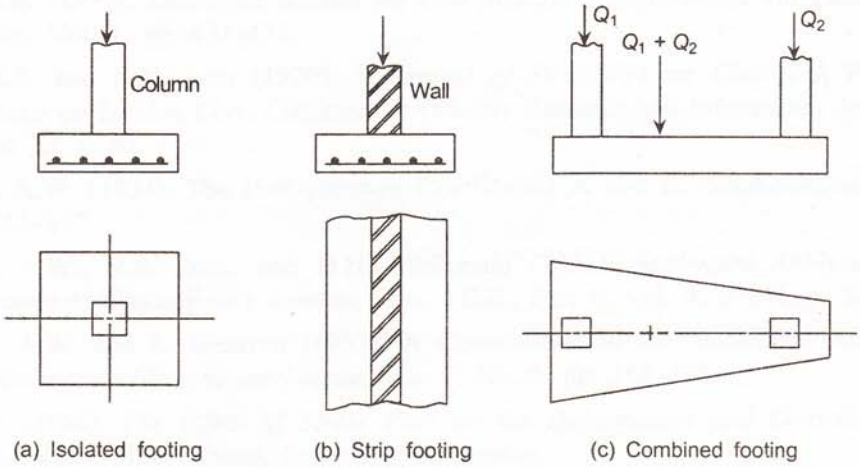


**Fig. 8.1** Isolated, strip, and combined footings.

The design of shallow foundation involves determination of:

1. depth of foundation,
2. allowable bearing pressure and size of foundation, and
3. settlement of the foundation.

## 8.2 DESIGN OF FOOTINGS

### 8.2.1 Depth of Footing

The minimum depth at which a foundation should be placed depends on the soil profile, structural requirement, ground water condition, and so on. The following factors should generally be taken into consideration in determining the depth of foundations.

(a) Depth of top soil, rubbish fill, if any.
(b) Depth of poor surface deposit such as peat, muck, or sanitary land fill.
(c) Location of ground water table and its seasonal fluctuation.
(d) Depth to poor or better underlying strata.
(e) Depth of adjacent footings if any.

If the subsoil near the ground surface consists of a heterogeneous fill of uncertain properties or compressible soil like peat, muck etc. the foundation should, preferably, be taken below the fill. Figure 8.2 is a clear representation of the same. It is also desirable that the foundation be taken below the zone of seasonal fluctuation of water table where the soil is not subjected to seasonal volume changes due to alternate wetting and drying. For this, the foundation is generally placed 1–2 m below ground surface. However, if the water table fluctuates over a great depth, it may not be economical to take the foundation to the desired level. The foundation may then be placed at some convenient depth and the design done for the highest position of the water table. The depth of foundation is also influenced by the location of underground facilities below the building. In case where a stiff clay is underlain by a softer material, the foundation should be placed as high above as possible so that the pressure bulb may be restricted within the stiff clay.

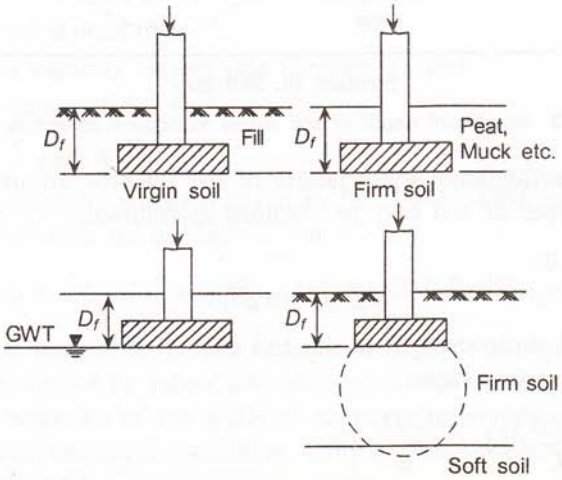


**Fig. 8.2** Depth of footing.

In sandy strata, if there is marked increase in density of sand with increasing depth, it may be tempting to take the foundation deeper than normal in order to take advantage of the higher bearing capacity. This procedure may not be economical if it involves deep excavation below the water table involving large scale dewatering. Further, there may be problems with the stability of side slopes and adjacent structures.

### 8.2.2 Allowable Bearing Capacity

The net allowable bearing pressure on footings should be determined from considerations of bearing capacity and settlement, so as to satisfy the required design criteria. The methods of bearing capacity and settlement analysis have already been described in Chapters 6 and 7.

First, it is necessary to establish the depth of soil which is significantly affected by the foundation loading. As a general rule, this depth may be taken as twice the width of footing. All the strata contained within the significant depth of soil are to be considered in the design. The relevant soil parameters for each stratum need to be evaluated from appropriate soil tests. Figure 8.3 shows typical examples of the significant depth of soil for different size of footing.

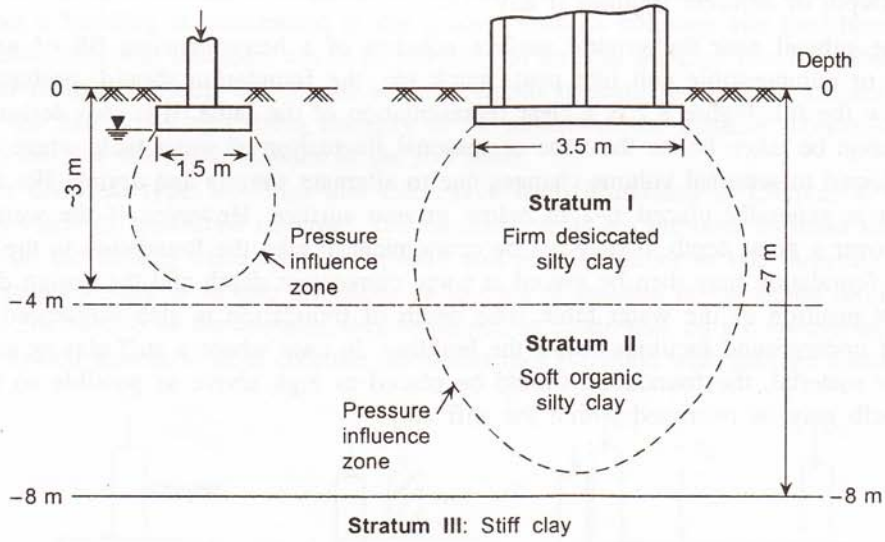


**Fig. 8.3** Significant depth of soil below foundation (pressure bulb).

Keeping under consideration shear failure of the soil, the ultimate bearing capacity of footings on different types of soil may be obtained as follows:

(a) *Cohesive soil* ($\phi = 0$)

$$q_{\text{ult}}(n) = c_u N_c \tag{8.1}$$

where, $c_u$ = undrained shear strength of the soil and

$N_c$ = bearing capacity factor

$$= 5\left(1 + \frac{0.2B}{L}\right)\left(1 + \frac{0.2D_f}{B}\right)$$

($B$ and $L$ are the width and length of footing)

The shear strength of the soil within the failure zone below the footing, that is, within a depth approximately equal to the width of footing, should be used in design. In view of the natural variation of soil properties at a building site, there is usually a wide spectrum of test results and the designer is required to exercise his judgment in selecting the design shear strength. For a stratified deposit, a weighted average shear strength may be used in design. However, it is to be realized that if the major portion of the failure surface is contained in stratum I, the bearing capacity of the foundation would be determined primarily by the undrained shear strength of stratum I. Figure 8.4 depicts a failure surface in stratified soil.

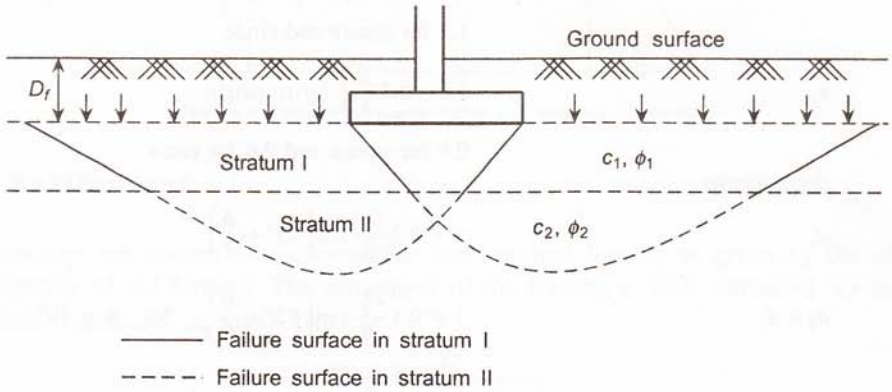


**Fig. 8.4** Failure surface in stratified soil.

(b) *Granular soils* ($c = 0$)

$$q_{ult}(n) = q(N_q - 1) + 0.5s\gamma' BN_\gamma \tag{8.2}$$

where,

$q$ = effective surcharge at the foundation level,
$\gamma'$ = effective unit weight of the soil below the foundation,
$B$ = width of foundation,
$N_q$, $N_\gamma$ = bearing capacity factors (see Chapter 6), and
$s$ = shape factor (0.5–1.0).

(c) *Soil having both c and $\phi$*

The general bearing capacity equation given in I.S. 6403—1981 may be used to determine the bearing capacity of soils having both $c$ and $\phi'$.

$$q_n = cN_c s_c d_c i_c + q(N_q - 1)s_q d_q i_q + 0.5\gamma BN_\gamma s_\gamma d_\gamma i_\gamma \tag{8.3}$$

The shape, depth, and inclination factors to be used in Eq. (8.3) are given in Table 8.1. The effect of water level should be taken into account in determining the values of $q$ and $\gamma'$. $N_c$, $N_q$, and $N_\gamma$ are functions of the angle of shearing resistance of the soil obtained from laboratory tests or from empirical correlation with the field standard penetration resistance, $N$ (for details, see Chapter 6).

**Table 8.1** Shape, depth, and inclination factors as per IS:6403—1981

| *Factors* | *Value* |
|---|---|
| *Shape factors* | |
| $s_c$ | $\left(1 + 0.2\frac{B}{L}\right)$ for rectangle |
| | 1.3 for square and circle |
| $s_q$ | $\left(1 + 0.2\frac{B}{L}\right)$ for rectangle |
| | 1.2 for square and circle |
| $s_\gamma$ | $\left(1 - 0.4\frac{B}{L}\right)$ for rectangle |
| | 0.8 for square and 0.6 for circle |
| *depth factors* | |
| $d_c$ | $1 + 0.2\frac{D_f}{B}\tan\left(45° + \frac{\phi}{2}\right)$ |
| $d_q = d_\gamma$ | $1 + 0.1\frac{D_f}{B}\tan\left(45° + \frac{\phi}{2}\right)$, for $\phi > 10°$ |
| | 1 for $\phi < 10°$ |
| *Inclination factors* | |
| $i_c = i_q$ | $\left(1 - \frac{\alpha}{90}\right)$ |
| $i_\gamma$ | $\left(1 - \frac{\alpha}{90}\right)$ $\alpha$ in degrees |

From the ultimate bearing capacity, the net allowable bearing capacity of a footing, $q_{all}(n)$, is obtained as

$$q_{all}(n) = \frac{q_{ult}(n)}{F} \tag{8.4}$$

where, $F$ = factor of safety (normally 2.5–3.0).

### 8.2.3 Effect of Ground Water Table

The effect of ground water table on the bearing capacity of shallow foundations has been discussed in Chapter 6.

The effective surcharge, $q$ at the foundation level is to be determined by using the appropriate density (bulk or submerged) of the soil above the foundation level. For ground water table coinciding with the ground surface, submerged density is to be used for the full depth of soil above foundation level. $\gamma'$ on the other hand, is the effective unit weight of the soil below the foundation. As the failure zone extends to a depth approximately equal to the width of footing, the effective unit weight within this zone is to be considered. For the water table at or above the foundation level, submerged density should be used while for the water

table at a depth greater than $B$ below the footing, bulk density is to be used. For any intermediate position of the water table, the effective unit weight may be obtained, from interpolation between $\gamma$ and $\gamma'$, as shown in Fig. 8.5.

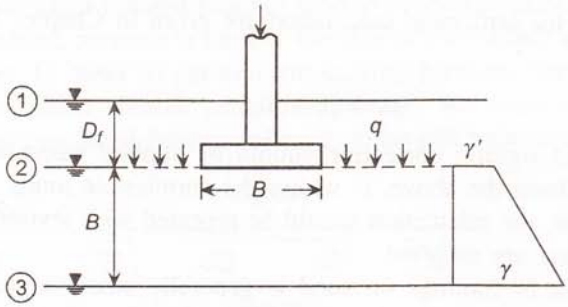


**Fig. 8.5** Effect of water table on bearing capacity.

## 8.2.4 Settlement

Trial dimensions are chosen to accommodate the required footing as given by the allowable bearing capacity of the footing. The settlement of the footing is then estimated for the actual net foundation pressure, $q_n$ given by,

$$q_n = \frac{Q}{\text{Area of footing}} \tag{8.5}$$

where $Q$ = net load on the footing.

For footings on clay,

(a) *Immediate settlement*

$$\rho_i = \frac{q_n B}{E}(1 - \nu^2) I_\rho \tag{8.6}$$

where, $q_n$ = net foundation pressure,
$B$ = width of foundation,
$E$ = modulus of elasticity of the soil within the zone of influence,
$I_\rho$ = influence coefficient, and
$\nu$ = Poisson's ratio.

(b) *Consolidation settlement*

$$\rho_c = \mu \sum \frac{C_c}{1 + e_0} H \log \frac{p_o + \Delta p}{p_o} \tag{8.7}$$

where, $C_c/(1 + e_0)$ = compressibility index of the clay,
$H$ = thickness of compressible stratum,
$p_o$ = in-situ effective overburden pressure at centre of stratum,
$\Delta p$ = increase of vertical stress at the centre of stratum due to the foundation loading, and
$\mu$ = pore-pressure correction factor.

If the coefficient of volume compressibility, $m_v$ is used, the consolidation settlement is given by

$$\rho_c = \mu \sum m_v \Delta p H \tag{8.8}$$

The detailed procedures for settlement calculation are given in Chapter 7.

(c) *Total settlement*

$$\rho_f = \rho_i + \rho_c \tag{8.9}$$

The depth correction and rigidity correction should be applied wherever applicable. If the settlement, as estimated from the above, is within the permissible limits, the foundation may be considered final. If not, the calculation should be repeated with revised footing dimensions until the settlement criteria are satisfied.

Although settlement of footings on sand is generally small, unless the sand is loose ($N < 10$)—it may be necessary to check the anticipated settlement to see if it exceeds the tolerable limits. As has been discussed in Chapter 7, the semi-empirical methods would be preferable to any theoretical analysis (See subsection 7.4.2).

Some complications arise when two different kinds of soil (say, sand and clay or vice versa) fall within the influence zone. In such cases, the settlement of the sand layer can be obtained separately and added to the settlement caused by the clay strata. There is usually no problem in determining the consolidation settlement of the relevant depth of clay strata using appropriate expressions. However, if the clay stratum is of lesser thickness than the depth of pressure bulb, the immediate settlement due to the clay layer may be overestimated. The designer may apply his judgment in evaluating the immediate settlement of individual stratum giving due importance to the relative contribution of each stratum.

## 8.2.5 Dimensioning Footing Foundations

### (a) Isolated footings

As a general rule, square footings give the most economic structural design for a given column load. In case of space restriction, it may be necessary to go for rectangular footings, as shown in Fig. 8.6.

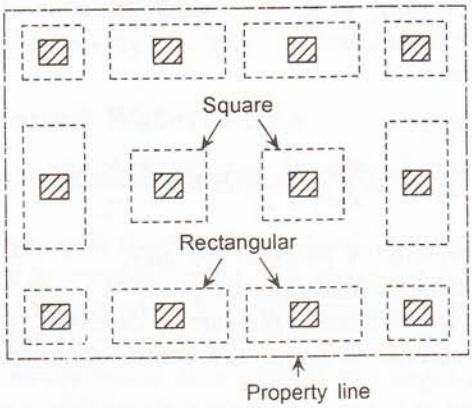


**Fig. 8.6** Square and rectangular footings.

### (b) Combined footings

Two or more columns in a building frame may be supported on a single footing, either rectangular or trapezoidal when isolated footings tend to overlap or extend beyond the property line. If the allowable bearing pressure is known, the size of the footing may be determined for a permissible settlement. In order to get uniform bearing pressure, the footing should be so proportioned that the resultant column loads pass through the centroid of the footing area. Figure 8.7 shows typical combined footings of rectangular and trapezoidal shape.

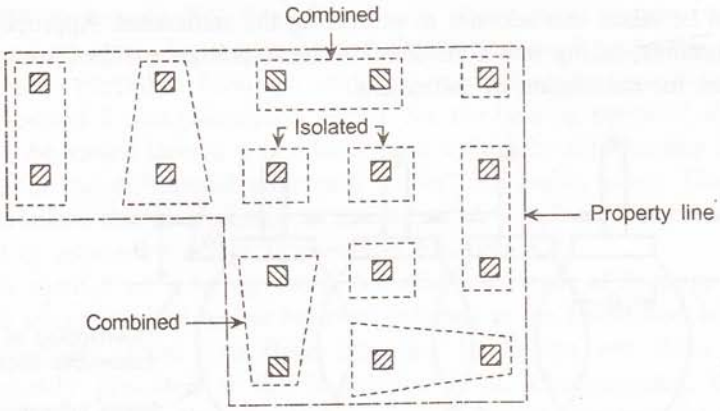


**Fig. 8.7** Combined footings.

### (c) Strip footings

Strip footings are provided below load bearing walls or a row of columns in building frame. Even if the column loads vary a little, the longitudinal extent of the footing normally ensures a uniformly distributed load below the footing. A pedestal may be provided if a singly reinforced strip footing along the width is desired below closely spaced columns. This is depicted in Fig. 8.8.

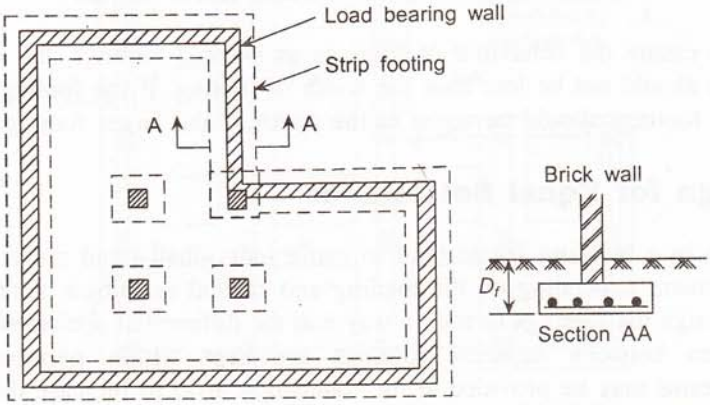


**Fig. 8.8** Strip footings.

### 8.2.6 Interference effect

When a number of closely spaced columns are required to be supported on isolated footings, the pressure bulbs under individual footings tend to overlap, as shown in Fig. 8.9. According to Boussinesq stress analysis, the pressure bulb below a footing extends to a distance of $B/2$ on either side of the footing (where $B$ is the width of footing). If two adjacent footings come to within a distance $B$ from each other, the pressure bulbs overlap and the soil below the depth, $D$ behaves as if it is loaded by a combined footing. The settlement of the footing as determined for an isolated foundation is no longer valid. The effect of superposition of stresses should be taken into account in estimating the settlement. Appropriate stress analysis for adjacent footings, taking into consideration the interference effect, may be done to obtain the soil stresses for calculation of settlement.

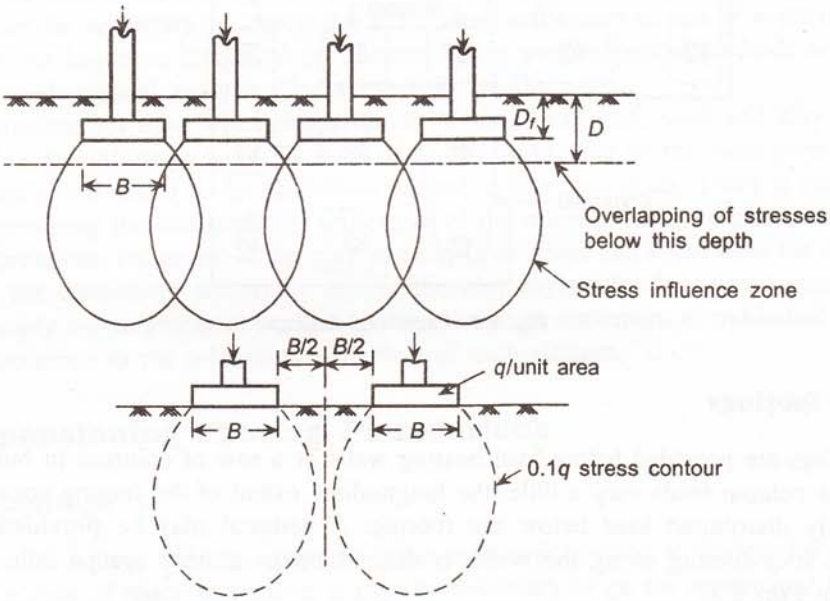


**Fig. 8.9** Interference effect in closely spaced footings.

In order to ensure the behaviour of footings as isolated footings, the spacing between adjacent footings should not be less than the width of footing. If the footing size varies, the spacing between footings should be equal to the width of the larger footing.

### 8.2.7 Design for Equal Settlement

Isolated footings in a building frame tend to settle individually and the columns undergo differential settlement depending on the loading and subsoil condition. Attempts should be made either to design the footings in such a way that the differential settlement and hence, the angular distortion between adjacent footings are kept within permissible limits or interconnected beams may be provided at the foundation level to increase the rigidity of the foundation.

The basic factors which affect the settlement of footings on a given soil are the intensity of loading and the size of the loaded area. The settlement increases in almost direct proportion to these parameters. It is a common experience that even though the foundation pressure is the same under all footings, a bowl shaped deformation trough is obtained with greater settlement at the centre than along the edges of the building mainly due to greater load in the central columns and the overlapping of stresses from adjacent footings. Hence, to produce uniform settlement, it may be necessary to adjust the pressure with size of footing, that is, to impose greater pressure under smaller footings than under larger ones and also to use larger pressure under the footings along the edge of the building. The principle was utilized in the CB1 Esplanada Building, Sao Paulo which was founded on moderately compact fine to medium sand. A pressure of 550 kN/m$^2$ was used under the outer footings and 400 kN/m$^2$ under the inner footings, with the result that the maximum differential settlement did not exceed 8 mm (Skempton, 1955). So, the bearing pressure of footings in a building frame may be varied though it is always kept within the safe bearing capacity so as to have the maximum and differential settlement within permissible limits. This may require a number of trials before the final design is arrived at. A simple calculation for achieving uniform settlement of adjacent footings is shown in Example 8.4.

A satisfactory method of reducing the differential settlement of footings in a building frame is to provide interconnected beams between columns at the foundation level. A framed structure is tied laterally, from first floor onwards, by beams and slabs but no such connection is generally provided at the foundation level. Consequently, the individual footings can settle differentially. Providing interconnected beams increases the rigidity of the foundation and differential settlement is substantially reduced. An approximate way of analysis would be to estimate the settlement of individual footings as isolated/strip footings and then to design interconnected beams to resist the bending moment at the joints due to the differential settlement. For more accurate design, theoretical analysis of the building frame may be done with predetermined sections of the interconnected beams and footings. Figure 8.10 shows a typical strip foundation with interconnected beams.

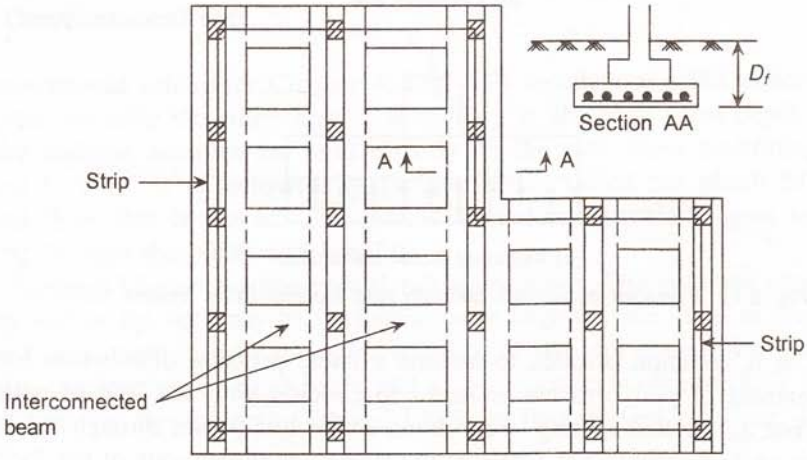


**Fig. 8.10** Strip footings with interconnected beams.

### 8.2.8 Structural Design of Footings

Structural designing of footings is mostly done by the conventional 'rigid' method. Here, the footing is assumed to be infinitely rigid so that the displacement of the footing does not affect the pressure distribution. However, in actual practice, the pressure distribution below a footing depends on the footing rigidity and the soil type. In loose sand, the soil near the edges of the footing tends to displace laterally whereas the soil towards the inside remains confined. Cohesive soil has high shear stress concentration near the edges which leads to local yielding even at high factor of safety against bearing capacity failure. Bowles (1988) indicates the probable pressure distribution beneath rigid footings for different soil types, refer Fig. 8.11.

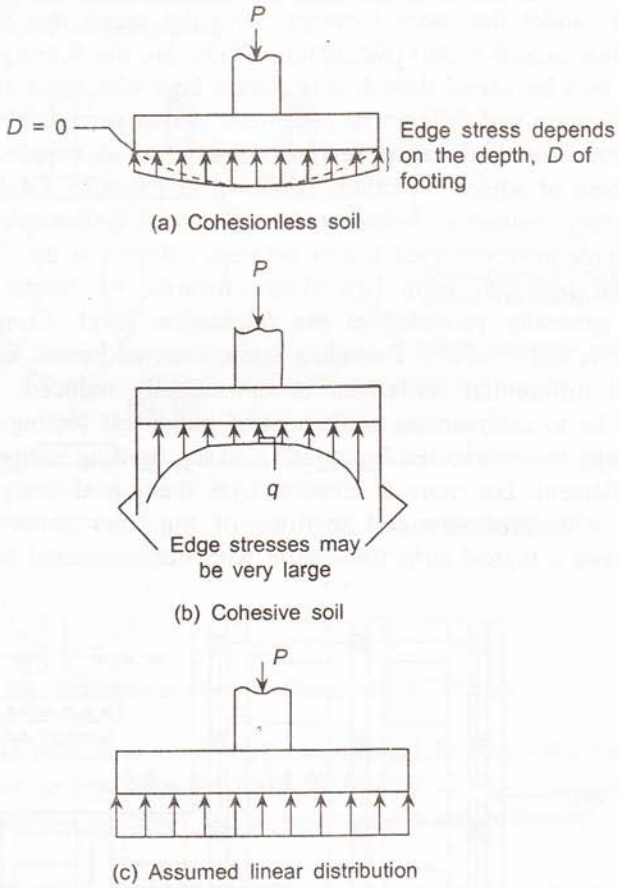


**Fig. 8.11** Pressure distribution beneath rigid footings (after Bowles 1988).

However, it is common practice to assume a linear pressure distribution for practical design. The centroid of soil pressure is made to concide with the line of action of the resultant load. For an isolated footing, the column centre line passes through the centroid of the footing area while for combined footings, the shape and dimensions of the footing are to

be determined to achieve this condition. Once the pressure distribution has been obtained for the chosen geometry of the footing, the structural design of the footing is made to resist the shear forces and bending movement for the appropriate support conditions. For isolated footings, the cantilever bending moment at the column face will normally determine the amount of reinforcement to be provided. In case of combined footings, the design is a simply supported beam with overhang on both sides while a strip footing is designed as a continuous beam with support at the column locations.

## 8.3 DESIGN OF RAFT FOUNDATION

A raft foundation usually covers the entire area of the building, thereby distributing the total load to a larger area than a footing foundation and reduces the bearing pressure to a minimum. The choice between a raft and a footing foundation depends on the soil properties and the weight of the building. If a preliminary design with footing foundations reveals that the sum of the footing areas required to support the structure exceeds 60% of the total building area, a raft foundation covering the entire area of the building should be preferred. Moreover, where the soil properties vary largely throughout the site, the amount of differential settlement may be excessive for a footing foundation, but with a raft foundation the effect of weak zones scattered at random tend to even out. Therefore, the settlement pattern is less erratic and the differential settlement is also reduced considerably. Also, a raft foundation provides increased rigidity which reduces the differential movement of the superstructure.

### 8.3.1 Types of Raft Foundation

Two types of raft foundation are in common use which form a subject matter of discussion in this subsection.

#### (a) Conventional raft

In conventional raft (refer Chapter 4, Fig. 4.7) foundation, a flat concrete slab of uniform thickness covering the entire area of a building is placed at some depth beneath the ground surface and the columns are built directly on the raft. Then backfilling is done upto the ground level. This is followed by further filling, called the plinth filling, on which the ground floor slab is placed. The ground floor load, therefore, goes to the raft by direct bearing through the plinth and backfill.

Figure 8.12 shows some typical raft foundations. The columns may be placed directly on the slab or the slab may be thickened under large column loads to give sufficient strength against shear and support moment. Rigidity of the raft foundation may be increased by cellular construction or rigid beam and slab construction. Figure 8.13 shows a simple raft foundation for the fourteen-storeyed block of flats at Golden Lane, London (Skempton, 1955).

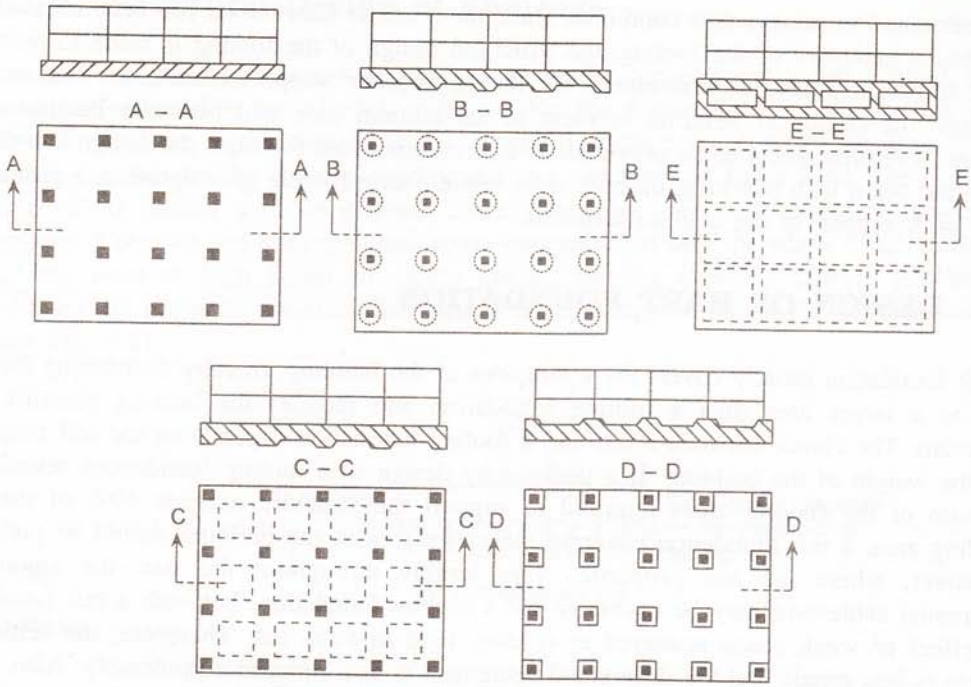


**Fig. 8.12** Typical raft foundations.

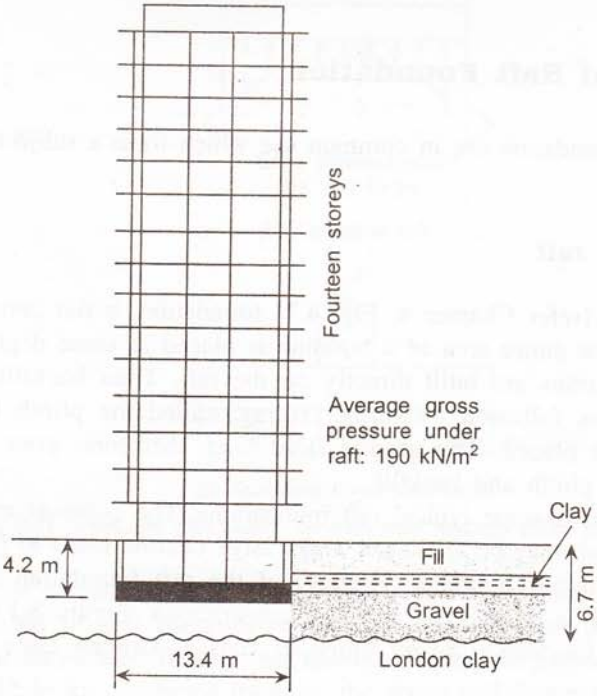


**Fig. 8.13** Raft foundation for Golden Lane flats, London (Skempton, 1955).

**(b) Buoyancy raft foundation**

With the increased number of tall buildings now being built for various commercial and residential purposes, raft foundations have been coveniently combined with the principle of floatation. Buoyancy rafts (refer Chapter 4, Fig. 4.8), with or without basement, are placed at some depth beneath the ground surface, but no backfilling is done on the raft. A structural slab is made, usually a little above the ground level to serve as the ground floor of the building. The space between the ground floor slab and the raft is kept void such that the net foundation pressure gets reduced and remains within the permissible bearing pressure on the foundation.

That is,

$$q_{net} = q_{gross} - \gamma D_f \tag{8.10}$$
$$< q_{all}(n)$$

where, $q_{gross}$ = gross foundation pressure,
$\gamma D_f$ = total overburden pressure at the foundation level, and
$q_{all}(n)$ = net permissible bearing pressure.

When a buoyancy raft has sufficient head room below the ground floor slab, the space may be utilized as a basement floor below the ground. Although a basement is, in effect, a buoyancy raft, it is not necessarily designed for the purpose. The main function of a basement is to provide additional floor space in the building and the fact that it reduces the net bearing pressure may be quite incidental. A buoyancy raft may, however, be designed solely for the purpose of providing support to the structure and to reduce the total and differential settlements within permissible limits.

## 8.3.2 Bearing Capacity

The mechanism of bearing capacity failure of raft foundation is similar to that of footings, except that the former involves a much bigger and deeper zone of failure.

The net ultimate bearing capacity of a raft foundation $q_{ult}(n)$ is, therefore, given by the same expressions as or footings, as illustrated by Eqs. (8.1)–(8.3). However, raft foundations being much larger than footings, the pressure bulb as well as the failure surface extend to considerable depth below the foundation. A typical raft foundation on normal Calcutta soil is shown in Fig. 8.14. As seen, more than one stratum with different shear parameters are involved. A weighted average strength or the strength or the most predominant stratum within the failure zone may be used to determine the bearing capacity.

## 8.3.3 Settlement

The immediate and consolidation settlements of raft foundations on clay are obtained in the same manner as for footings, see Eqs. (8.5) and (8.6). The compression of all the strata within the significant depth below the foundation are to be calculated separately and the summation of all these settlements will give the total settlement of the foundation. Use of Eq. (8.6) to calculate the immediate settlement presumes that the subsoil behaves as homogeneous, isotropic, elastic medium. In case of non-homogeneous/stratified deposit, this is somewhat approximate, but is often accepted for practical purposes. More rigorous analysis, taking into account the variation of subsoil properties, can also be done. Depth correction is not significant for raft

foundations because of small $D_f/B$ ratio but rigidity correction is generally applicable. Pore-pressure correction is to be applied giving due weightage to the contribution of the most significant layers in the settlement calculation.

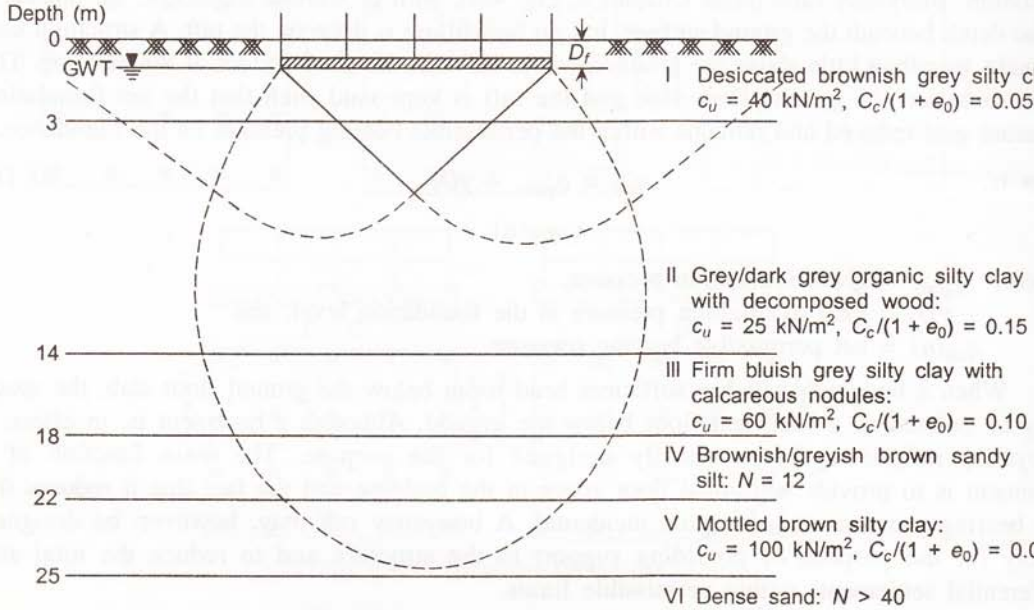


**Fig. 8.14** Bearing capacity of raft foundation.

## 8.3.4 Floating Foundation

A *floating foundation* is a particular case of buoyancy raft foundation where the net foundation pressure is zero, that is

$$q_{net} = q_{gross} - \gamma D_f \tag{8.11}$$
$$= 0$$

This condition can be achieved by excavating the soil to such a depth that the weight of soil removed is equal to the weight of the building, including that of the substructure. This principle can be adopted to construct even multistorey buildings on very soft clay by taking the foundation to the desired depth and providing one or more basement floors below the ground surface.

Though examples of fully floating foundation (i.e., zero net pressure) are often found, it is only in exceptional cases that such a foundation is necessary. An excellent example of almost a fully buoyant foundation is the New England Mutual Life Insurance Building in Boston, Massachussets (Casagrande and Fadum, 1942). The building covers an area of 104 m × 61 m and consists of one 10-storey section with two 2-storey and two 4-storey sections to be supported on a soil containing 21 m of very soft Boston blue clay. The construction of a 10.7 m basement has been found to be extremely successful even with such differential loading. Out of a total settlement of 62.5 mm (including the resettlement of the heaved soil), more than 35 mm occurred during construction of foundation. The long-term

settlements due to consolidation of the clay were reduced as can be seen from the very flat slope of the settlement curve in Fig. 8.15.

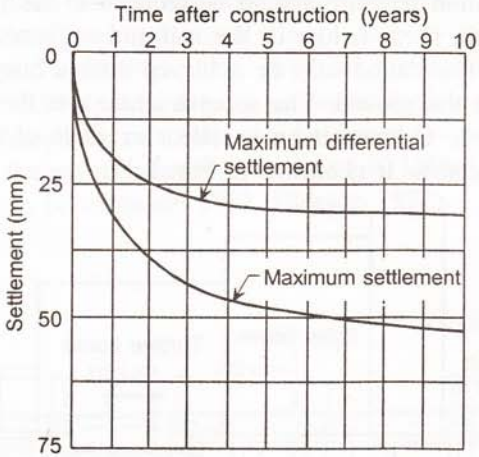


**Fig. 8.15** Settlement of Liberty Mutual Life Insurance Building, Boston (Casagrande and Fadum, 1942).

In the high Paddington project, a thirty four-storey building was built on overconsolidated London clay by providing a 18 m basement which reduced the foundation pressure to 100 kN/m$^2$ while the gross pressure remained 425 kN/m$^2$. This is depicted through Fig. 8.16. The construction of a box type foundation provides extra stiffness to the structure which reduces the chance of excessive differential settlement (Skempton, 1955).

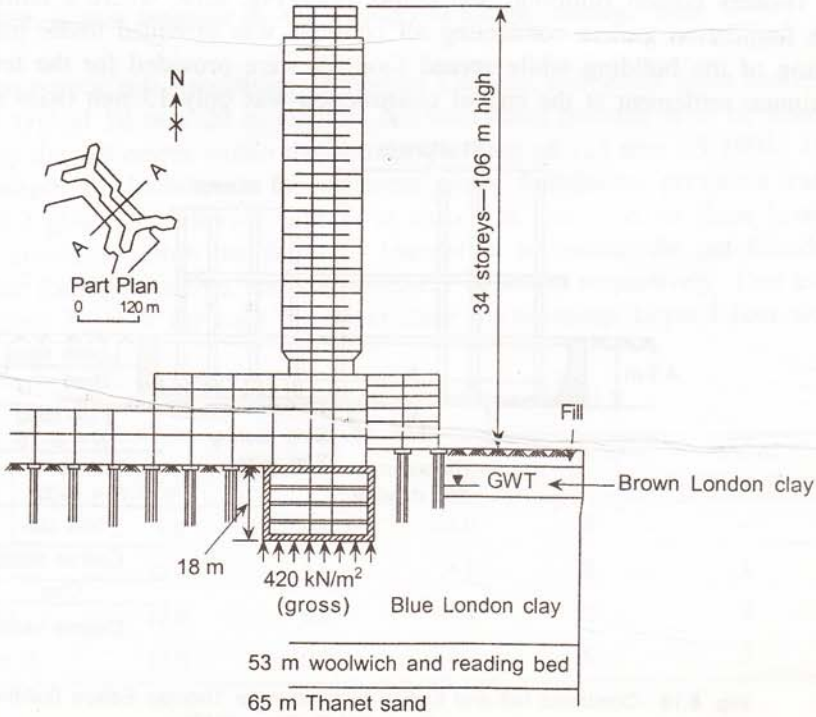


**Fig. 8.16** Buoyancy raft foundation for High Paddington Project (Skempton, 1955).

Glossop (1972) indicated two types of floating foundations depending on whether floatation is required to reduce the settlement or to prevent shear failure of the subsoil. In either case, the net foundation pressure should be reduced to such an extent that the design criteria with respect to both, shear failure of the soil and settlement, are satisfied.

Increased rigidity of foundation may be achieved with a buoyancy raft by providing a cellular construction below the ground. The superstructure and the cellular raft provided for the Cossipore Power Station, Calcutta is an excellent example of a near floating foundation on soft normal Calcutta deposit. It is shown in Fig. 8.17.

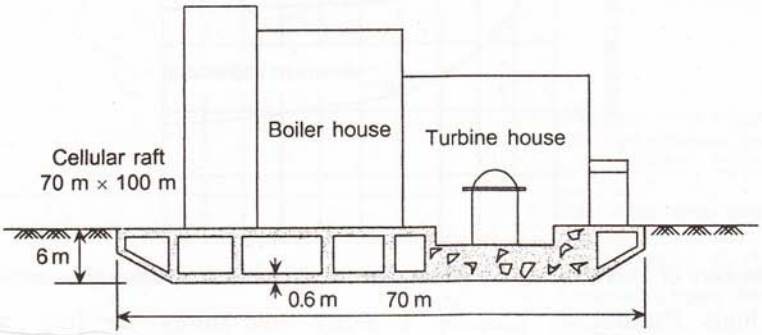


**Fig. 8.17** Cellular raft foundation for Cossipore Power Station, Calcutta (Skempton, 1955).

When the height of a building varies, it is possible to combine rafts under the heavier part with footings under the lighter part of the building. A good example of this is found in the Thomas Edison Building, Sao Paulo, refer Fig. 8.18, where a reinforced concrete mat with foundation girders connecting all columns was provided under the twenty one-storey section of the building while spread footings were provided for the ten-storey block. The maximum settlement at the end of construction was only 15 mm (Rios and P. Silva, 1948).

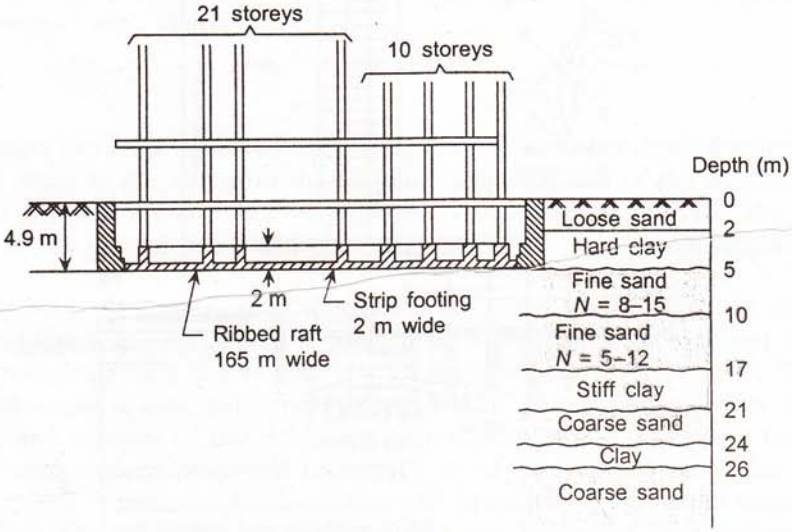


**Fig. 8.18** Combined raft and footing foundation for Thomas Edison Building, Sao Paulo (Rios and P. Silva, 1948).

### 8.3.5 Basement Raft

Buoyancy raft foundation can be conveniently used to provide basements for multistorey buildings in soft clay. This gives additional floor space to a building but requires no additional ground coverage. Depending on the depth of foundation multiple basements may be accommodated. Figure 8.19 depicts Albany telephone building in New York which was founded on a 7 m deep buoyancy raft with two basement floors. The subsoil consisted of sensitive plastic clay. But the net foundation pressure of 40 kN/m$^2$ restricted the settlement of the building to only 60 mm (Casagrande 1932, Glossop 1972).

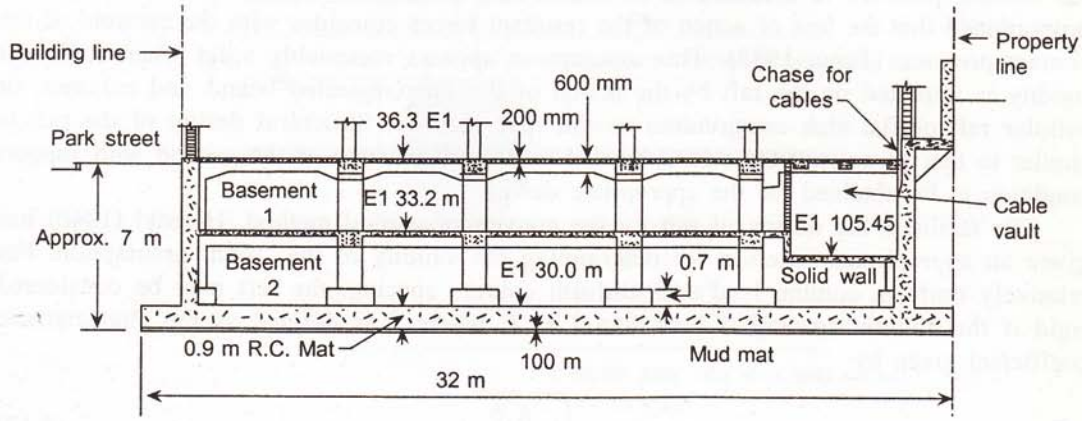


**Fig. 8.19** Multiple basement for Albany telephone building (Glossop, 1972).

Analysis of buoyancy raft foundation in normal Calcutta soil gives some interesting observations. For a typical 10 m × 20 m raft, the net foundation pressure is to be restricted to 40 kN/m$^2$ to keep the settlement within the permissible limit of 125 mm (IS 1904 : 1966). Accordingly, the depth of foundation for different gross foundation pressures can be calculated. Table 8.2 gives the relevant data. It is clear that one, two, or three levels of basement may be provided within the depth of foundation to restrict the net foundation pressure to 40 kN/m$^2$ for eight, twelve, and sixteen-storey buildings respectively. That means, four upper storeys can be built for each basement floor for buildings beyond four storeys high.

**Table 8.2** Depth of basement in normal Calcutta soil

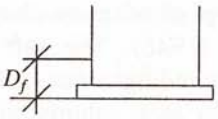


$q_{net} = q_{gross} - \gamma D_f$

$= q_{gross} - 1.8\, D_f$

| $q_{gross}$ (t/m$^2$) | $D_f$(m) | $q_{net}$ (t/m$^2$) | *No. of storeys* | *No. of basement floors* |
|---|---|---|---|---|
| 4.0 | — | 4.0 | 4 | — |
| 10.0 | 3.3 | 4.1 | 8 | 1 |
| 16.0 | 6.6 | 4.1 | 12 | 2 |
| 22.0 | 10.0 | 4.0 | 16 | 3 |

### 8.3.6 Structural Design of Raft Foundation

A raft foundation can be structurally designed in the same way as the reinforced concrete floors of a framed building. However, in a foundation raft, the floor is inverted so that its dead weight can be subtracted from the upward soil reaction.

#### (a) Rigid method

Raft foundations are mostly designed by the rigid method. This assumes the raft to be fully rigid and ensures that the deflection of the raft does not affect the soil contact pressure. Also, the contact pressure is assumed to be distributed on a plane surface and the raft is so proportioned that the line of action of the resultant forces coincides with the centroid of the contact pressure (Teng, 1972). This assumption appears reasonably valid when sufficient rigidity is imparted on the raft by the action of the interconnected beams and columns, or cellular raft or flat slab construction as the case may be. Structural design of the raft is similar to that of an inverted slab subjected to upward reaction of the ground with support condition to be obtained for the appropriate design.

To facilitate the design of raft by the conventional rigid method, Hetenyi (1946) has given an approximate criterion for determining the validity of the 'rigid' assumption. For relatively uniform column load and uniform column spacing, the raft may be considered rigid if the column spacing is less than $1.75/\lambda$, where $\lambda$ is defined as the characteristic coefficient given by

$$\lambda = \sqrt{4\frac{K_s b}{4E_c I}} \tag{8.12}$$

where,

$K_s$ = coefficient of subgrade reaction (pressure required to cause unit displacement),
$b$ = width of a strip of raft between centres of adjacent bays,
$E_c$ = modulus of elasticity of concrete, and
$I$ = moment of inertia of the strip of width $b$.

#### (b) Elastic method

In the simplified elastic method, the soil is assumed to consist of infinite number of elastic springs each acting independently. The Winkler model is considered valid. The springs are assumed to be able to resist both tension and compression while the soil deformation is considered proportional to the pressure. The elastic constant of the springs is determined by the coefficient of subgrade reaction of the soil (defined as the unit pressure required to produce unit settlement). The analysis is carried out following the concept of beam on elastic foundation, the rigorous analysis for which was done by Hetenyi (1946). The raft is considered as a plate and the column loads are distributed in the surrounding areas in the zone of influence. The bending moment and shear force are calculated for each column point and the data are superimposed to obtain the moment and shear for the raft foundation. American Concrete Institute has recommended a procedure for design (ACI 1966, 1988). Computer programs are now available to carry out the complex mathematical calculations for

practical use. Finite element formulation can also be used to work out a computer program. Given the scope of this book, the details are not discussed here.

**Example 8.1**

An isolated column in a building frame, with a column grid of 3.5 m × 3.5 m carries a superimposed load of 450 kN. The subsoil condition is shown in Fig. 8.20. Design a suitable square footing for the column.

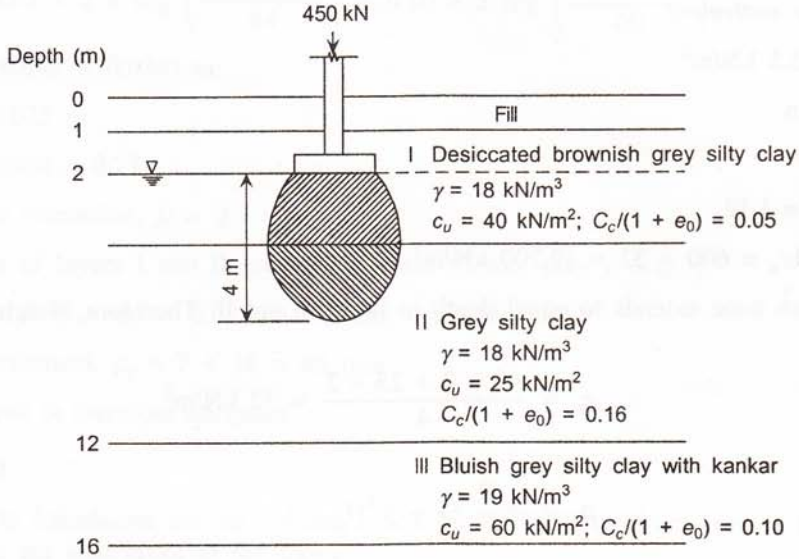


**Fig. 8.20** Subsoil condition for Example 8.1.

Given superimposed load = 450 kN

Take footing size = 2 m × 2 m

$$q_{net} = \frac{450}{2 \times 2} = 112.5 \text{ kN/m}^2$$

Place foundation below fill and at depth of G.W.T. i.e.

$$D_f = 2 \text{ m}$$

***Solution***

(a) *Bearing capacity*

$$N_c = 5\left(1 + 0.2\frac{B}{L}\right)\left(1 + 0.2\frac{D_f}{B}\right)$$

$$= 7.2$$

Failure surface lies in stratum I. Hence, take $c_u = 40$ kN/m².

Cohesive soil: $q_{ult}(n) = c_u N_c$

$$= 40 \times 7.2$$

$$= 288 \text{ kN/m}^2$$

$$Fs = \frac{288}{112.5} = 2.56 > 2.5$$

(b) *Immediate settlement*

$q_u = 112.5 \text{ kN/m}^2$

$B = 2 \text{ m}$

$\nu = 0.5$

$I_{\rho(\text{centre})} = 1.12$

$E = 600 c_u = 600 \times 32 = 19{,}200 \text{ kN/m}^2$

Stress influence zone extends to equal depth in layers I and II. Therefore, weighted average is

$$\therefore \quad c_u = \frac{40 \times 2 + 25 \times 2}{4} = 32 \text{ kN/m}^2$$

and

$$\rho_i = \frac{q_n B}{E}(1 - \nu^2) I_\rho$$

$$= \frac{112.5 \times 2}{19{,}200} \times 0.75 \times 1.12$$

$$= 0.0098 \text{ m}$$

Depth correction:

$$\frac{D}{\sqrt{LB}} = \frac{2}{\sqrt{2 \times 2}} = 1$$

and

$$\frac{L}{B} = 1$$

$\therefore$ Correction factor = 0.73

$\therefore$ $(\rho_i)_{corr} = 0.73 \times 0.0098 = 0.007 \text{ m} = 7 \text{ mm}$

(c) *Consolidation settlement*

$$\rho_c = \sum \frac{C_c}{1 + e_0} H \log \frac{p_o + \Delta p}{p_o}$$

Influence zone extends to depth of 4 m below footing, that is, 2 m in stratum I and 2 m in stratum II. Hence, consider settlement due to both.

At A: $p_o = 18 \times 2.0 + 8 \times 1.0 = 44 \text{ kN/m}^2$

$\Delta p$ (for $Z/B = 1/2$) $= 0.6 \times 112.5 = 67.5 \text{ kN/m}^2$

At B: $p_o = 18 \times 2.0 + 8 \times 2.0 + 8 \times 1.0 = 60 \text{ kN/m}^2$

$\Delta p$ (for $Z/B = 3/2$) $= 0.15 \times 112.5 = 16.9 \text{ kN/m}^2$

$$\therefore \quad \rho_c = 0.05 \times 2 \times \log\left(\frac{44 + 67.5}{44}\right) + 0.16 \times 2 \log\left(\frac{60 + 16.9}{60}\right)$$

$$= (0.041 + 0.034) \text{ m}$$

$$= 0.075 \text{ m}$$

Depth correction = 0.73

Pore-pressure correction, $\mu = 0.7$

(Contribution of layers I and II are nearly equal. Hence, take $\mu = 0.7$)

$\therefore \quad (\rho_c)_{\text{corr}} = 0.73 \times 0.7 \times 0.075 = 0.038 \text{ m} = 38 \text{ mm}$

$\therefore$ Total settlement, $\rho_f = 7 + 38 = 45$ mm

The foundation is therefore adequate

**Example 8.2**

Design a strip foundation for the column row C in the building frame shown in Fig. 8.21. The soil data are also given in the figure.

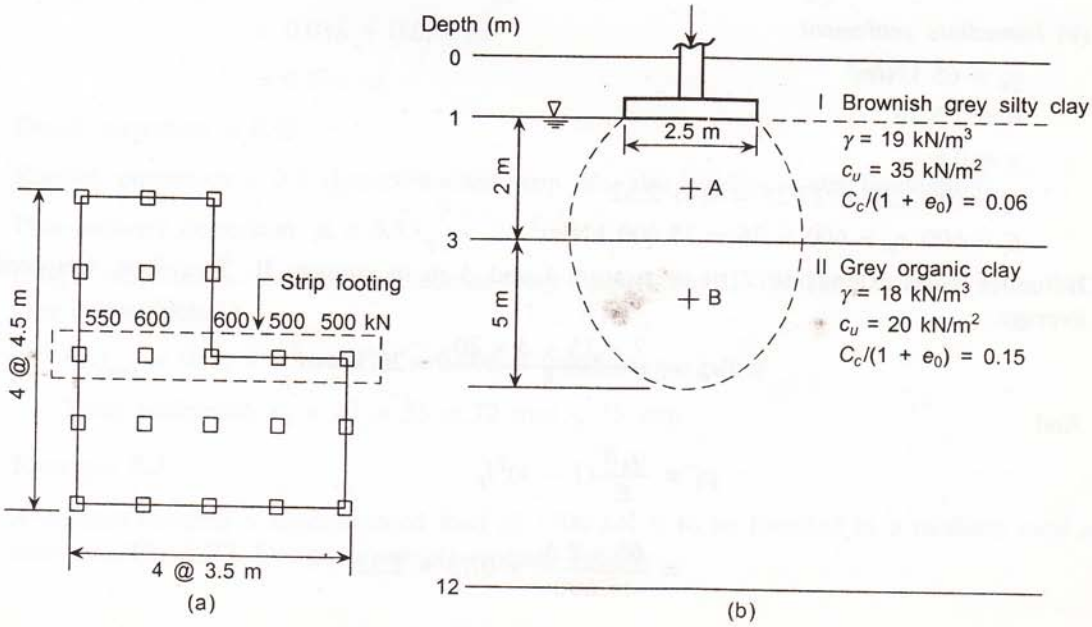


**Fig. 8.21** Building frame (Example 8.2).

Total load, $Q_{net}$ = 550 + 600 + 600 + 500 + 500 = 2750 kN

Take footing of size = 17 m × 2.5 m

(that is, extend length of footing by 1.5 m beyond outermost columns)

$$\therefore \quad q_{net} = \frac{2750}{17 \times 2.5} = 65 \text{ kN/m}^2$$

***Solution***

(a) *Bearing capacity*

$$N_c = 5\left(1 + 0.2\frac{D_f}{B}\right)\left(1 + 0.2\frac{B}{L}\right)$$

$$= 5\left(1 + 0.2\frac{1}{2.5}\right)\left(1 + 0.2\frac{2.5}{17}\right)$$

$$= 5.6$$

$$\therefore \quad q_{ult}(n) = c_u N_c$$

$$= 35 \times 5.6$$

$$= 196 \text{ kN/m}^2$$

Failure zone is restricted in stratum I. Hence, take $c_u$ of stratum I.

$$Fs = \frac{196}{65} = 3.0 > 2.5$$

(b) *Immediate settlement*

$q_n$ = 65 kN/m$^2$

$B$ = 2.5 m

$\nu$ = 0.5

$I_\rho$ = (for $L/B$ = 17/25 = 6.8) 2.32

$E$ = 600 $c_u$ = 600 × 26 = 15,600 kN/m$^2$

Influence zone extends to 2 m in stratum I and 3 m in stratum II. Therefore, weighted average,

$$c_u = \frac{2 \times 35 + 3 \times 20}{5} = 26 \text{ kN/m}^2$$

And

$$\rho_i = \frac{q_n B}{E}(1 - \nu)^2 I_\rho$$

$$= \frac{65 \times 2.5}{15{,}600} \times 0.75 \times 2.32$$

$$= 0.018 \text{ m}$$

Depth correction:

$$\frac{L}{B} = \frac{17}{2.5} = 6.8$$

$$\frac{D}{\sqrt{LB}} = \frac{1.5}{\sqrt{2.5 \times 1.7}} = 0.23$$

∴ Correction factor = 0.95

∴ $(\rho_i)_{corr} = 0.95 \times 0.018 = 0.017 \text{ m} = 17 \text{ mm}$

(c) *Consolidation settlement*

$$\rho_c = \sum \frac{C_c}{1 + e_0} H \log \frac{p_o + \Delta p}{p_o}$$

Two layers (I and II) are involved in the pressure influence zone.

At A: $p_o = 19 \times 1.0 + 9 \times 1.0 = 28 \text{ kN/m}^2$

$\Delta p$ [for $Z/B = 1.6/2.5 = 0.4$] $= 0.85 \times 65 = 55.2 \text{ kN/m}^2$

At B: $p_o = 19 \times 1.0 + 9 \times 2.0 + 8 \times 1.5 = 49 \text{ kN/m}^2$

$\Delta p$ (for $Z/B = 3.5/2.5 = 1.4$) $= 0.42 \times 65 = 27.3 \text{ kN/m}^2$

$$\therefore \quad \rho_c = 0.04 \times 2 \log \frac{28 + 55.2}{28} + 0.15 \times 2 \log \frac{49 + 27.3}{49}$$

$$= 0.038 + 0.058 \text{ m}$$

$$= 0.096 \text{ m}$$

Depth correction = 0.95

Rigidity correction = 0.8 (Interconnected strip provides rigidity to the foundation)

Pore-pressure correction, $\mu = 0.75$

(Major contribution to settlement comes from strata I and II. Hence, $\mu$ correction for N.C. clay is considered.)

∴ $(\rho_c)_{corr} = 0.95 \times 0.8 \times 0.75 \times 0.096 = 0.055 \text{ m} = 55 \text{ mm}$

∴ Total settlement, $\rho_f = 17 + 55 = 72 \text{ mm} < 75 \text{ mm}$

**Example 8.3**

A column carrying a superimposed load of 1500 kN is to be founded in a medium sand as shown in Fig. 8.22. Design a suitable isolated footing.

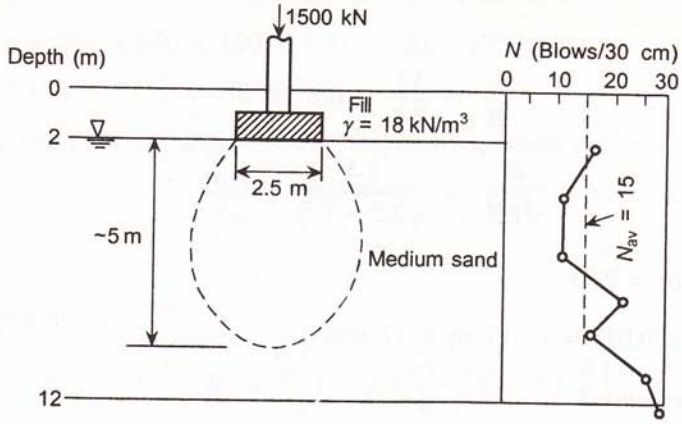


**Fig. 8.22** Example 8.3.

Average $N$ value, $N_{av} = 15$

$$\phi' = 34° \text{ (Eq. (2.5))}$$

$$N_q = 30$$

$$N_\gamma = 41$$

$$Q_{net} = 1500 \text{ kN/m}^2$$

Assume footing size = 2.5 m × 2.5 m

$$\therefore \quad q_{net} = \frac{1500}{2.5 \times 2.5} = 240 \text{ kN/m}^2$$

***Solution***

(a) *Bearing capacity*

$$s_q = 1.2;\ s_\gamma = 0.8;\ d_q = d_\gamma = 1.15;\ i_q = i_\gamma = 1.0$$

$$q_{ult}(n) = q(N_q - 1)s_q d_q i_q + 0.5\gamma B N_\gamma s_\gamma d_\gamma i_\gamma$$

$$= [18 \times 2(30 - 1) \times 1.2 \times 1.15 \times 1.0] + (0.5 \times 9 \times 2.5 \times 41 \times 0.8 \times 1.15 \times 1.0)$$

$$= 1440 + 424$$

$$= 1864 \text{ kN/m}^2$$

$$Fs = \frac{1864}{240} = 7.8 > 2.5$$

(b) *Settlement*

Considering single layer of 5 m depth

$$\delta = \frac{2.3 p_o}{E} H \log \frac{p_o + \Delta p}{p_o}$$

$$p_o = 18 \times 2 + 9 \times 2.5 = 58.5 \text{ kN/m}^2$$

$$\Delta p = (\text{for } Z/B = 1.0) = 0.35 \times 240 = 84 \text{ kN/m}^2$$

$$E = 39 + 4.5 \times 15 = 1065 \text{ kg/cm}^2 = 10{,}650 \text{ kN/m}^2 \text{ (refer Eq. (2.6))}$$

$$\therefore \quad \delta = \frac{2.3 \times 58.5}{10{,}650} \times 5 \log \frac{58.5 + 84}{58.5}$$

$$= 0.024 \text{ m}$$

$$= 24 \text{ mm}$$

**Example 8.4**

Three columns in a building frame spaced 4 m apart carry vertical superimposed loads of 500 kN, 720 kN and 600 kN. Design suitable isolated footings for the columns for equal settlement. Subsoil condition is shown in Fig. 8.23.

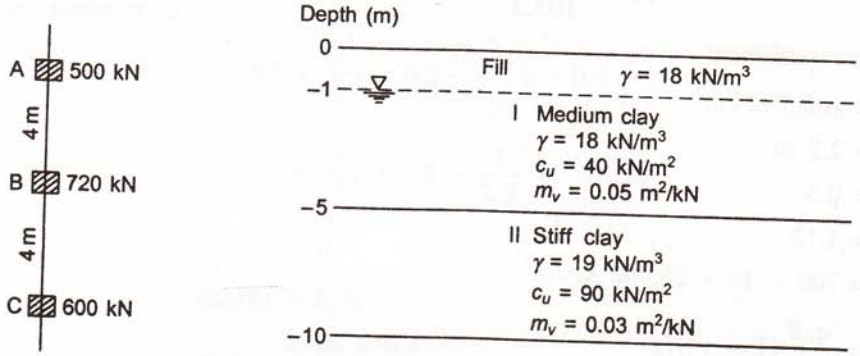


**Fig. 8.23** Subsoil condition (Example 8.4).

***Solution***

Approximate $q_{ult}(n)$ of stratum I

$$= c_u N_c$$

$$= 40 \times 6.0 = 240 \text{ kN/m}^2$$

$$q_{all}(n) = \frac{240}{2.5} = 96 \text{ kN/m}^2 \text{ (for } Fs = 2.5)$$

Choosing approximate footing size accordingly and carrying out detailed analysis,

**Column A**

Take footing size = 2.2 m × 2.2 m

Area = 4.84 m²

$$q_{net} = \frac{500}{4.84} = 103.3 \text{ kN/m}^2$$

(a) *Bearing capacity*

Failure surface in layer I: Take $c_u = 40$ kN/m$^2$

$$N_c = 5\left(1 + 0.2\frac{D_f}{B}\right)\left(1 + 0.2\frac{B}{L}\right)$$

$$= 5\left(1 + 0.2 \times \frac{1}{2.2}\right)(1 + 0.2 \times 1)$$

$$= 6.55$$

$$q_{ult}(n) = c_u N_c$$

$$= 40 \times 6.55$$

$$= 262 \text{ kN/m}^2$$

$$Fs = \frac{262}{103.3} = 2.54 > 2.5$$

(b) *Immediate settlement*

$q_n = 103.3$ kN/m$^2$

$B = 2.2$ m

$\nu = 0.5$

$I_\rho = 1.12$

$E = 700 \times 40 = 28{,}000$ kN/m$^2$

$$\rho_i = \frac{q_n B}{E}(1 - \nu^2)I_\rho$$

$$= \frac{103.3 \times 2.2}{28{,}000} \times 0.75 \times 1.12$$

$$= 0.007 \text{ m}$$

Depth correction:

$$\frac{D}{\sqrt{LB}} = \frac{1}{2} = 0.5$$

$$\frac{L}{B} = 1.0$$

$\therefore$ Correction factor = 0.85

$\therefore$ $(\rho_i)_{corr} = 0.007 \times 0.85 = 0.006$ m = 6 mm

(b) *Consolidation settlement*

$$\rho_c = \Sigma m_v \Delta p H$$

At A: $p_o = 18 \times 1.0 + 8 \times 2.2 = 35.6$ kN/m$^2$

$\Delta p$ (for $Z/B = 1$) $= 0.35 \times 103.3 = 36$ kN/m$^2$

$$\therefore \quad \rho_c = m_v \Delta p H$$

$$= 0.05 \times 36.5 \times 4.4 = 0.080 \text{ m}$$

.0005

Depth correction = 0.85

Pore-pressure correction = 0.7

$$\therefore \quad (\rho_c)_{\text{corr}} = 0.85 \times 0.7 \times 0.08 = 0.048 \text{ m} = 48 \text{ mm}$$

$$\therefore \quad \rho_f = 6 + 48 = 54 \text{ mm}$$

**Column B**

Take footing size of 3 m × 3 m

$$\text{Area} = 9 \text{ m}^2$$

$$\therefore \quad q_{\text{net}} = \frac{720}{9} = 80 \text{ kN/m}^2$$

(a) *Bearing capacity*

$$N_c = 5\left(1 + 0.2\frac{D_f}{B}\right)\left(1 + 0.2\frac{B}{L}\right)$$

$$= 5\left(1 + 0.2 \times \frac{1}{2.9}\right)(1 + 0.2)$$

$$= 6.4$$

$$q_{\text{ult}}(n) = c_u N_c$$

$$= 40 \times 6.4$$

$$= 256 \text{ kN/m}^2$$

$$Fs = \frac{256}{80} = 3.2$$

(b) *Immediate settlement*

$$q_n = 89 \text{ kN/m}^2$$

$$B = 28 \text{ m}$$

$$\nu = 0.5$$

$$I_{\rho(\text{centre})} = 1.12$$

$$c_u = \frac{40 \times 4 + 2 \times 80}{6}$$

$$= 53 \text{ kN/m}^2$$

Influence zone extends approximately to 4 m in stratum I and 2 m in stratum II. Therefore, weighted average taken is

$$E = 700 \times 53 = 37{,}000 \text{ kN/m}^2$$

$$\rho_i = \frac{q_n B}{E}(1 - \nu^2) I_\rho$$

$$= \frac{80 \times 3}{37{,}000} \times 0.75 \times 1.12$$

$$= 0.0054$$

Depth correction:

$$\frac{L}{B} = 1$$

$$\frac{D}{\sqrt{LB}} = 0.33$$

$\therefore$ Correction factor = 0.9

$\therefore$ $(\rho_i)_{\text{corr}} = 0.9 \times 0.0054 = 0.005 \text{ m} = 5 \text{ mm}$

Consolidation settlement

$$\rho_c = \sum m_v \Delta p H$$

$$= (0.05 \times 4 \times 36.8) + (0.03 \times 2 \times 9.6)$$

for point A ($Z/B = 0.66$), $\Delta p = 0.46 \times 80 = 36.8 \text{ kN/m}^2$

$$= 0.074 + 0.006$$

for point B ($Z/B = 1.67$), $\Delta p = 0.12 \times 80 = 96 \text{ kN/m}^2$

$$= 0.080 \text{ m}$$

Depth correction = 0.9

Pore-pressure correction = 0.7

$\therefore$ $(\rho_i)_{\text{corr}} = 0.9 \times 0.7 \times 0.086 = 0.050 \text{ m} = 50 \text{ mm}$

$\therefore$ $\rho_f = 5 + 50 = 55 \text{ mm}$

**Column C**

Take footing size of 2.5 m × 2.5 m, and

$$\text{area} = 6.25 \text{ m}^2$$

$$\therefore \quad q_{\text{net}} = \frac{600}{6.25} = 96 \text{ kN/m}^2$$

*Settlement*

By similar calculation as in the previous parts,

$$\rho_i = 5 \text{ mm}$$

$$\rho_c = 50 \text{ mm}$$

$$\rho_f = 5 + 50 = 55 \text{ mm}$$

| *Column* | *Footing size* (m × m) | $q_{net}$ (t/m$^2$) | *Settlement* (mm) |
|---|---|---|---|
| A | 2.2 × 2.2 | 10.3 | 54 |
| B | 3.0 × 3.0 | 8.3 | 55 |
| C | 2.5 × 2.5 | 9.6 | 55 |

**Example 8.5**

Design a raft foundation for the buildings shown in Fig. 8.24.

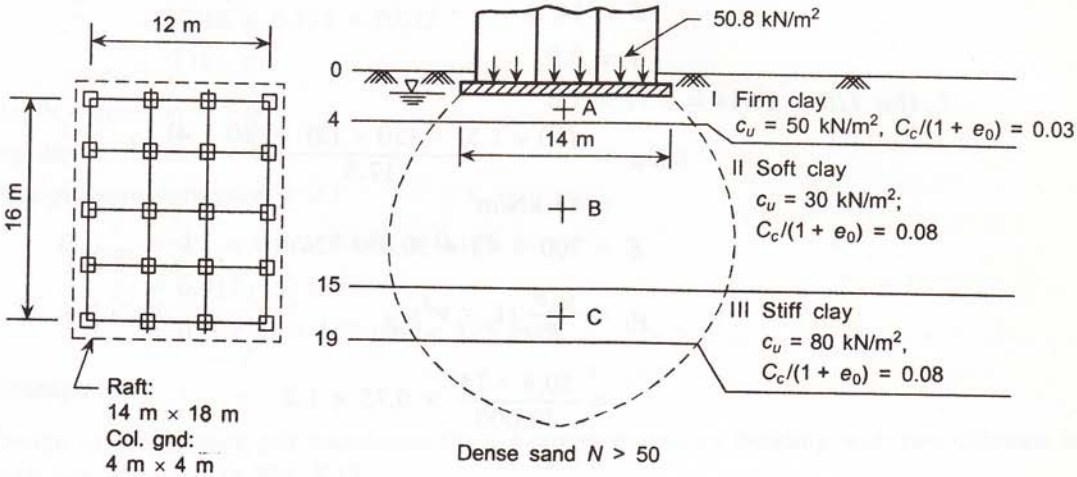


**Fig. 8.24** Example 8.5.

***Solution***

$$\text{Total load} = 720 \times 10 + 560 \times 10$$
$$= 7200 + 5600 = 12{,}800 \text{ kN}$$

Consider raft of size = 14 m × 18 m

$$\therefore \quad q = \frac{12{,}800}{14 \times 18} = 50.8 \text{ kN/m}^2$$

Depth of foundation, $D_f = 1.5$ m

(a) *Bearing capacity*

$$N_c = 5\left(1 + 0.2\frac{B}{L}\right)\left(1 + 0.2\frac{D_f}{B}\right)$$

$$= 5\left(1 + 0.2 \times \frac{14}{18}\right)\left(1 + 0.2 \times \frac{1.5}{14}\right)$$

$$= 5.8$$

$$q_{ult}(n) = c_u N_c$$

$$= 30 \times 5.8$$
$$= 174 \text{ kN/m}^2$$
$$Fs = \frac{174}{58} = 3.0$$

Major portion of failure zone lies in stratum II, hence, we have taken $c_u = 30$ kN/m$^2$

(b) *Immediate settlement*

$$q_n = 50.8 \text{ kN/m}^2$$
$$B = 14 \text{ m}$$
$$\nu = 0.5$$
$$I_\rho \text{ (for } L/B = 18/14 = 1.3) = 1.2$$
$$(c_u)_{av} = \frac{(50 \times 1.5) + (30 \times 12) + (80 \times 4)}{17.5}$$
$$= 43 \text{ kN/m}^2$$
$$E = 700 \times 43 = 30{,}000 \text{ kN/m}^2$$
$$\therefore \quad \rho_i = \frac{q_n B}{E}(1 - \nu^2) I_\rho$$
$$= \frac{50.8 \times 14}{30{,}000} \times 0.75 \times 1.2$$
$$= 0.21 \text{ m}$$

Depth correction = 1.0

Rigidity correction = 0.8

$\therefore \quad (\rho_i)_{corr} = 0.8 \times 0.021 = 0.017$

(c) *Consolidation settlement*

$$\rho_c = \sum \frac{C_c}{1 + e_0} H \log \frac{p_o + \Delta p}{p_o}$$

At A: $p_o = 1.5 \times 18 + 8 \times 0.75 = 33$ kN/m$^2$

$\Delta p$ (for $Z/B = 0.75/14 = 0.05$) $= 0.98 \times 50.8 = 49.8$ kN/m$^2$

At B: $p_o = 18 \times 1.5 + 8 \times 1.5 + 7 \times 6$

$= 27 + 12 + 42$

$= 81$ kN/m$^2$

$\Delta p$ (for $Z/B = 7.5/14 = 0.53$) $= 0.74 \times 50.8 = 37.5$ kN/m$^2$

At C: $p_o = 18 \times 1.5 + 8 \times 1.5 + 7 \times 12 + 8 \times 2$

$= 27 + 12 + 84 + 16$

$= 139$ kN/m$^2$

$$\Delta p = \left(\text{for } Z/B = \frac{15.5}{14}\right) 0.35 \times 50.8 = 17.8 \text{ kN/m}^2$$

$$\frac{\Delta p}{p_o} = \frac{12.9}{139} = 0.09 < 0.1 \quad \text{Hence, soil below stratum III is not significant.}$$

$$\rho_c = 0.03 \times 1.5 \times \log \frac{33 + 49.8}{33} + 0.08 \times 12 \log \frac{81 + 37.5}{81}$$

$$+ 0.06 \times 4 \log \frac{139 + 17.8}{139}$$

$$= 0.018 + 0.158 + 0.012$$

$$= 0.188 \text{ m}$$

Depth correction = 1.0

Rigidity correction = 0.8

Pore-pressure correction = 0.7

$$\therefore \quad (\rho_c)_{\text{corr}} = 0.8 \times 0.7 \times 0.188 = 0.105 \text{ m}$$

$$\rho_f = 0.017 + 0.105$$

$$= 0.122 \text{ m} = 122 \text{ mm} < 125 \text{ mm}$$

**Example 8.6**

Design of a buoyancy raft foundation for a 4-storey dormitory building with two columns in each bay, depicted in Fig. 8.25.

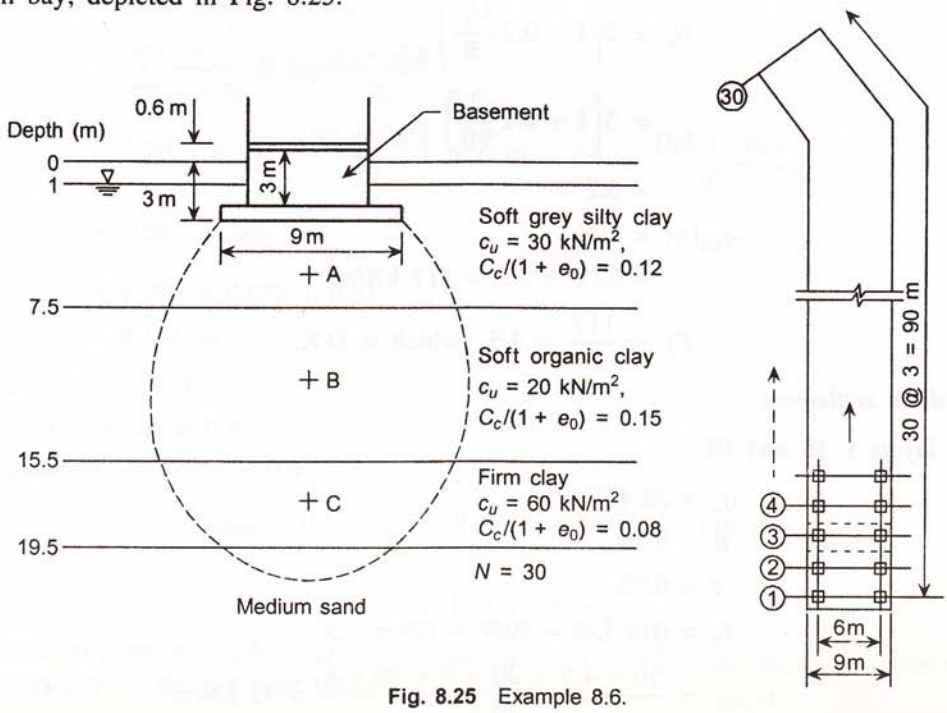


**Fig. 8.25** Example 8.6.

***Solution***

Size of raft = 9 m × 90 m
Area of each column bay = 3 m × 9 m = 27 m$^2$
Load in each bay = 2 × 900 = 1800 kN

Gross foundation pressure

for superstructure $q = \dfrac{1800}{27} = 67$ kN/m$^2$

Assume basement to be 25%. Thus, $q_{(\text{basement})} = 17$ kN/m$^2$

$\therefore \quad q_{\text{gross}} = 84$ kN/m$^2$

Provide depth of foundation, $D_f = 3$ m.

$$q_{\text{net}} = q_{\text{gross}} - \gamma D_f$$
$$= 84 - 18 \times 3$$
$$= 30 \text{ kN/m}^2$$

(a) *Bearing capacity*

Consider 9 m depth below raft

$$\therefore \quad c_u = \frac{25 \times 4.5 + 20 \times 4.5}{9} = 22.5 \text{ kN/m}^2$$

and

$$N_c = 5\left(1 + 0.2\frac{D_f}{B}\right)$$
$$= 5\left(1 + 0.2\frac{3}{90}\right)$$
$$= 5.2$$
$$q_{\text{ult}}(n) = c_u N_c$$
$$= 22.5 \times 5.2 = 117 \text{ kN/m}^2$$
$$Fs = \frac{117}{33} = 3.5 \quad \text{which is O.K.}$$

(b) *Immediate settlement*

Consider layers I, II, and III.

$$q_u = 32 \text{ kN/m}^2$$
$$B = 9 \text{ m}$$
$$\nu = 0.75$$
$$I_\rho = (\text{for } L/B = 90/9 = 10) = 2.5$$
$$(c_u)_{\text{av}} = \frac{30 \times 4.5 + 20 \times 8 + 60 \times 4}{16.5} = 32 \text{ kN/m}^2$$

$$E = 600 \times 32 = 19{,}200 \text{ kN/m}^2$$

$$\rho_i = \frac{q_n B}{E}(1 - \nu) I_\rho$$

$$= \frac{30 \times 9 \times 0.75 \times 2.5}{19{,}200}$$

$$= 0.026 \text{ m}$$

Deptn correction = 1.0
Rigidity correction = 0.8

$$(\rho_i)_{\text{corr}} = 0.08 \times 0.026 = 0.02 \text{ m} = 20 \text{ mm}$$

(c) *Consolidation settlement*

Consider layers I, II, and III.

At A: $p_o = 18 \times 1.0 + 8 \times 4.25 = 52 \text{ kN/m}^2$

$\Delta p = 0.96 \times 30 = 28.8 \text{ kN/m}^2$

At B: $p_o = 18 \times 1 + 8 \times 6.5 + 8 \times 4.0$

$= 102 \text{ kN/m}^2$

$\Delta p = 0.55 \times 30 = 16.5 \text{ kN/m}^2$

At C: $p_o = 18 \times 1 + 8 \times 6.5 + 8 \times 8 + 8 \times 2$

$= 150 \text{ kN/m}^2$

$\Delta p = 0.36 \times 33 = 10.8 \text{ kN/m}^2$

$$\therefore \quad \rho_c = \sum \frac{C_c}{1 + e_0} H \log \frac{p_o + \Delta p}{p_o}$$

$$= 0.10 \times 4.5 \log \frac{52 + 28.8}{52} + 0.15 \times 8 \log \frac{102 + 16.5}{102}$$

$$+ 0.08 \times 4 \log \frac{150 + 12}{150}$$

$$= 0.086 + 0.078 + 0.01$$

$$= 0.174 \text{ m}$$

Depth correction = 1.0

Rigidity correction = 0.8

Pore-pressure correction = 0.8

$$(\rho_c)_{\text{corr}} = 0.8 \times 0.8 \times 0.174 = 0.110 \text{ m} = 110 \text{ mm}$$

Total settlement,

$$\rho_f = 20 + 110 = 130 \text{ mm}$$

Marginal extra settlement beyond the permissible limit of 125 mm may be allowed in view of the rigidity of the raft foundation.

## REFERENCES

Bowles, J.E. (1988), *Foundation Analysis and Design*, McGraw-Hill Book Company, International ed., Singapore.

Casagrande, A. (1936), *The Determination of Preconsolidation Load and its Practical Significance*, Proc. Ist Int. Conference on Soil Mechanics and Foundation Engineering, Cambridge, Mass, Vol. 3.

Casagrande, A. and R.E. Fadum, (1942), *Application of Soil Mechanics in Designing Building Foundations*, Proc. American Society of Civil Engineers, Nov. 1942.

Glossop, R. (1972), *Floating Foundations, Foundation Engineering Handbook* Ist ed., Van Nostrand Reinhold Co., New York.

Hetenyi, M. (1946), *Beams on Elastic Foundation*, The University of Michigan Press, Ann Arban, Mi, USA.

IS 1904 (1966), *Code of Practice for Design of Shallow Foundations*, Bureau of Indian Standards, New Delhi.

Rios, L. and P. Silva, *Foundations in Down Town, Sao Paulo*, Proc. 2nd Int. Conf. Soil Mech (Rotterdam) Vol. 4, p. 69.

Skempton, A.W. (1955), *Foundations for High Buildings*, Proc. Institution of Civil Engineers, London. Pt. 3, Vol. 4, p. 246.

Terzaghi, K. (1938), *Settlement of Structures in Europe and Methods of Observation*, Proc. ASCE, Vol. 103, p. 1432.

# 9 Pile Foundations

## 9.1 INTRODUCTION

Piles are relatively long and slender structural members used to transmit foundation loads through soil of low bearing capacity to deeper strata (soil or rock) having high bearing capacity. They are also used in normal ground conditions to resist uplift and lateral forces.

The principal uses of piles are:

1. To carry vertical compression load from buildings, bridges, and so on.
2. To resist horizontal or inclined loads by retaining wall, bridge pier, water front structures and structures subjected to wind or seismic loads.
3. To resist uplift forces in transmission towers and underground structures below water table.

Piles are described as end bearing piles and friction piles depending on the manner in which the load is transmitted into the surrounding soil. These can be defined as follows:

If the pile rests in a hard and relatively incompressible stratum, for example, rock or dense sand/gravel, the pile derives most of its carrying capacity from end bearing at the pile tip. Such piles are called *end bearing* or *point-bearing* piles. Figure 9.1(a) depicts end-bearing piles. The soft compressible layer through which the pile passes may not carry any significant load by side friction.

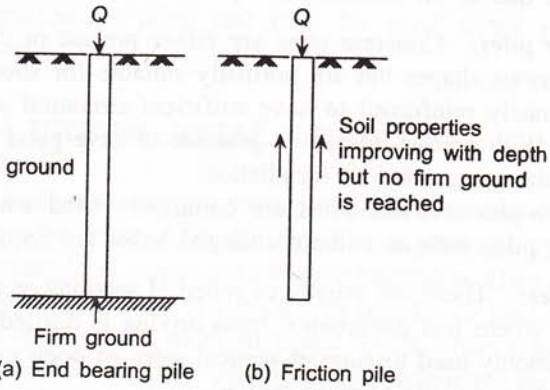


**Fig. 9.1** Piles: methods of load transfer.

If the pile does not reach an incompressible stratum but is driven for some depth into a penetrable soil, the carrying capacity of the pile is derived primarily from skin friction or adhesion between the embedded surface of the pile and the surrounding soil. Such piles are called *friction piles*, as shown in Fig. 9.1(b).

Although, in common terminology, piles are often referred to as friction piles or end-bearing piles—in reality, there is no pile that transmits the load to the surrounding soil solely by friction or solely by end bearing. The distinction only serves to indicate the relative magnitude of the load that is transmitted by friction and by end bearing. For example, a straight pile embedded in homogeneous clay will mostly transfer the load by friction and a pile with its tip resting in dense sand underlying soft clay can be considered an end bearing pile.

The relative magnitude of the skin friction and the base resistance of a pile, however, depends on various factors such as,

1. Geometry of the pile shaft—its shape, length, and diameter and whether it is with or without enlarged base.
2. Subsoil stratification along the pile shaft and the properties of soil in which the pile is embedded and where the tip of the pile rests.
3. Method of construction of the pile, that is, driven pile, bored pile, and so on.

## 9.2 CLASSIFICATION

Piles are classified according to their composition or method of installation.

### 9.2.1 Classification Based on Composition

(a) ***Timber piles:*** In India, timber piles are mostly made up of sal tree trunks and are called salballah piles. These are commonly available in length between 4–6 m, with diameter ranging from 15–25 cm. These may be suitable where good bearing stratum is available at a relatively shallow depth. Now a days, use of timber piles is restricted due to the necessity for preservation of forests.

(b) ***Concrete piles:*** Concrete piles are either precast or cast-in-situ. *Precast* piles may be of various shapes but are normally suitable for short lengths. These piles should be adequately reinforced to have sufficient structural strength to withstand handling stresses. With precast piles, it is possible to have good control on quality as they are cast on the ground before installation.

*Cast-in-situ* concrete piles are commonly used where relatively long and large diameter piles with or without enlarged bases are required to support heavy loads.

(c) ***Steel piles:*** These are usually of rolled H sections or pipe sections. These piles may be used where less disturbance from driving is desired. H-piles and steel sheet piles are commonly used to support vertical sides of open excavation. Steel sheet piles are also used to provide seepage barrier.

### 9.2.2 Classification Based on Method of Installation

(a) ***Driven piles:*** These may comprise of timber, steel, or precast concrete. The piles are driven by the impact of a hammer or by vibrations induced by a vibratory hammer.

When a pile is driven into the soil, it displaces a volume of the soil equal to the volume of the pile. So, these piles are also called *displacement piles*. In granular soils, the driving operation densifies the soil and increases strength of the soil in the vicinity. When piles are driven in saturated clay, the soil instead of being compacted gets remoulded often with reduction of strength. The soil, however, regains strength with time due to consolidation and thixotropic hardening. Because of the displacement of soil by the piles, there may be ground heaving around the piles. Also, driving of piles imparts vibration to surrounding soil, which in some cases, may be detrimental to structures located very close to the site.

(b) ***Driven cast-in-situ-piles:*** These piles are also a kind of driven pile. Steel casing is driven into the ground with a shoe at the bottom. The hole is then filled up with concrete, and the casing is gradually lifted as the concrete is poured.

(c) ***Bored piles:*** These piles are formed in prebored holes in the ground either using a casing or by circulation of a drilling fluid, such as bentonite slurry. Concrete is poured into the hole by displacing bentonite and then gradually lifting the casing.

Bored piles may be of the following types:

(i) Small diameter bored piles—generally upto 600 mm diameter.
(ii) Large diameter bored piles—diameter generally greater than 600 mm. They are advantageous where heavy structural loads are to be supported.
(iii) Under-reamed piles—one or more bulbs of larger diameter than that of the shaft are formed by suitably enlarging the borehole with special tools to increase the end resistance. These piles are suitable when a good bearing stratum is available at a relatively shallow depth. The uplift capacity of these piles is high. In India, these piles are widely used to provide suitable foundations in expansive soils.

Bored piles are non-displacement piles and may be used when pile driving is detrimental to adjoining structures.

## 9.3 PILE BEHAVIOUR UNDER AXIAL LOAD

Figure 9.2 shows a typical load settlement diagram for a pile under gradually increasing load. At small deformations, say upto the point A in the figure, the pile–soil system behaves elastically, as indicated by the linear load versus settlement relationship. Upto this point, the entire load is carried by skin friction and there is virtually no transfer of load to the pile tip. With more deformation, the pile shaft carries more frictional forces while a part of the load is transferred to the pile tip also. At B, the pile tip carries the maximum skin friction that can be mobilized in the soil. Therefore, further increase of load on the pile is carried out at the pile tip and the pile is said to have failed, at C, when the tip load has also reached its

maximum value. Thus, the load carrying capacity of a pile may be determined from separate evaluation of the ultimate skin friction and the ultimate base resistance.

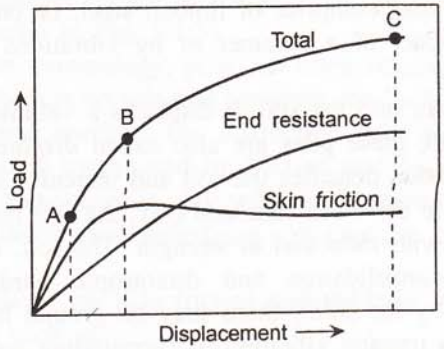


**Fig. 9.2** Load settlement relationship of piles.

Thus,

$$Q_p = Q_f + Q_b - W_p - W_e \tag{9.1}$$

where $Q_p$ is the load carrying capacity of the pile,
$Q_f$ is the maximum skin friction on the pile shaft,
$Q_b$ is the ultimate tip resistance,
$W_p$ is the weight of the pile, and
$W_e$ is the weight of soil displaced by the pile.

In general, $W_p$ and $W_e$ are small in relation to $Q_p$ and their differences even smaller. Thus, for practical purposes

$$Q_p = Q_f + Q_b \tag{9.2}$$

Therefore, it is apparent, that full mobilization of $Q_f$ and $Q_p$ are primarily dependent on the movement of the pile in the soil (refer Fig. 9.2). Cooke (1974), and Cooke and Price (1973) have shown that, for an elastic soil, full mobilization of skin friction in a cylindrical pile occurs at vertical displacement of 0.5–1% of the pile diameter. On the other hand, full mobilization of base resistance requires a much greater deformation—even upto 20% of the base diameter (Whitaker, 1976). This suggests that skin friction is mobilized almost fully before any appreciable base resistance develops in the soil. Therefore, the entire problem of load distribution through piles has to be viewed as a pile–soil interaction where the response of the soil to a given deformation in terms of skin friction and end bearing has to be taken into account.

An evaluation of the zone of soil that is influenced by piling is important to determine the soil properties that come into play in resisting the movement of the pile in the soil. Meyerhof (1959) and Kerisel (1961) considered the influence zone as shown in Fig. 9.3. According to Meyerhof (1959), the shear zone at the base causing bearing capacity failure of the soil extends to some distance above the pile tip. The zone of skin friction may extend laterally to a distance of three to four times the diameter of the pile while compaction of the pile may occur upto a distance of five to six times the diameter. Cooke and Price (1973) have, however, observed that displacement of the soil may extend to a radial distance of ten

diameters around the pile. Pile driving causes significant changes in the soil within the zone of influence. Therefore, it is important to study the various factors that affect the soil during piling.

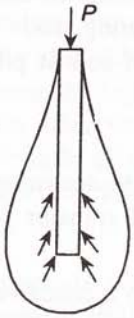


**Fig. 9.3** Stress influence zone around piles.

## 9.4 PILE CAPACITY TO RESIST AXIAL FORCES

The load carrying capacity of a pile is controlled by its structural strength and the supporting strength of the soil. The smaller of the two is considered for design purposes. There are three apporaches to the computation of pile capacity based on soil support. These are:

(a) Static analysis
(b) Dynamic analysis
(c) Load test

### 9.4.1 Structural Capacity of Piles

The structural capacity of a pile is its strength as a column. When the pile is completely embedded in soil, the restraint offered by the soil is generally sufficient to consider the pile as a short column (except for the case of a long pile in very soft clay). Pre-cast concrete piles are adequately reinforced to withstand handling and driving stresses. Cast-in-situ piles are also reinforced to increase column strength and also to resist moment that may have developed due to horizontal load or eccentricity of vertical loads. Reinforcements are also helpful in resisting tensile stresses that may develop due to heave resulting from driving of adjacent piles in clay.

### 9.4.2 Pile Capacity from Static Analysis

The static analysis relates the shear strength of the soil to the skin friction along the pile shaft and end bearing at the pile tip. The carrying capacity of a pile is given by the sum of the ultimate bearing capacity of the soil at the pile tip and the ultimate adhesion between the pile and the surrounding soil, (refer Fig. 9.2).

$$Q_{\text{ult}} = \sum A_s f_s + A_p q_p \tag{9.3}$$

where

$f_s$ = unit skin friction in each layer,
$A_s$ = pile area providing skin friction in each layer,
$A_p$ = pile area providing end bearing, and
$q_p$ = ultimate bearing capacity of soil at pile tip.

## Piles in cohesive soil

A total stress approach is generally used to determine the shaft and tip resistances of piles in cohesive soil considering that the load transfer from the pile to the soil occurs under undrained condition.

***Driven piles:*** When a pile is driven into a cohesive soil, two effects of pile driving become significant.

The clay is displaced laterally and in an upward direction, resulting in a ground heave. The soil close to the pile shaft gets disturbed to cause remoulding of the clay. This may lead to considerable loss in strength of the soil. This has been discussed by Flaate (1972) who observed appreciable increase in water content and corresponding reduction of shear strength of the soil between two adjacent driven piles in clay. With time, soft clay regains this strength either completely or partially by thixotropic hardening (Skempton and Northey, 1952). A corresponding increase in load carrying capacity of the pile with time is shown in Fig. 9.4 (Tomlinson, 1994). On the other hand, in stiff clays, extensive cracking of the soil occurs during pile driving. Clay in the upper part of the pile *breaks away from the shaft and may never regain contact with it* (Tomlinson, 1977). Thus, the effect of pile driving on the shear strength of the clay differs with the soil consistency. Considerable gain in strength may be observed with time in soft clays while no appreciable effect may be noted in stiff clays.

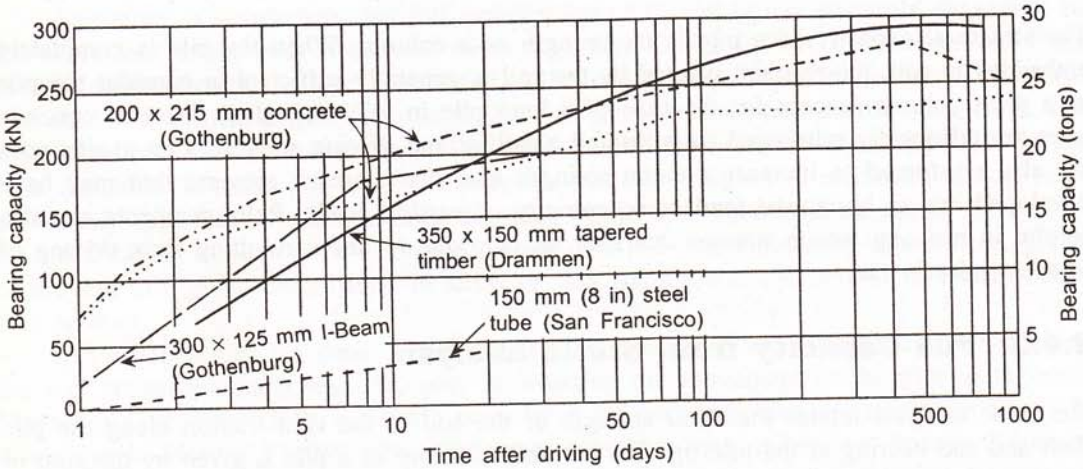


**Fig. 9.4** Gain in load carrying capacity with time of driven piles in soft clay (Tomlinson, 1994).

High pore-pressure is developed in the clay due to pile driving forces. This pore-pressure often takes time to dissipate. When reconsolidation of the clay occurs, the soft clay

tends to stick to the pile shaft. In the case of stiff clays, the high pore-pressure dissipates quickly through the cracks and fissures and often a negative pore-pressure is set up in the surrounding clay. Tomlinson carried out extensive research on the behaviour of driven piles in stiff clays. Steel tubular piles were driven into stiff London clay and were subjected to load test 1 month, 3 months, and 1 year after driving. Examination of the soil around the pile showed that gaps had been created near the top of the pile during driving which had not closed even after one year. Tomlinson observed three zones of adhesion of varying magnitude in a driven pile. Below a length of 8 × diameter at the top where the gap occurred, there was a length of partial adhesion followed by a length of very close adhesion where most of the frictional resistance of the pile developed.

***Bored piles:*** In bored piles, the in-situ soil is removed from the hole by drilling and the void is later filled with concrete. Water and/or drilling fluid is used to stabilize the borehole before concreting. Boring causes release of lateral stresses on the walls of the borehole. The soil in contact with the borehole undergoes swelling and migration of pore water occurs towards the exposed clay face. Use of drilling fluid such as bentonite, may considerably minimize this migration of pore water.

When concrete is poured in the borehole to make the pile, there is further migration of water from the green concrete into the surrounding soil which causes further softening of the clay. Meyerhof and Murdock (1953) measured 4–8% increase of water content in stiff fissured clay close to the interface of the soil with concrete.

## Pile in cohesionless soil

Drained condition generally prevails in cohesionless soil. Accordingly, pile capacity is determined from effective stress analysis.

***Driven piles:*** The effect of pile driving in cohesionless soil is to compact the soil and, thereby, increase its shearing resistance. The question of loosening of the soil, as in the case of clays, does not normally arise. Whatever loosening may occur during withdrawal of casing, is more than compensated by the vibration caused by ramming of the concrete and the density of the soil is not likely to come down below its original value.

***Bored piles:*** Boring a hole in granular soil generally causes a loosening of the soil, thereby reducing its relative density. This causes a marked reduction in both the skin friction and the end bearing. Further, if bentonite slurry is used to stabilize the hole, there often remains a screen of bentonite between the hole and the pile. It is believed that this may result in a reduction of the frictional resistance.

Sliwinski and Fleming (1974), and Broms and Hill (1973) have observed some reduction of skin friction of bored piles made with bentonite slurry as compared with those made without bentonite slurry. On the other hand, Touma and Reese (1973), did not find any significant difference in behaviour between the piles installed with or without bentonite slurry. However, if chances of reduction of skin friction is anticipated, measures to expell the bentonite screen (say, by grouting or other means) may be adopted (Tomlinson, 1977).

## 9.5 FRICTIONAL RESISTANCE

We have, so far discussed the various factors that affect the soil during pile driving. The quantitative evaluation of frictional resistance should take into account the effect of all these factors on the shear behaviour of the soil. Although the frictional resistance is basically a function of the shear strength of the soil, this friction develops as an adhesion between the pile and the soil and not as pure friction between soil particles. The complex nature of stresses developed around a pile, the effects of remoulding and/or stress release of the soil, and a somewhat indeterminate nature of the pore-pressure dissipation and pile soil interaction make it difficult to analyze the problem of skin friction evaluation.

Paton (1895) applied Rankine's earth pressure theory to obtain the bearing capacity of piles (see Whitaker, 1976). The frictional resistance along the pile shaft was expressed as,

$$F_s = \mu\gamma \frac{L}{2} \frac{1 - \sin\phi}{1 + \sin\phi} A_s \tag{9.4}$$

where $\mu$ is the coefficient of friction between the pile and the soil,
$\gamma$ is the density of the soil,
$L$ is the length of the pile,
$\phi$ is angle of internal friction of the soil, and
$A_s$ is surface area of the pile.

The major uncertainty in using Eq. (9.4) to evaluate the skin friction lies in the estimation of $\mu$ and $\phi$ of the soil. In particular, no distinction is made between clay and sand, and the choice of these parameters for actual conditions that exist around a pile during and after driving leads to difficulties.

Burland (1973) developed a method of calculation of shaft friction from the effective stress principle. It is assumed that the zone of distortion around the pile being small, the pore-pressure dissipates quickly and loading takes place under drained condition. It is further assumed that there is no effective cohesion in the soil due to remoulding of the soil around the pile. The unit skin friction at any depth is then given by,

$$f_s = kp \tan\delta \tag{9.5}$$

where $k$ is the lateral earth pressure coefficient,
$p$ is the effective overburden pressure at the depth considered, and
$\delta$ is the angle of friction between the pile and the soil.

It poses extreme difficulties to select appropriate values of $k$ and $p$. $p$ is initially small due to high pore-pressure developed during driving but its value soon increases with dissipation of pore water pressure. In driven piles, $k$ is also likely to be high initially because of the driving forces whereas in bored piles, $k$ is observed to have small value due to swelling of the soil. These values may ultimately attain some stability after installation but uncertainties still remain regarding the time required for drainage of the soil around the pile and about values of $k$ and $p$ that should be applicable in a field situation. Burland made a further simplifying assumption that $k = k_0$ ($k_0$ is the coefficient of earth pressure at rest) and obtained the following expression for the total shaft friction:

$$F_s = \pi B \sum_0^L pk_0 \tan\delta(\Delta L) \tag{9.6}$$

Owing to the uncertainties involved in selecting field parameters for analytical solutions, attempts for evaluation of frictional resistance of piles have been based on semi-empirical approaches.

### 9.5.1 Frictional Resistance in Cohesive Soil

When a pile is installed in a cohesive soil, either by methods of driving or boring, the immediate deformation of the soil takes place essentially under undrained condition. In this case, $\phi = 0$ analysis (Skempton, 1948) would be valid. The unit skin friction between the soil and the pile may then be considered to be a function of the undrained shear strength of the clay. Notwithstanding the fact that this shear strength may undergo change with time due to thixotropic hardening or due to dissipation of excess pore-pressure, the unit ultimate skin friction may be expressed by the equation,

$$f_s = \alpha c_u \tag{9.7}$$

where $c_u$ is the undrained shear strength of the clay, and
$\alpha$ is an adhesion factor.

The total frictional resistance of the piles would then be,

$$F_s = \sum A_f \alpha c_u \tag{9.8}$$

where $A_f$ is the surface area of the pile shaft in contact with the soil in different layers.

While the undrained shear strength of the clay, $c_u$ can be determined from field vane shear test or from laboratory triaxial test, a proper assessment of the adhesion factor is required for the evaluation of the unit skin friction. This adhesion factor gives a measure of the part of the undrained shear strength of the soil that is mobilized as skin friction.

#### Driven piles in cohesive soil

Extensive research by Tomlinson (1965, 1977) has shown that the adhesion factor depends on the consistency of the soil, as represented by its cohesive strength. In addition, the penetration depth of the pile appears to have some effect on the adhesion factor. Figure 9.5 illustrates following three different cases.

(i) In the case of short piles in uniform clay, the gap formed near the pile during driving may occupy a large part of the penetration depth. The average adhesion factor would, accordingly, be low. For large penetration depth, the gap would be small compared to the pile length and a higher average adhesion factor may be adopted. Figure 9.5(a) shows the variation of adhesion factor with undrained shear strength for piles in uniform clay.

(ii) If the pile is driven through a soft clay with an underlying stiff clay, a skin of soft clay would be dragged into the gap formed near the top of the stiff clay. This would reduce the adhesion over a certain length of penetration depth into the stiff clay, the effect being more predominant in the case of short penetration lengths. The corresponding adhesion factors for different values of $c_u$ are shown in Fig. 9.5(b).

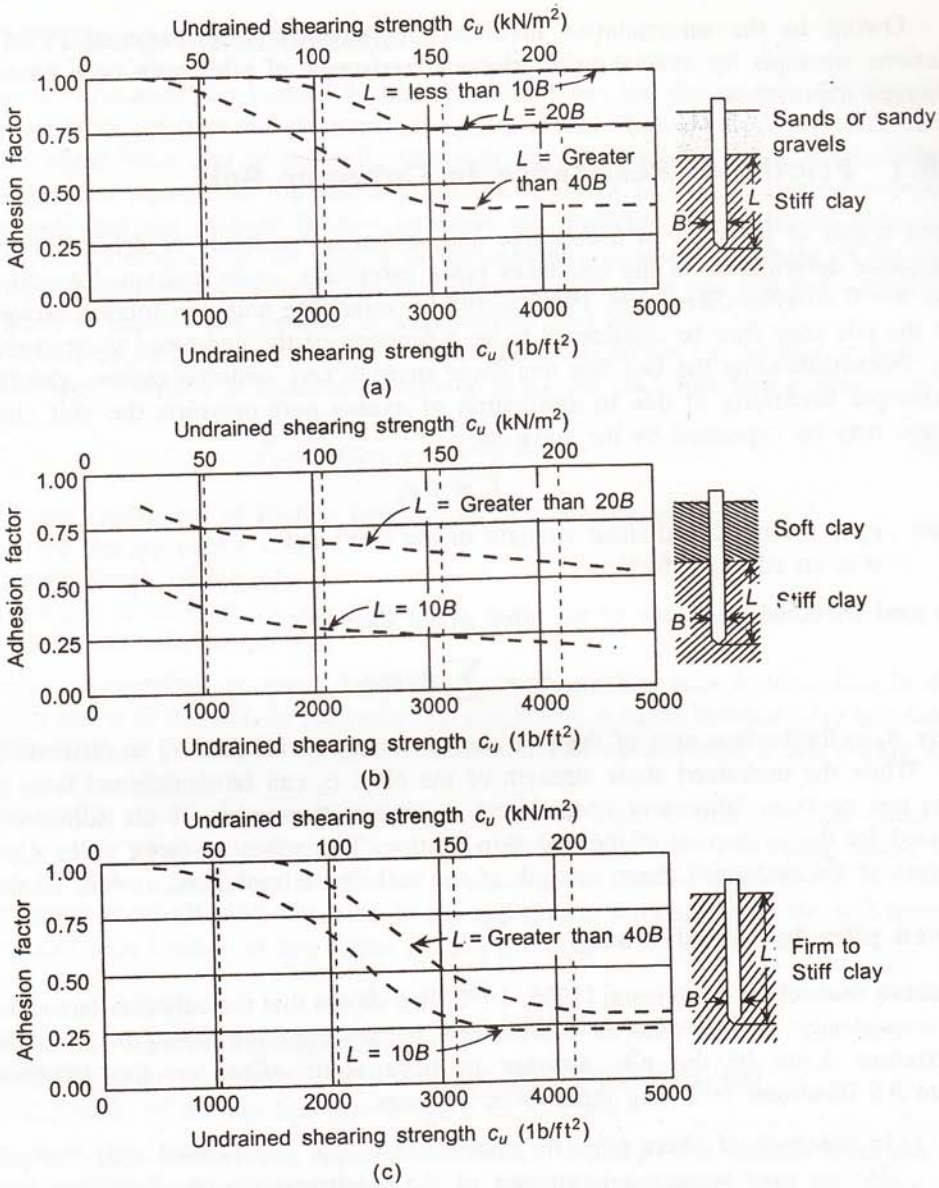


**Fig. 9.5** Skin friction in cohesive soil and adhesion factor.

(iii) If the pile is driven through a granular soil into a stiff clay, the gap near the top of the stiff clay explained previously will be filled with a sand skin and the corresponding adhesion factors would be higher. The design curves for adhesion factor are shown in Fig. 9.5(c). In general, deep piles will show higher adhesion factor for all values of shear strength.

Tomlinson (1977) points out that the adhesion factors given in Fig. 9.5 are applicable to driven piles of uniform cross-section. The adhesion factors for driven and cast-in-situ piles may be

slightly less than the precast piles because of the migration of water from the green concrete into the surrounding soil, although the extent of reduction cannot be precisely determined.

Vijayvergiya and Focht (1972) employed a different approach to the determination of adhesion factor for driven piles in cohesive soils. They suggested that pile driving forces would mobilize passive resistance in the soil and this would influence the development of skin friction in pile shaft. The unit skin friction could then be expressed as a function of the passive earth pressure.

$$f_s = \lambda (p_0 + 2c_u) \tag{9.9}$$

where $p_0$ is the average vertical effective stress between the ground surface and the pile tip,
$c_u$ is the average undrained shear strength along the pile shaft, and
$\lambda$ is a dimensionless coefficient.

The values of $\lambda$ for different penetration depths of piles in clay as proposed by Vijayvergiya and Focht are shown in Fig. 9.6. When calculating $p_0$, due account of the ground water table should be taken. McClelland (1974) compared the results of 47 pile tests, mostly from U.S.A. with the predictions based on Tomlinson's and Vijayvergiya and Focht's adhesion factor. Better correlation was obtained with the latter.

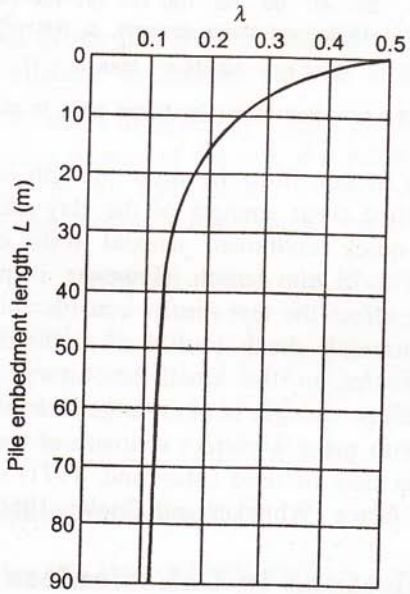


**Fig. 9.6** Values of $\lambda$ (Vijayvergiya and Focht, 1972).

## Bored piles in cohesive soil

In bored piles, as discussed earlier, softening of the clay occurs in the vicinity of the borehole. This results in a reduction of the adhesion factor which should be duly taken into account in design. This effect is more pronounced in stiff clay than in soft clay. Skempton (1959) observed an adhesion factor as low as 0.3 for bored piles in stiff London Clay. This factor is likely to vary with time that is allowed between boring and casting of the concrete. Greater time gap would allow more swelling of the surrounding clay and thereby reduce the

adhesion factor. For bored piles, the adhesion factor may best be obtained from correlation with undrained strength of the clay as shown in Fig. 9.7.

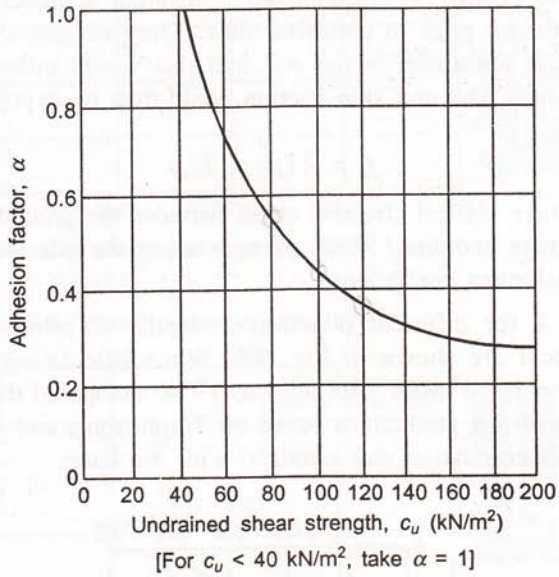


**Fig. 9.7** Adhesion factor for bored piles in clay.

The determination of skin friction from the shear strength of the clay requires a proper evaluation of the in-situ undrained shear strength of the clay mass. This strength is usually determined from laboratory quick undrained triaxial tests on cylindrical samples of dimensions 37.5 mm diameter × 75 mm length. However, in practice, anisotropy, rate of strain, sample size, and so on affect the test results considerably (Bishop, 1966). There is often a large scatter in the strength–depth profile of fissured clays due to the random presence or otherwise of fissures in the small laboratory specimens (Skempton and La Rochelle, 1955) and the average strength is often larger than the representative strength of the clay mass in-situ. In order to make a correct estimate of the in-situ strength, either the lower limit of the strength data may be used (Marsland, 1971) or the average strength may be multiplied by an empirical factor (Whitaker and Cooke, 1966).

## 9.5.2 Frictional Resistance in Cohesionless Soil

The classical formula for calculation of the unit skin friction at any depth on a pile shaft in a cohesionless soil is given by the equation

$$f_s = K_s p \tan \delta \tag{9.10}$$

where,

$K_s$ is the coefficient of lateral earth pressure which depends on the relative density of the soil,

$p$ is the effective overburden pressure at the depth considered, and

$\delta$ is the angle of friction between the pile and soil.

The unit skin friction, according to Eq. (9.9). Varies linearly with depth along the pile shaft. This is shown in Fig. 9.8. The total frictional resistance for a pile of depth $D_f$ can be obtained as

$$Q_f = \frac{1}{2} K_s \gamma' D_f \tan \delta A_f \tag{9.11}$$

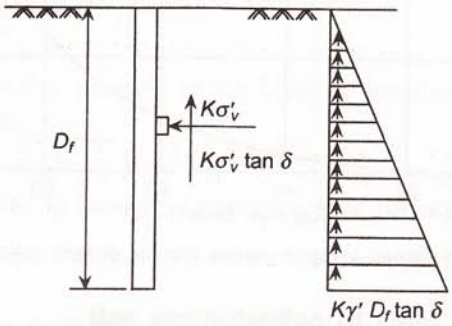


**Fig. 9.8** Skin friction in piles within sand.

where,

$A_f$ is the area of the pile shaft in contact with the soil and

$\gamma' D_f$ is the effective overburden pressure at the pile tip.

The values of $K_s$ and $\delta$ as given by Broms (1966) are shown in Table 9.1. While $K_s$ is a function of the relative density of the soil, $\delta$ is related to the angle of shearing resistance of the soil and the nature of pile soil contact. In piles with liner, the skin friction is even less than direct soil–concrete friction and a reduced value of $\delta$ should be used.

**Table 9.1** Values of $K_s$ and $\delta$ (Broms 1966)

| *Installation method* | $K_s$ | *Pile–soil interface* | $\delta$ |
|---|---|---|---|
| Driven piles, large displacement | 1.5–2.0 | Steel/sand | $0.5\phi'$–$0.7\phi'$ |
| Driven piles, small displacement | 1.0–2.0 | Precast concrete/sand | $0.8\phi'$–$1.0\phi'$ |
| Bored and cast-in-situ piles | 0.7–1.0 | Cast-in-situ concrete/sand | $1.0\phi'$ |

## Driven piles in cohesionless soil

In driven piles, Poulos and Davis (1980) have recommended the use of the relationship

$$\delta = \frac{3}{4}\phi' + 10° \tag{9.12}$$

to determine the angle of pile soil friction accounting for the effect of pile driving, $\phi'$ being the angle of shearing resistance prior to installation of the pile.

Tomlinson (1977) has proposed a relationship between average unit skin friction and relative density, based on the results of actual pile load tests, as depicted by Fig. 9.9. According to this relationship, the skin friction attains a peak value of 107 kN/m$^2$ (10 t/m$^2$) for high relative density.

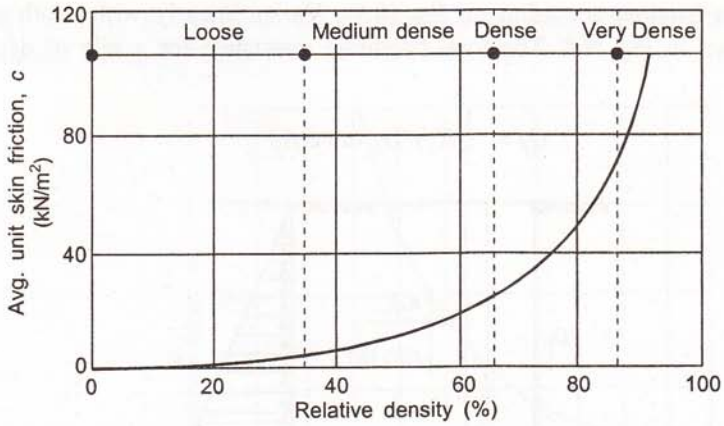


**Fig. 9.9** Unit skin friction in sand versus relative density (after Tomlinson, 1977).

## Bored and cast-in-situ piles in cohesionless soil

For bored and cast-in-situ piles in cohesionless soil, there may be a marked reduction in the relative density of the soil around the walls of the borehole after drilling. This may lead to a reduction of skin friction on the pile shaft. If appreciable loosening of the soil is anticipated a low angle of shearing resistance should be used in calculating skin friction by Eq. (9.9). The presence of a bentonite skin on the face of the borehole may also cause a reduction of skin friction. Poulos and Davis (1980) suggest reduction in $\phi$ of sand in bored piles by 3°. That is,

$$\phi = \phi' - 3° \tag{9.13}$$

Touma and Reese (1974) suggest a value of 0.7 for the earth pressure coefficient, $K_s$ for calculating skin friction of bored piles in sand.

The skin friction mobilized in cohesionless soil may be best understood by considering the value of $K_s \tan \delta$ in Eq. (9.10). Vesic (1967) and Meyerhof (1976) have done extensive work on model piles. They gave the relationships between $K_s \tan \delta$ and $\phi'$ as shown in Fig. 9.10. The effect of pile installation on the skin friction coefficient is clearly seen.

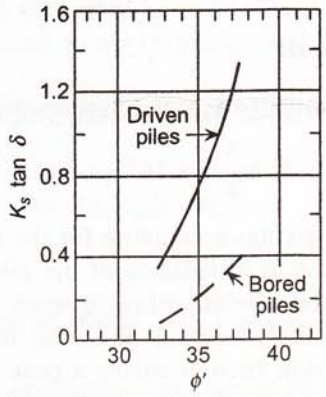


**Fig. 9.10** Relationship between $K_s \tan \delta$ and angle of shearing resistance, $\phi'$ (Poulos and Davis, 1980).

## 9.6 END BEARING

The ultimate bearing capacity of shallow foundation has been discussed in Chapter 5. The general equation for bearing capacity of a foundation is given by

$$q_{ult} = cN_c + qN_q + 0.5B\gamma' N_\gamma \tag{9.14}$$

where $c$ = cohesion of the soil,

$q$ = effective overburden pressure at the level of foundation,

$B$ = width of footing,

$\gamma'$ = effective unit weight of soil, and

$N'_c$, $N'_q$, and $N'_\gamma$ = bearing capacity factors suitably corrected for shape and depth.

For a pile having depth $D_f$ and diameter $D$, the ultimate bearing capacity at the pile tip becomes

$$q_p = cN'_c + qN'_q + 0.5\gamma' DN'_\gamma \tag{9.15}$$

Now the pile diameter, $D$ is generally small compared to the depth $D_f$. So, the term $\gamma DN'_\gamma$ is small and often neglected. End bearing at the pile tip is then obtained as

$$q = cN'_c + qN'_q \tag{9.16}$$

### 9.6.1 End Bearing in Cohesive Soil

For cohesive soil having $\phi = 0$, under undrained condition

$$q_p = c_u N_c \tag{9.17}$$

where, $N_c$ = bearing capacity factor.

For $\phi = 0$ and for deep foundations, which a pile may be treated as, $N_c$ may be taken to be equal to 9 on the basis of analytical and experimental evidences (Skempton, 1951). However, for deep piles in homogeneous clay, contribution of end resistance is small in comparison to the shaft resistance.

### 9.6.2 End Bearing in Cohesionless Soil

For a cohesionless soil having $c = 0$, the end bearing is

$$q_p = qN'_q \tag{9.18}$$

where

$q$ = effective vertical stress at the pile tip and

$N'_q$ = bearing capacity factor which is a function of $\phi'$.

Different investigators have obtained different relations between $N_q$ and $\phi'$ depending on the shape of failure surface considered. Figure 9.11 shows some assumed failure surfaces and corresponding relationships between $N_q$ and $\phi$.

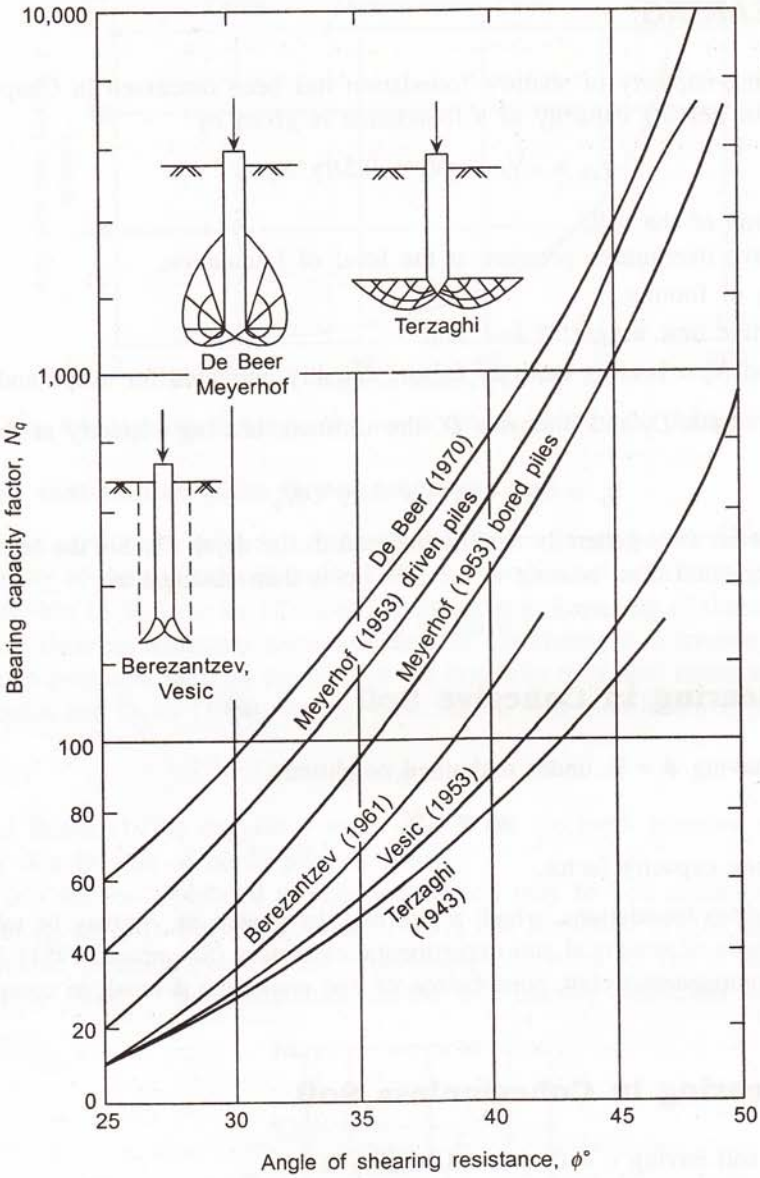


**Fig. 9.11** Variation of $N_q$ with $\phi'$ as obtained by different investigators.

It can be seen that Terzaghi (1943) gives the lower bound and De Beer (1970) gives the upper bound values of $N_q$. Comparison of observed point resistances of piles in sand by Nordlund (1969) and Vesic (1967) reveal that $N_q$ values established by Berezantzev et al. (1961) give better estimates of point resistance. Although $N_q$ values of Berezantzev are dependent on the relative embedment depth $D_f/B$, the variation is small. An average Berezantzev curve has been given in IS 2911 (part I, 1979), Fig. 9.12.

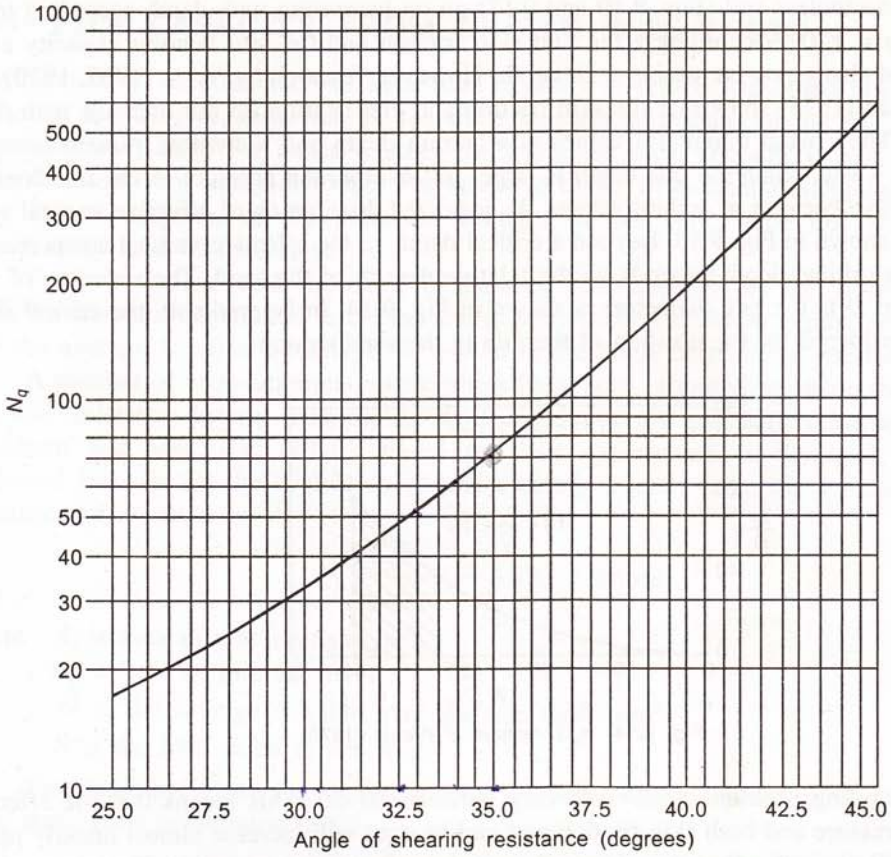


**Fig. 9.12** Variation of $N_q$ with $\phi'$ (Berezantzev, 1961).

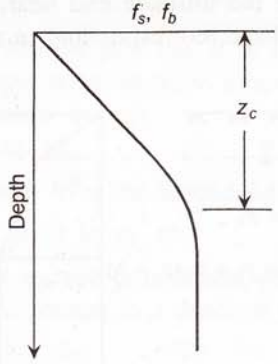


**Fig. 9.13** Concept of critical depth in cohesionless soil (after Vesic, 1970).

## 9.7 CRITICAL DEPTH

The effective overburden pressure required for calculation of frictional resistance and end

bearing in cohesionless soil (Eqs. 9.10 and 9.17) go on increasing with depth according to the relationship $q = \gamma' D_f$. Accordingly the unit skin friction and the unit bearing capacity at the pile tip should also go on increasing with depth. However, research by Vesic (1967, 1970), and Hanna and Tan (1973) show that the skin friction and end bearing do not increase with depth indefinitely. They reach maximum values at a certain depth and thereafter, remain constant. According to Vesic, when the pile depth is large, full overburden pressure in the soil does not become effective because of arching action. An idealized distribution of effective vertical stress with depth is shown in Fig. 9.13. Beyond a critical depth $z_c$, the effective vertical stress remains constant. This critical depth depends on the relative density of the sand. The variation of $z_c/D$ with $\phi'$ (where $D$ is the pile diameter) is shown in Fig. 9.14. In layered soil, the critical depth should be considered for the position of the pile in the sand stratum.

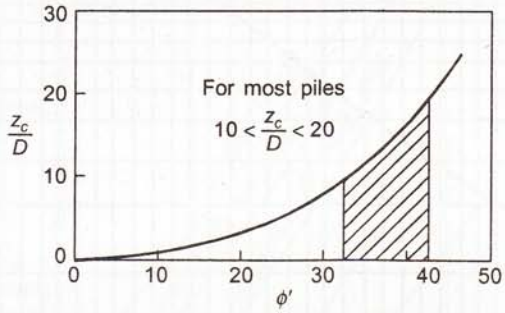


**Fig. 9.14** $z_c/D$ versus $\phi'$ (Vesic, 1970).

In most piling problems, $z_c/D$ will vary between 10–20. This means that the effective overburden pressure and both skin friction and end bearing will increase almost linearly upto a depth of 10–20 times the diameter of the pile and thereafter remain constant. The ultimate skin friction should therefore be obtained from the trapezoidal distribution of skin friction with depth, as shown in Fig. 9.15, while the ultimate end bearing should be determined for the maximum overburden pressure mobilized, corresponding to the critical depth $z_c$.

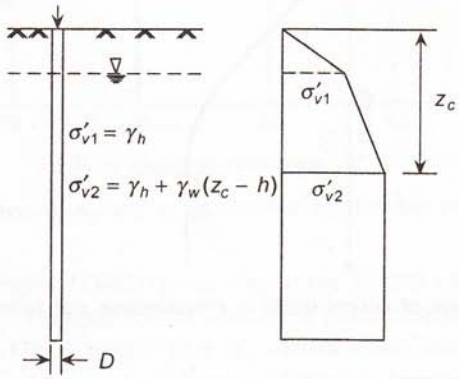


**Fig. 9.15** Distribution of skin friction with depth.

## 9.8 PILE CAPACITY FROM IN-SITU SOIL TESTS

The methods of determination of axial load capacity of driven and bored piles as described earlier in the Chapter, make use of the shear strength parameters of the soil as determined from laboratory tests. For cohesive soils, the undrained shear strength, $c_u$ can be determined from the field vane shear test also. For sensitive clays, in particular, sampling disturbances may cause reduction of the cohesive strength of the soil. Vane test results may be conveniently used in such clays.

For cohesionless soil, the angle of shearing resistance of the soil is best determined from the standard penetration test. This test is performed at different depths within boreholes and the average $N$ value for a layer is related to the angle of shearing resistance, $\phi'$.

A number of semi-empirical relationships have been proposed to obtain the skin friction and end resistance directly from the standard penetration test and static cone penetration test. Thorburn and MacVicar (1970), based on their experiences in Scotland, proposed an empirical formula for the evaluation of pile capacity directly from the standard penetration resistance of the sand as

$$Q_u = \frac{\bar{N}}{6} A_f + 4NA_p \quad \text{tonnes} \tag{9.19}$$

where $A_f$ is area of pile strength (m$^2$),
$A_p$ is area of pile tip (m$^2$),
$\bar{N}$ is the average $N$ value over the pile shaft, and
$N$ is the SPT value at pile base.

Tomlinson has given the relationship for ultimate bearing capacity of displacement piles from static cone penetration test.

$$Q_u = q_c A_p + \frac{\bar{q}_c}{200} A_s \tag{9.20}$$

where

$q_c$ = cone resistance in t/m$^2$ at pile tip. It is taken as the average value of cone resistance over a depth equal to three times the pile diameter above the tip and one pile diameter below the tip,
$A_p$ = area of pile tip in sq. m.,
$\bar{q}_c$ = average cone resistance over the embedded length of the pile shaft, and
$A_s$ = surface area of pile shaft in sq. m.

For taking unit base resistance as $q_c$, the pile should penetrate at least 8 diameter into the bearing stratum and sand should be present to a depth of at least 3 diameter beneath the base.

## 9.9 UNDER-REAMED PILES

Under-reamed piles are often used as load bearing and anchor piles in expansive clays. A single under-reamed pile is suitable for anchor pile while double under-reamed piles are used to increase the load bearing capacity of the pile, this is shown in Fig. 9.16. The ultimate capacity of an under-reamed pile is given by

$$Q_u = \sum \alpha c_{u1} f_s + \frac{\pi d_0^2}{4} c_{u2} N_c \tag{9.21}$$

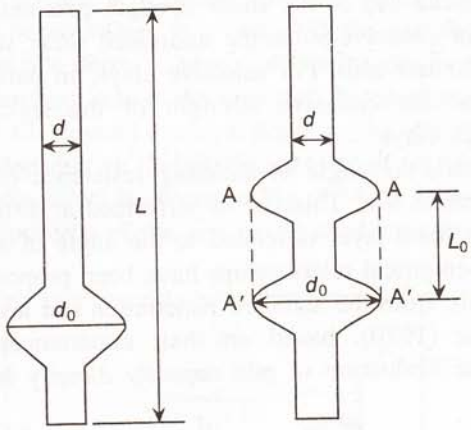


**Fig. 9.16** Under-reamed pile.

where $c_{u1}$ = undrained shear strength of the clay along pile shaft,
$\alpha$ = adhesion factor,
$d_0$ = diameter of under-reamed,
$c_{u2}$ = undrained shear strength of the clay at pile tip, and
$N_c$ = bearing capacity factor.

For double and multi-under-reamed piles, the soil between the bulbs acts as part of the pile and the frictional resistance for the length, $L_0$ may be calculated for the diameter, $d_0$ while for rest of the pile length above the under-ream, the skin friction develops over the diameter $d$. Mohan et al. (1967) suggest an optimum spacing of $1.25d_0 - 1.5d_0$ between bulbs and under-reamed diameter, $d_0$ approximately equal to $2.5d$.

Under-reamed piles are not normally recommended for cohesionless soil owing to doubts about formation of bulb in soils having no cohesion.

## 9.10 ALLOWABLE LOAD ON PILES FROM STATIC ANALYSIS

The load carrying capacity of a pile is determined from separate evaluation of the ultimate skin friction and the ultimate base resistance. The two are added together to arrive at the ultimate capacity of the pile, refer Eq. (9.2). However, this would imply a total settlement of the order of 20–30% of the pile diameter if the ultimate base resistance is to be fully mobilized, the skin friction having already mobilized at a settlement of only 0.5–1% of the pile diameter. For large diameter piles (diameter > 600 mm) that are now being increasingly used, this means a total settlement which may go beyond the permissible limit for an engineering structure. Therefore, the allowable load on a pile has to be restricted to the extent by which the settlement is to be restricted for the pile. A factor of safety of 2.5 generally ensures that the settlement is well within the permissible limits, that is,

$$Q_a = \frac{Q_u}{2.5} \tag{9.22}$$

where, $Q_a$ = allowable load on pile.

However, it may be noted that a concept of overall factor of safety does not necessarily imply identical factors of safety with respect to both frictional resistance and base resistance of a pile. Tomlinson (1977) has observed that for a large diameter bored pile in stiff clay, an overall factor of safety equal to 2.0 will result in the mobilization of full frictional resistance (i.e., $FS = 1$) while only 22% of the ultimate base resistance will come into play (i.e $FS = 5$). Settlement of a pile foundation will, therefore, be primarily governed by the compression of the soil around the pile shaft where the load is transmitted to the soil by skin friction.

Design of a pile foundation involves not only the determination of the allowable load on a pile from consideration of ultimate resistance of single pile but also ensuring the stability of the pile group where a large number of closely spaced piles are provided to support the column load. The entire soil including the pile group will be stressed as a block and the settlement of the pile group will have to be evaluated under the working load and the design should ensure that the settlement is acceptable. Group action of piles is discussed in Section 9.12.

## 9.11 DYNAMICS OF PILE DRIVING (DYNAMIC ANALYSIS)

The resistance to penetration of a pile during driving may be related to its static bearing capacity by applying the principal of conservation of energy as

$$WH = RS \tag{9.23}$$

where $W$ = weight of driving hammer,
$H$ = height of fall of hammer,
$R$ = resistance to penetration, and
$S$ = pile penetration under each blow.

The left hand side of Eq. (9.23) is the energy supplied per blow, and the right hand side is the corresponding work done to facilitate the penetration of pile. The basic elements involved in the driving analysis is shown in Fig. 9.17.

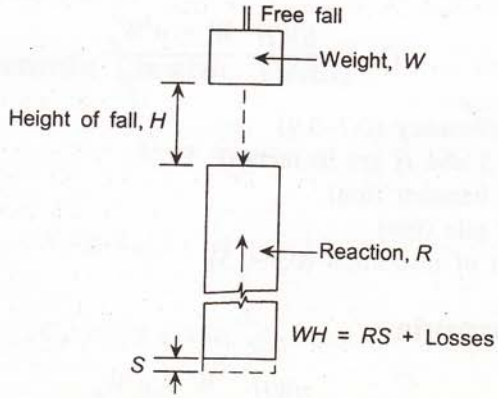


**Fig. 9.17** Dynamics of pile driving.

Equation (9.23) is, to some extent, a simplification of a complex field problem. In reality, following uncertainties tend to influence the measured response of the pile to the driving energy:

1. The soil resistance is not constant during pile driving because of elasticity and damping characteristics of soil.
2. The elastic compression of the cap block, cushion, pile, and soil absorb some energy and does not contribute to the penetration of pile.
3. Some energy is lost through impact, and the sound and heat generated during the hammer blow.
4. A pile is a long, slender member and at any instant, different lengths of the piles experience different kinds of motion in the soil.

Notwithstanding the above uncertainties a number of pile driving formulae have been developed to determine the ultimate capacity of the pile during driving. They differ mainly in the manner of accounting for energy losses involved in the driving operation. Some of the commonly used formulae are discussed in the subsequent parts of this section.

### 9.11.1 ENR Formula

The earliest pile driving formula assumes that for a given hammer blow, the resistance increases in an elastic manner as the pile is displaced, remains constant for further displacement, and finally falls to zero as the pile rebounds. Equating the energy supplied to the work done, the following formula was obtained.

$$WH = Q_u(S + C) \tag{9.24}$$

where $W$ = weight of hammer (ton),
$H$ = fall of hammer (ft),
$S$ = penetration per blow (in),
$R$ = pile resistance (ton), and
$C$ = constant which accounts for elastic settlement of pile-soil system (1.0 in for drop hammer and 0.1 in for single acting steam hammer)

Equation (9.24) has subsequently been revised to a more generalized form,

$$Q_u = \frac{EWH}{S + C} \frac{W + n^2 W_p}{W + W_p} \tag{9.25}$$

where $E$ = hammer efficiency (0.7–0.9)
$C$ = 0.1 in (if $S$ and $H$ are in inches)
$W$ = weight of hammer (ton)
$W_p$ = weight of pile (ton)
$n$ = coefficient of restitution (0.4–0.5)

### 9.11.2 Hiley Formula

$$Q_u = \frac{\eta WH}{S + C/2} \frac{W + n^2 W_p}{W + W_p}$$

Here, $Q_u$, $W$, $H$, $n$, $S$, and $W_p$ have the same meaning as in Eq. (9.25).

$\eta$ = efficiency of hammer blow (0.75–1.0)

$C$ = a factor which accounts for energy losses due to elastic compression of pile, $C_1$, elastic compression of the head assembly, $C_2$, and elastic compression of the soil, $C_3$, that is,

$$C = C_1 + C_2 + C_3$$

The approximate values of $C_1$, $C_2$, and $C_3$ to be used in Hiley formula for concrete piles are given in Table 9.2.

**Table 9.2** Values of $C_1$, $C_2$, $C_3$ in Hiley formula

| | |
|---|---|
| $C_1$ = 0.075–0.10 in, for hard driving | |
| $C_2 = R_u L/AE_p$, | where $R_u$ = ultimate test load, $L$ = Length of pile, $A$ = Cross sectional area of pile, and $E_p$ = Elastic modulus of pile material. |
| $C_3$ = 0.1 in (0 for hard soil and 0.2 for resilient soil) | |

## 9.11.3 Simplex Formula

This formula has been found to give quite good prediction of load carrying capacity for driven piles in alluvial deposits. The ultimate capacity is given by:

$$Q_u = NWH\frac{\sqrt{(L/50)}}{L(1+S)} \tag{9.26}$$

where $Q_u$ = ultimate load in tons,

$L$ = embedded length of pile in ft.,

$W$ = weight of hammer in tons,

$N$ = total number of blows,

$S$ = penetration for last blow in inches, and

$H$ = drop of hammer in ft.

## 9.11.4 Janbu's Formula (Janbu, 1953)

$$Q_u = \frac{EH}{K_u S} \tag{9.27}$$

where

$$K_u = C_d\left(1 + \sqrt{1 + \frac{\lambda}{C_d}}\right);$$

$$C_d = 0.75 + 0.14\left(\frac{W_p}{W}\right), \text{ and}$$

$$\lambda = \frac{EHL}{A_p E_p S^2}$$

The ultimate pile capacity as determined from the pile driving formulae may be used to determine the safe load capacity of a pile by using a factor of safety. In view of the uncertainties involved in the calculation, a high factor of safety, not less than 3, should be used. The early ENR formula even recommended a factor of safety equal to 6.

Sorensen and Hansen (1957), Housel (1966), and Olsen and Flaate (1967) made comprehensive studies on the use of different pile driving formulae in predicting the pile capacity. It appears from their studies, "if driving formulae are to be used, those which involve the least uncertainty are the Hiley and Janbu formulae while the most uncertain is the ENR formula", (Poulos and Davis, 1980).

### 9.11.5 Wave Equation

It has been long recognized that the phenomenon of pile driving involves transmission of compression waves down the pile. Smith (1960) gave a practical method of solving the wave equation using a digital computer for studying the dynamic behaviour of a pile during driving. The analysis involves dividing the pile into a number of segments, each beam represented by a weight joined to the adjacent weights by springs. The hammer, pile cap, cap block, and cushion block are also represented by weights and springs. The soil resistance is represented by a Kelvin rheological model consisting of spring and dash pot. A set of equations can be set up considering dynamic equilibrium of each element. The pile resistance corresponding to a given set observed in the field can be obtained by solving the set of simultaneous equations. The procedure has been described by Bowles (1968, 1974).

The success of this method is handicapped by the lack of knowledge of essential parameters involved in the equation. Nowadays, with the advent of sophisticated equipment such as Pile Driving Analyzer (PDA) and suitable transducers which can be attached to piles to measure the relevant parameters, for example, velocity, acceleration, and so on, the method is becoming increasingly popular. A number of computer program have been developed to get direct output of the pile capacity from the PDA.

### 9.11.6 Limitations of Dynamic Analysis

Most of the dynamic formulae are based on assumptions which have little regard for the driving of an actual pile. For instance, Newtonian Impact Theory is not valid for pile driving because of the presence of cushioning material. Also it is difficult to correctly estimate the various energy losses involved in pile driving. Although Smith's wave equation is theoretically more sound, it's practical usefulness is limited by the lack of precise information about quake, damping factor, and distribution of resistance through the shaft and the base.

One major limitation of dynamic analysis is that the dynamic resistance can hardly be equal to the static bearing capacity. Even if this may be assumed to be true at the time of driving or immediately afterwards, the situation is likely to change with time, and, as a result, there may be significant difference between the actual pile capacity and the value obtained from dynamic analysis. Nevertheless, dynamic analysis may be used in pile driving to obtain assessment of the variation of soil consistency with depth. It gives a good indication if the pile has reached good bearing stratum. Also, through proper correlation with load test data, a dynamic formula can be used to have a very good control over the pile installation.

## 9.12 PILE GROUPS

Piles are commonly used in groups with a foundation slab or pile cap cast over the pile heads to distribute the load to the piles. Although the piles in a group are generally identical, the group capacity is not necessarily the same as the capacity of single pile multiplied by the number of piles in the group. Also, the settlement of a pile group may be different from the settlement of a single pile subjected to the same average load per pile. This is because of interaction among piles which is known as *group action*.

Figure 9.18 shows the pressure bulb of a single pile and that of a group of piles installed in a homogeneous medium. In case of a closely spaced group, the pressure bulb of individual piles overlap and a much larger bulb is formed. This is likely to result in a larger settlement. Also, due to overlapping of stresses, the capacity of individual piles may decrease and result in a lower capacity of the group.

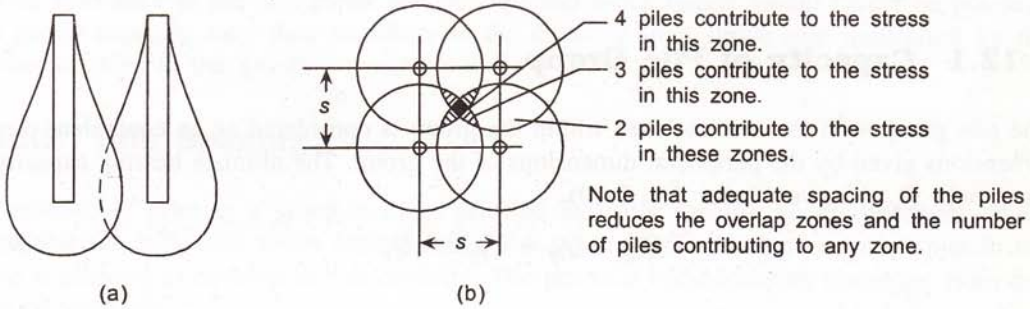


**Fig. 9.18** Pressure bulb for single pile and pile group.

A vivid example of this effect is seen in the foundations of the Charity Hospital Building in New Orleans, (Terzaghi, 1942), as depicted in Fig. 9.19. A steel framed building with stone facing was founded on 13 m long timber piles. Soil investigation was done prior to design to a depth of 15 m and the piles were driven into the dense sand below the soft

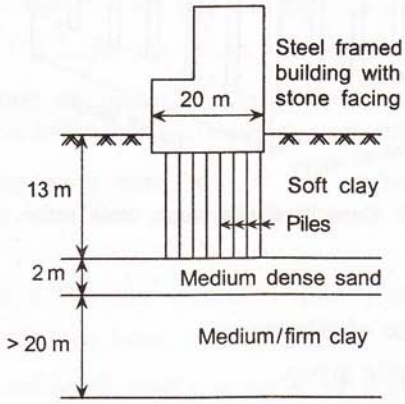


**Fig. 9.19** Foundation for Charity Hospital Building, New Orleans (Terzaghi, 1942).

clay. Against an estimated working load of 15 ton, a single pile was tested for a maximum load of 30 ton and gave a settlement of only 6 mm. On this basis, a maximum settlement of 6 mm was anticipated for the building. However, two years after construction, the building had settled 270 mm with a maximum differential settlement of 200 cm. Obviously, as later investigation revealed, the pressure bulb below the pile group extended well into the compressible clay below the sand layer which caused large settlement of the building. In the Hotel Sao Paulo building which is founded on spread footings supported on RCC piles, the settlement of the pile group under full structural load was 15 mm while the test pile showed settlement of only 3 mm (Vargas, 1948). Another good example of this group effect is an apartment house in Vienna where the settlement of the building was 20 times more than that of the test pile under the same load (Terzaghi, 1955).

Theoretical analysis of pile groups considering interaction of piles is quite complicated. Load carrying capacity and settlement of pile groups are generally determined by methods based on empirical evidences obtained chiefly from model tests and field observations.

### 9.12.1 Capacity of Pile Group

The pile group with the soil enclosed within the group is considered as an equivalent pier of dimensions given by the peripheral dimensions of the group. The ultimate bearing capacity of the group, $Q_{ug}$ is given (refer Fig. 9.20).

$$Q_{ug} = Q_{fg} + Q_{pg} \leq nQ_u \tag{9.28}$$

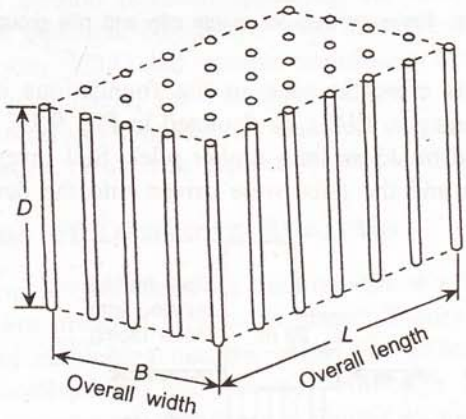


**Fig. 9.20** Capacity of pile group: block action.

where

$Q_{fg}$ = frictional resistance of pile group,

$Q_{pg}$ = point bearing of pile group,

$Q_u$ = capacity of a single pile, and

$n$ = no. of piles in the group.

For friction piles in clay,

$$\left.\begin{aligned} Q_{fg} &= 2(B + L)D_f c_u \\ Q_{pg} &= (B \times L)9c_u \end{aligned}\right\} \tag{9.29}$$

where

$B$ = width of pile group,

$L$ = length of pile group,

$D_f$ = depth of piles,

$c_u$ = average undrained shear strength of clay along the pile depth, and

Terzaghi and Peck (1967) recommended $FS = 3$ to obtain allowable load on the pile group. This approach appears reasonable for friction piles in clay. For piles resting in sand, end bearing resistance of the pile group will be high and block failure would hardly be possible. The group capacity may then be taken as the capacity of a single pile multiplied by the number of piles in the group.

### 9.12.2 Pile Spacing

The spacing of piles in a group is to be selected basically keeping under consideration the factor that the influence zones around individual piles do not overlap and each pile in the group is allowed to develop its full capacity. The practical considerations important from this point of view are

(a) *The type of soil and the method of installation:* Larger spacing may be required for driven piles in saturated clay to minimize the effect of heaving.

(b) *The minimum spacing*: Should be such that with due tolerance for error in layout and verticality, reasonable gap is maintained between adjacent piles.

(c) *The efficiency of the group:* The bearing should be such that the group efficiency is close to unity, that is, each pile can develop its full capacity.

(d) *The economy:* The larger the group, the more costly is the cap.

The building codes provide minimum allowable spacing of piles in a group. I.S. 2911 (part I), 1979, suggests the following guidelines for spacing:

(a) For piles bearing on a hard stratum and deriving their strength mainly from end bearing, the minimum spacing shall be $2.5d$, $d$ being the diameter of the pile.

(b) For friction piles in clay, the minimum spacing shall be $3d$.

(c) For piles driven through loose sand or fill, the minimum spacing may be $2d$.

However, the most commonly used spacing is $3d$. Figure 9.21 shows some typical pile groups with different number of piles.

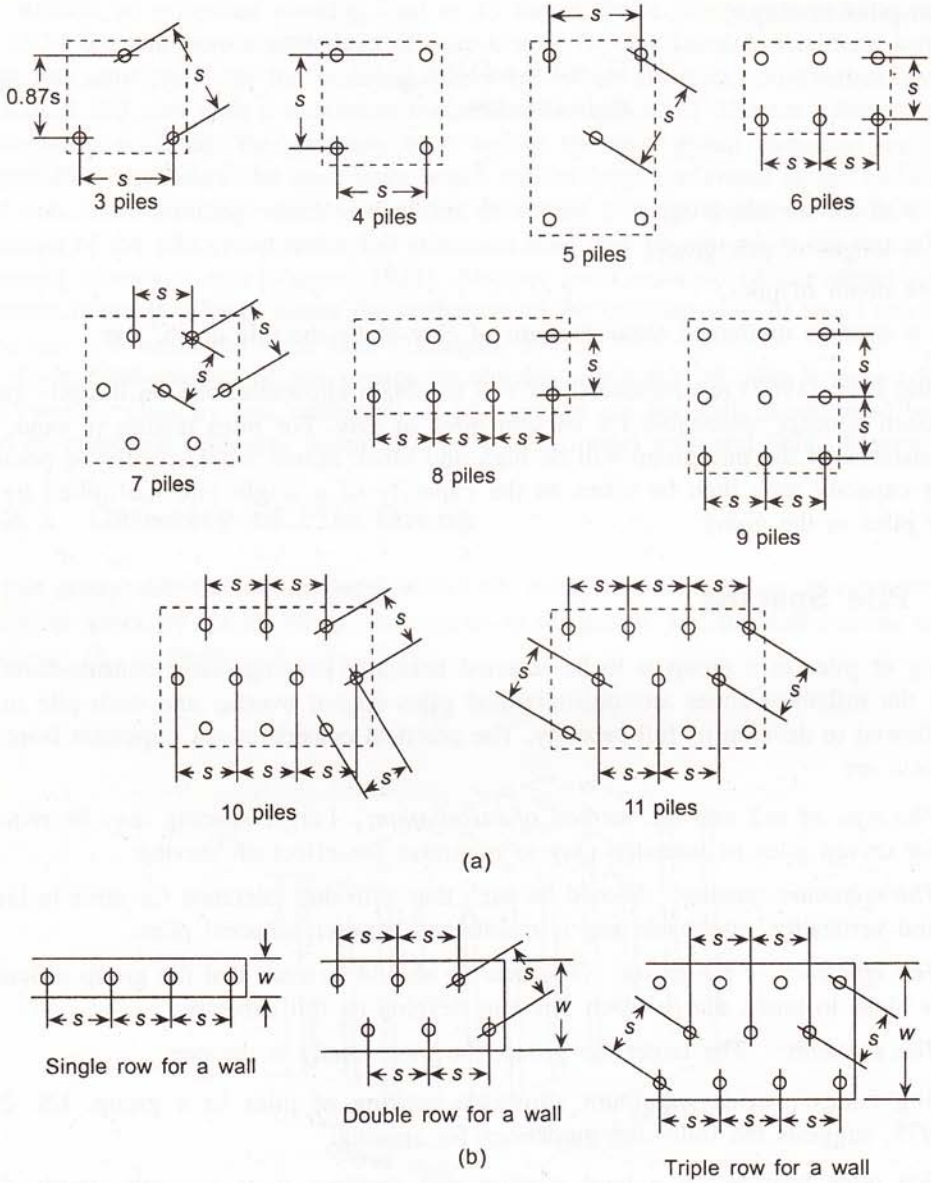


**Fig. 9.21** Typical pile groups.

## 9.12.3 Pile Group Subjected to Vertical Load and Moment

A pile group may be subjected to moments due to horizontal load or eccentrically applied vertical load. The following approximate method is commonly used in practical design of group of identical piles subjected to vertical load and moments. The cap is assumed to be rigid, and the reaction of any pile is assumed to be proportional to the displacement of the pile head.

Figure 9.22 shows a pile group subjected to a vertical load, $V$ at its CG = 0 (CG = centre of gravity) and moments $M_{xx}$ and $M_{yy}$ about XX and YY axes respectively, passing through 0. Due to vertical load, $V$ there is uniform deflection and reaction. Therefore, pile reaction due to $V = V/N$, where $N$ represents no. of piles.

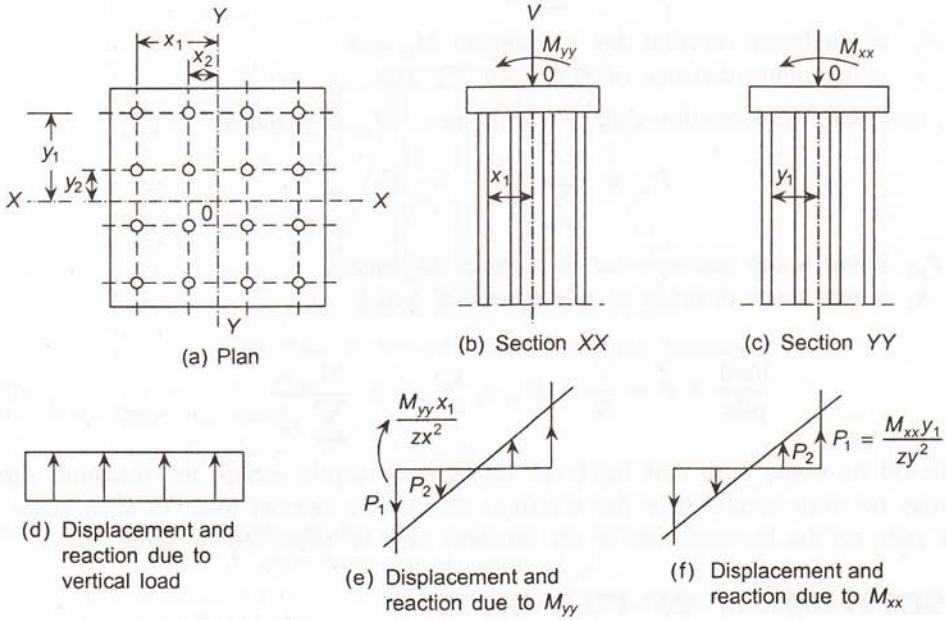


**Fig. 9.22** Pile group subjected to vertical load and moment.

Due to $M_{yy}$, there is tilting of the cap about 0, and the displacement of the head of each pile is proportional to the distance of the pile from 0, as shown.

For a row of $N$ piles,

$$\frac{P_{y_1}}{x_1} = \frac{P_{y_2}}{x_2} = \cdots = \frac{P_{y_n}}{x_n}$$

This gives,

$$P_{y_1} = P_{y_2}\frac{x_1}{x_2};\ P_{y_2} = P_{y_1}\frac{x_2}{x_1};\cdots;\ P_{y_n} = P_{y_1}\frac{x_n}{x_1}$$

But

$$M_{yy} = P_{y_1}x_1 + P_{y_2}x_2 + \cdots + P_{y_n}x_n$$

or

$$M_{yy} = P_{y_1}\frac{x_1^2}{x_1} + P_{y_2}\frac{x_2^2}{x_1} + \cdots + P_{y_n}\frac{x_n^2}{x_1}$$

$$= \frac{P_{y_1}}{x_1}(x_1^2 + x_2^2 + \cdots + x_n^2)$$

$$P_{y_1} = \frac{M_{yy}x_1}{\sum x_n^2} = \frac{M_{yy}}{z_{xx}}$$

On the other side of CG, the reaction is upward, that is, $P_y$ is negative. Thus,

$$P_{y_1} = \frac{\pm M_{yy} x_1}{\sum x_n^2} = \frac{\pm M_{yy}}{z_{xx}}$$

where $P_{y1}$ = maximum reaction due to moment $M_{yy}$ and
$x_1$ = maximum distance of pile from YY axis.

Similarly, maximum pile reaction due to the moment, $M_{xx}$ is given by

$$P_{x_1} = \frac{\pm M_{xx} y_1}{\sum y_n^2} = \frac{\pm M_{xx}}{z_{yy}}$$

where, $P_{x1}$ = maximum reaction due to moment $M_{xx}$ and
$x_1$ = maximum distance of pile from XX axis.

Thus,

$$\frac{\text{load}}{\text{pile}} = P = \frac{V}{N} \pm M_{yy} x_1 \sum x_n^2 \pm \frac{M_{xx} y_1}{\sum y_n^2} \tag{9.30}$$

It should be noted here that for large moment on a pile group, the reactions due to moment may be even greater than the reactions due to the vertical load. In such cases, the outermost piles on the leeward side of the moment may be subjected to uplift forces.

## 9.13 SETTLEMENT OF PILE GROUPS

As yet, there is no precise method of estimating the settlement of pile groups. The problem is still approached in an approximate manner.

### 9.13.1 Pile Groups in Cohesive Soil

The settlement of a pile group in predominantly cohesive soil is given by the sum of the immediate or elastic settlement and the long-term consolidation settlement of the subsoil. The procedure for calculating these settlements are similar to that for raft foundations with appropriate depth corrections as described in Chapters 7 and 8. However, it is, necessary to determine the load distribution around a pile group in order to obtain the size and depth of the equivalent raft from which the settlement is to be determined.

It requires rigorous mathematical analysis, for example, finite element technique, to determine the true stress distribution around a pile group (Poulos and Davis, 1980) but such analysis is highly complex and is seldom used in practical design because pile foundations, in any case are expected to undergo small settlement. Simplified method of load distribution has been suggested by Terzahi and Peck (1962) and Tomlinson (1967, 1977). Accordingly, total load, $Q$ is assumed to get dispersed from the foundation level at a slope of 4:1 upto the depth of an imaginary raft at depth $2D_f/3$, as shown in Fig. 9.23. Here, the size of the imaginary raft becomes $(B + D_f/6)(L + D_f/6)$. Thereafter, the load is assumed to get dispersed at a slope of 2:1 into the underlying strata. If the pile group passes through a very weak stratum to an underlying hard stratum, the load is assumed to spread at a slope 4:1 on an equivalent raft at a depth $2L/3$, where $L$ is the embedment of the pile in the stiff stratum.

Thereafter, a spread of 2:1 may be followed. For a wholly end bearing pile, the load is assumed to get transferred to an equivalent raft at the level of pile tip without any dispersion through the upper strata. It is, therefore, necessary to determine the compressibility characteristics of the soil below the depth $2D_f/3$. The settlement of the pile group may then be calculated in the usual way.

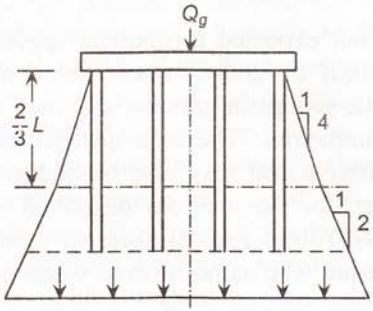


**Fig. 9.23** Settlement of pile group: load dispersion.

(a) *Immediate settlement*

$$\rho_i = \alpha \frac{q_n B}{E}\left(1 - \nu^2\right) I_\rho \tag{9.31}$$

where $q_n$ = net pressure on the equivalent raft at depth $2D_f/3$,
$B$ = width of equivalent raft at depth $2D_f/3$,
$\nu$ = Poisson's ratio of soil below the depth equivalent raft (may be taken as 0.5),
$E$ = elastic modulus of the soil below equivalent raft,
$I_\rho$ = influence coefficient, $f(L/B)$, and
$\alpha$ = depth correction factor, $f(D_f/B,\ L/B)$

The elastic modulus of the soil may be determined from the undrained shear strength of the soil by using the relationship $E = (500\text{–}1000)\, c_u$ as discussed in Chapter 7. The influence coefficient, $I_\rho$ and the depth correction factor, $\alpha$ are given by the elastic analysis of Boussinesq (1985) and Fox (1948) (refer Chapter 7).

(b) *Consolidation settlement*

The consolidation settlement of the pile group is obtained from the standard equation,

$$\rho_c = \left(\sum \frac{C_c}{1 + e_0} H \log \frac{p_o + \Delta p}{p_o}\right) \alpha\mu \tag{9.32}$$

or,

$$\rho_c = \left(\sum m_v \Delta p H\right) \alpha\mu$$

where $C_c/(1 + e_0)$ and $m_v$ are respectively the compressibility index and the coefficient of volume decrease for the appropriate stress level of the relevant strata,
$H$ is the thickness of strata,
$p_o$ and $\Delta p$ are the in-situ vertical effective stress and the increase of stress in the respective strata, and
$\alpha$ and $\mu$ are respectively the depth and pore-pressure correction factors.

To know the effective depth of soil below the pile group, the best method is to determine the stress increment ratio $\Delta p/p_o$ at different depths and consider the depth of soil for which $\Delta p/p > 0.1$.

## 9.13.2 Pile Groups in Cohesionless Soil

Pile foundations in sand are not expected to undergo appreciable settlement because of the low compressibility of medium to dense, where piles are usually terminated. Still, if necessary, the settlement of pile groups in granular soil may be determined by using the same methods as given for raft foundations. The load distribution in the soil and the equivalent raft concept proposed for cohesive soil may also be adopted to obtain the geometry of the problem to be solved. Further, for the methods described in Chapter 7 for foundations on sand, Schultze and Sherif (1973) used case histories to establish a method of predicting the settlement of foundation on sand. The same method when adopted for pile groups gives

$$\delta = \frac{Sq_u}{N^{0.81}\left(1 + 0.4\dfrac{D_f}{B}\right)} \tag{9.33}$$

where $S$ = settlement coefficient,
$q_u$ = average pressure on the equivalent raft,
$N$ = average SPT value over a depth $2B$ below the foundation level or $D_s$ if the depth of cohesionless soil is less than $2B$,
$D_f$ = depth of equivalent raft, and
$B$ = width of equivalent raft.

The settlement coefficient, $S$ varies with $D_f/B$ as shown in Fig. 9.24.

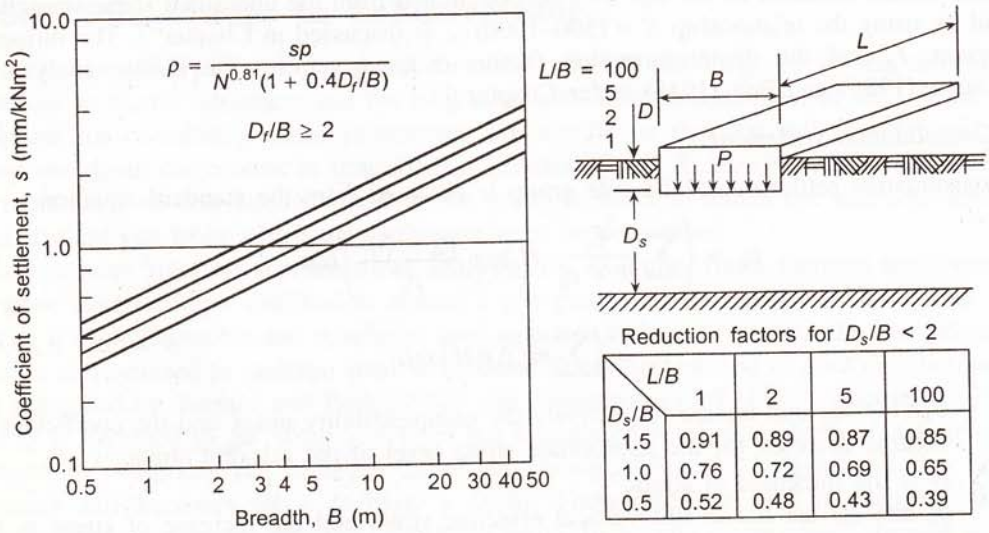


Reduction factors for $D_s/B < 2$

| $D_s/B$ \ $L/B$ | 1 | 2 | 5 | 100 |
|---|---|---|---|---|
| 1.5 | 0.91 | 0.89 | 0.87 | 0.85 |
| 1.0 | 0.76 | 0.72 | 0.69 | 0.65 |
| 0.5 | 0.52 | 0.48 | 0.43 | 0.39 |

**Fig. 9.24** Settlement coefficient, $S$ versus $D_f/B$ (Schultze and Sherif, 1973).

## 9.14 UPLIFT RESISTANCE OF PILES

A straight shaft pile, when subjected to uplift forces, derives its ultimate capacity from frictional resistance of the pile which can be determined in the same way as indicated for piles under compression (see Section 9.7). However, for cyclic loading, skin friction may be reduced by the degradation of soil strength at the pile–soil interface under repetitive load. In particular, for sandy soils, reduction in uplift capacity to 50% of the ultimate skin friction has been reported (St. John et al., 1983). Even for cohesive soils, Radhakrishnan and Adams (1973) have observed 30–50% reduction of uplift capacity in short augured piles. Such reduction in uplift capacity has been attributed to long term creep under sustained loading whereby the strength of the soil reaches its residual value. As a general rule, a factor of safety of 3–4 on the frictional resistance calculated for compression may be applied to determine the uplift capacity of piles. However, it should be noted that an upward movement of only 0.5–1% of the pile diameter is required to mobilize the peak frictional resistance.

In case of pile groups, the uplift resistance may be calculated by taking the resistance of the soil enclosed within the groups, as depicted in Fig. 9.25. For cohesionless soil, an assumed spread of 1:4 from the pile tip to the ground and the weight of soil block enclosed within the group give the frictional resistance. In such cases, Tomlinson suggests a factor of safety equals to unity against uplift since skin friction around the periphery of the group is ignored. The submerged weight of the soil below the ground water table should be taken.

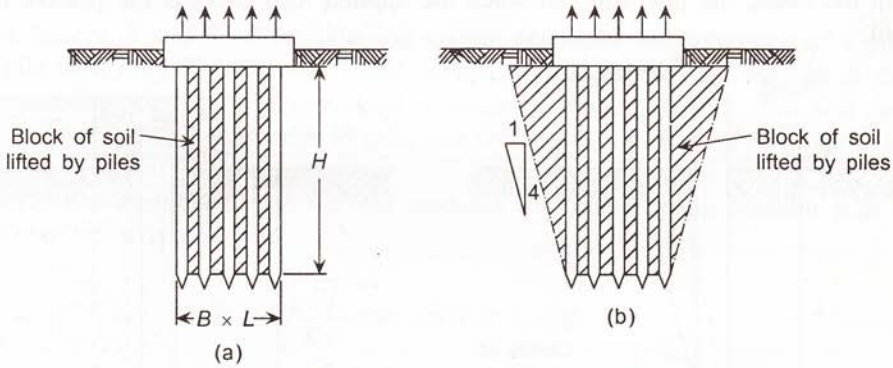


**Fig. 9.25** Uplift resistance of pile group.

For cohesive soils, the uplift resistance of the block may be obtained by summing up the undrained shearing resistance around the periphery of the block and the weight of soil enclosed by the group as

$$Q_u = 2(L + B)D_f c_u + W \tag{9.34}$$

where $L$ = length of the pile group,
$B$ = width of the pile group,
$D_f$ = depth of the pile group,
$c_u$ = average undrained shear strength of the clay, and
$W$ = weight of the soil enclosed within the block.

A safety factor of 3 should be used to determine the safe uplift capacity of the group.

## 9.15 PILES UNDER HORIZONTAL FORCES

Vertical piles can resist lateral forces to a certain extent depending on the strength and stiffness of the pile and the soil. According to I.S. 2911—1985, permissible lateral load of a vertical pile is 2–5% of the permissible vertical load. For greater horizontal load, additional reinforcement is to be provided in the pile or raker piles may be used.

Ultimate lateral resistance and load-deflection behaviour of a pile under lateral load is a complex problem of soil-structure interaction. The lateral load on the pile head is initially carried by the soil close to the ground surface resulting in elastic deformation of the soil. As the load increases, the soil yields and transfers the load to greater depths.

### 9.15.1 Failure Mechanisms

Short and long piles fail under different mechanisms. This subsection briefly discusses these failure mechanisms.

A short rigid pile, unrestrained at the head, tends to rotate or tilt as shown in Fig. 9.26, and passive resistance develops above and below the point of rotation on opposite sides of the pile. If the pile head is restrained by a cap, there will be lateral translation. In both the cases, the pile will fail when the applied load exceeds the passive resistance of the soil.

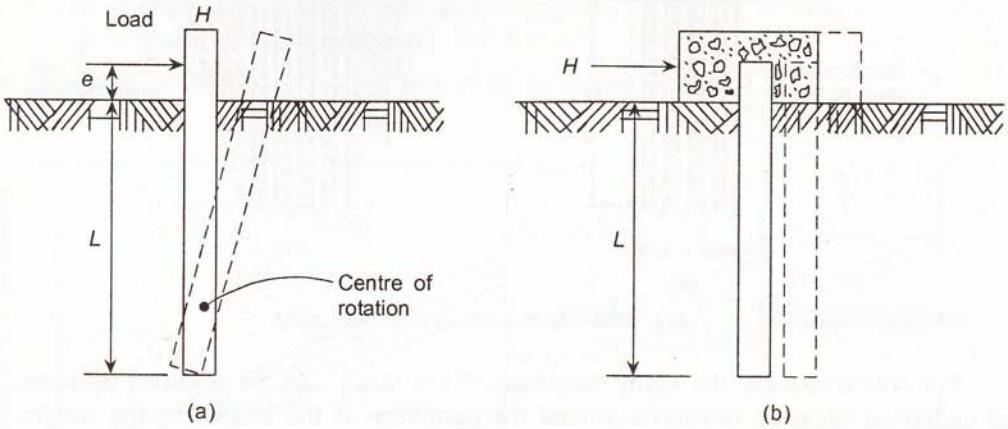


**Fig. 9.26** Failure mechanism of rigid pile under horizontal load: (a) free head, (b) fixed head.

For a long pile, the passive resistance is very large and pile cannot rotate or tilt. The lower portion remains almost vertical due to fixity while the upper part deflects in flexure. The pile fails when a plastic hinge is formed at the point of maximum bending moment, Fig. 9.27.

As a consequence, a short pile fails when passive resistance of soil is exceeded (soil failure) and a long pile fails when the moment capacity is exceeded (structural failure).

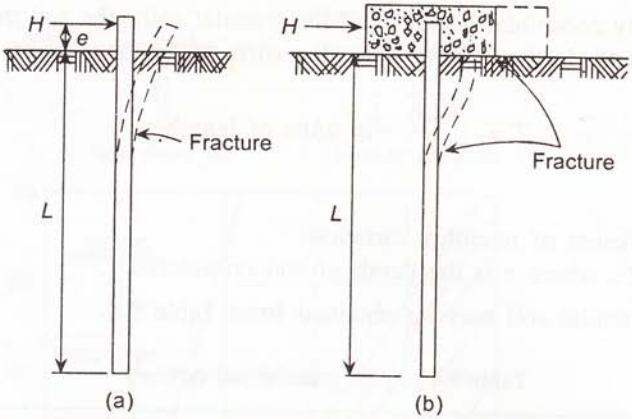


**Fig. 9.27** Failure mechanism of long pile under horizontal load: (a) free head, (b) fixed head.

For development of ultimate resistance, the lateral movement is generally too large. Therefore, after calculating the ultimate resistance and dividing by a factor of safety, it is necessary to check that the permissible deflection of pile head is not exceeded.

## 9.15.2 Stiffness Factors and Subgrade Modulus

The stiffness factors, $R$ and $T$, of the pile–soil system determine the behaviour of a pile as a short rigid pile or a long flexible one. These factors depend on the stiffness, $EI$ of the pile and the compressibility of the soil expressed in terms of a soil modulus. The soil modulus depends on the type of soil, the width of pile, and the depth of influence area and is related to Terzaghi's modulus of subgrade reaction.

For stiff overconsolidated clay, the soil modulus is assumed to be constant with depth, and the stiffness factor is given by

$$R = \sqrt[4]{\frac{EI}{KD}} \text{ in units of length} \tag{9.35}$$

where $K = K_1/1.5$ in which $K_1$ is Terzaghi's subgrade modulus in kg/m$^3$ or kN/m$^3$ and
$D$ = diameter of pile.

According to Terzaghi (1955), $K_1$ is related to the undrained shear strength of the clay as shown in Table 9.3.

**Table 9.3** Values of $K_1$ for different consistencies of clay (after Terzaghi)

| *Consistency* | *Unconfined comp. strength, $q_u$*(kN/m$^2$) | *Range of $K_1$* (kN/m$^3$) | *Recommended, $K_1$* (kN/m$^3$) |
|---|---|---|---|
| Stiff | 100–200 | 18–36 | 27 |
| Very stiff | 200–400 | 36–72 | 54 |
| Hard | >400 | >72 | >108 |

For soft normally consolidated clays and for granular soils, the soil modulus is assumed to increase linearly with depth. For this case, the stiffness factor is given by

$$T = \sqrt[5]{\frac{EI}{n_h}} \quad \text{in units of length} \tag{9.36}$$

where

$n_h$ = coefficient of modulus variation
= $K\,D/x$, where $x$ is the depth of soil considered.

The $n_h$ values for granular soil may be obtained from Table 9.4.

**Table 9.4** $n_h$ for granular soil (kN/m$^3$)

| *Type of sand* | | *Loose* | *Medium* | *Dense* |
|---|---|---|---|---|
| Dry or moist sand | (Terzaghi (1955)) | 2500 | 7500 | 20000 |
| Sub merged sand | | 1400 | 5000 | 12000 |

For soft normally consolidated clay,

$$n_h = 350 \text{ to } 750 \text{ kN/m}^3$$

For soft organic silt,

$$n_h = 150 \text{ kN/m}^3$$

The criteria for behaviour of a pile as a short pile or a long pile are related to the embedded length, $L$ as follows:

Long Pile: $L \geq 4T$ or $L \geq 3.5R$

Short Pile: $L \leq 2T$ or $L \leq 2R$

## 9.15.3 Ultimate Lateral Resistance

The method suggested by Broms (Broms, 1964; Poulos and Davis, 1980) appears to be most convenient for design. Broms assumed simplified distribution of soil resistance for cohesive and cohesionless soils and determined the ultimate capacity of short and long piles in terms of the flexural rigidity of the pile. The design charts prepared by Broms are given Fig. 9.28 through Fig. 9.31.

In Fig. 9.28, the variation of $H_u/c_uD^2$ versus $L/D$ (where $H_u$ = ultimate horizontal load, $c_u$ = undrained shear strength of soil, $D$ = pile dia, $L$ = embedded length) have been plotted for short piles in cohesive soils. Curves for both restrained and unrestrained piles with different eccentricity ratio have been presented. In Fig. 9.29, the corresponding plots for short piles in cohesionless soil with design curves for $H_u/K_pD^3\gamma$ versus $L/D$ ($K_p$ = coefficient of passive earth pressure and $\gamma$ = unit weight of soil) are presented. The curves for long piles in cohesive soil are given in Fig. 9.30. The normalized ultimate lateral resistance, $H_u/c_uD^2$ is plotted against normalized yield moment, $M_{\text{yield}}/c_uD^3$. Figure 9.31 shows corresponding curves for cohesionless soil, where normalized ultimate lateral resistance, $H_u/K_pD^3\gamma$ has been plotted against normalized yield moment, $M_{\text{yield}}/K_p\gamma D^4$.

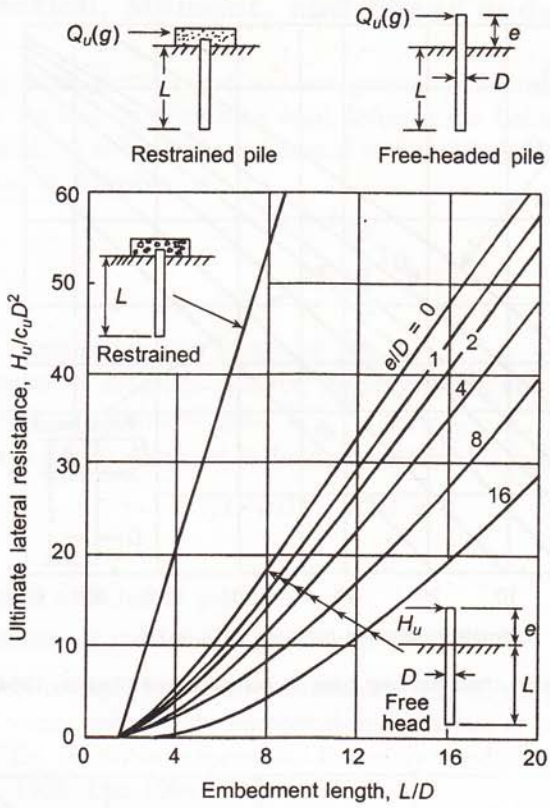


**Fig. 9.28** Design charts for short piles in cohesive soil (Broms 1964).

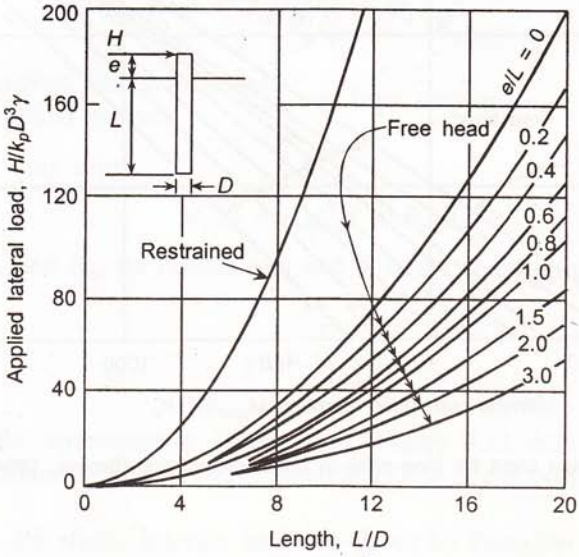


**Fig. 9.29** Design charts for short piles in cohesionless soil (Broms, 1964).

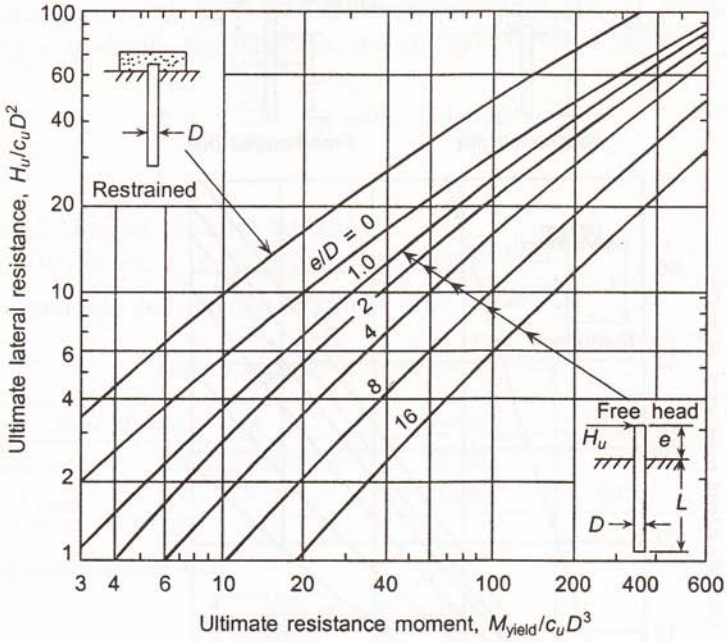


**Fig. 9.30** Design chart for long piles in cohesive soil (Broms, 1964).

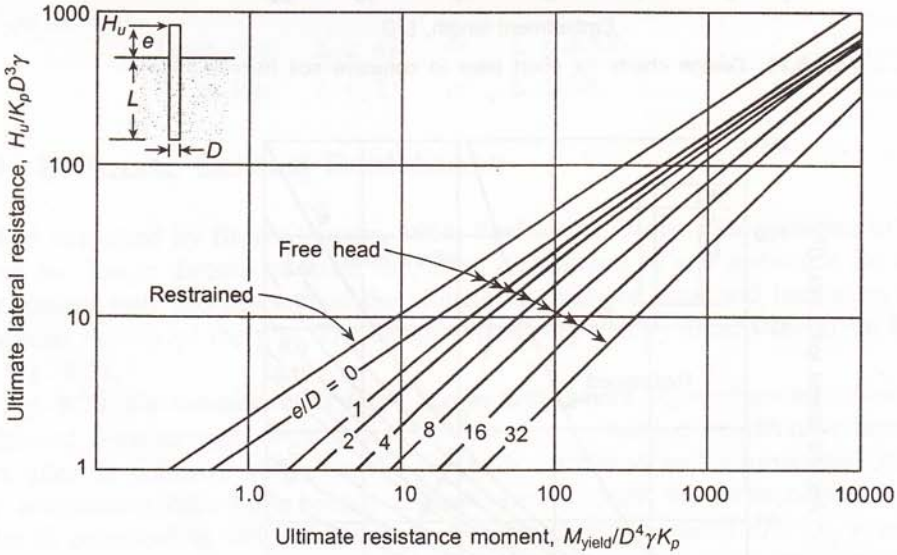


**Fig. 9.31** Design chart for long piles in cohesionless soil (Broms, 1964).

### 9.15.4 Deflection, Moment, and Shear under Working Load

Under the working load, the pile and soil are generally assumed to behave elastically, and Winkler model is applied to determine load-deformation behaviour of the pile. The soil pressure and deflection, $y$ at a point are assumed to be related through the horizontal modulus of subgrade reaction as follows:

$$p = Ky \tag{9.37}$$

or,

$$w = KDy \tag{9.38}$$

where

$w$ = soil reaction per unit length of pile,
$K$ = modulus of subgrade reaction (force/length$^3$), and
$D$ = diameter or width of pile.

The behaviour of the pile is assumed to be governed by the beam equation (Heteny, 1946)

$$E_p I_p D^4 y/D^4 + KDy = 0 \tag{9.39}$$

Where

$E_p$ = elastic modulus of pile and
$I_p$ = moment of inertia of pile section.

Closed form solution of Eq. (9.39) can be obtained for the simple case of constant $K$. For the cases where $K$ varies with depth, numerical analysis has to be applied.

A solution of Eq. (9.39) for appropriate boundary conditions gives the following results (Rees and Matlock 1956, Das 1998):

Pile deflection at any depth

$$x_z(z) = A_x \frac{Q_g T^3}{E_p I_p} + B_x \frac{M_g T^2}{E_p I_p} \tag{9.40}$$

where $Q_g$ = Applied lateral load and
$M_g$ = Applied moment } at frow surface

Moment in pile at any depth

$$M_z(z) = A_m Q_g T + B_m M_g \tag{9.41}$$

where $A_x$, $B_x$, $A_m$, and $B_m$ are coefficients and $T$ is the characteristic length of the pile–soil system given by

$$T = \sqrt{\frac{E_p I_p}{n_h}} \tag{9.42}$$

Table 9.4 gives the representative values of $n_h$. Figure 9.32 shows the variation of $A_x$, $B_x$, $A_m$, and $B_m$ for different values of $L/T$. Beyond $L/T > 5$, the coefficients remain essentially constant.

For cohesive soil, the elastic solution has been given by Davisson and Gill (1963). The pile deflection $x_z(z)$ is given by

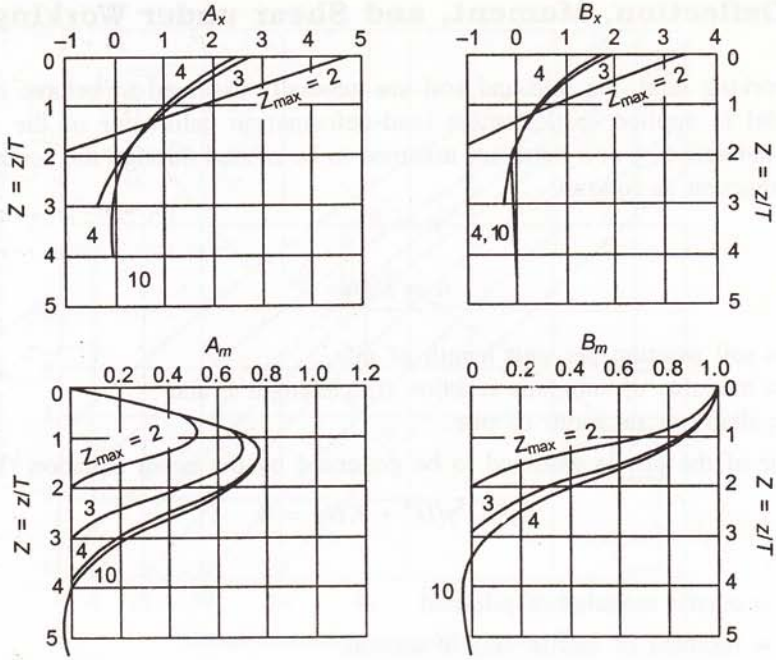


**Fig. 9.32** Pile deflection and moment in cohesionless soil: Elastic analysis (Reese and Matlock (1956), Das (1998)).

$$x_z(z) = A'_x \frac{Q_g R^3}{E_p I_p} + B'_x \frac{M_g R^2}{E_p I_p} \tag{9.43}$$

and

$$M_z(z) = A'_x Q_g R + B'_m M_g \tag{9.44}$$

where $A'_x$, $B'_x$, $A'_m$, and $B'_m$ are coefficients and $R = \sqrt{E_p I_p / K}$.

The variation of $A'_x$, $B'_x$, $A'_m$, and $B'_m$ with $z$ is given in Fig. 9.33.

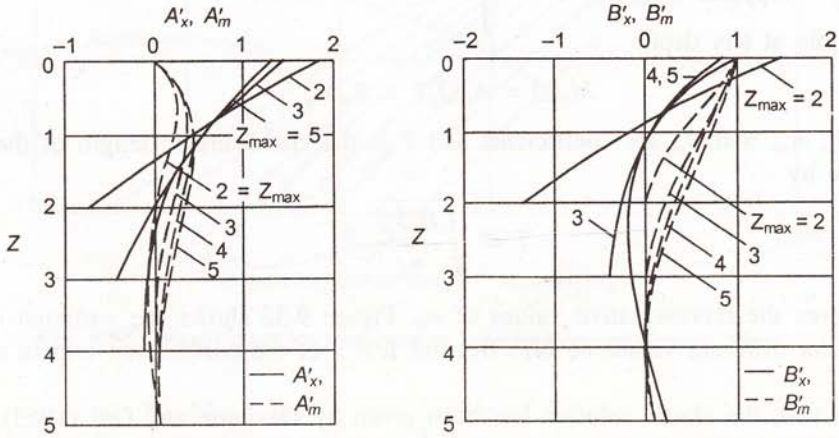


**Fig. 9.33** Pile deflection and moment in cohesive soil: Elastic analysis (Davisson and Gill, 1963).

Broms (1966) worked out a procedure for obtaining the deflection of the pile head from an ultimate load analysis. He presented the relationship between dimensionless parameters.

$$\frac{x_0(E_pI_p)^{3/5}(n_h)^{2/5}}{Q_gL} \text{ and } \eta L, \qquad \text{for sand}$$

and

$$\frac{x_0(KDL)}{Q_g} \text{ and } \beta L, \qquad \text{for clay.}$$

where $x_0$ = deflection at pile head,
$E_p$ = elastic modulus of pile,
$I_p$ = moment of inertia of pile section,
$n_h = \dfrac{K_z}{h}$ = constant of modulus of horizontal subgrade reaction,
$K$ = modulus of subgrade reaction,
$D$ = diameter of pile,
$L$ = length of pile,
$Q_g$ = working load,

$$\eta = \sqrt{\frac{n_h}{E_pI_p}}$$

$$\beta = \sqrt{\frac{KD}{4E_pI_p}}$$

These relationships are illustrated through Figs. 9.34 and 9.35.

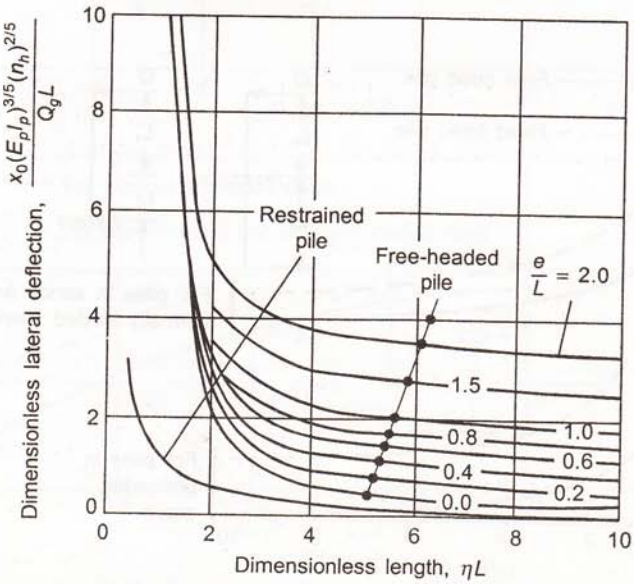


**Fig. 9.34** Deflection of pile head under working load: Cohesionless soil (Broms, 1966).

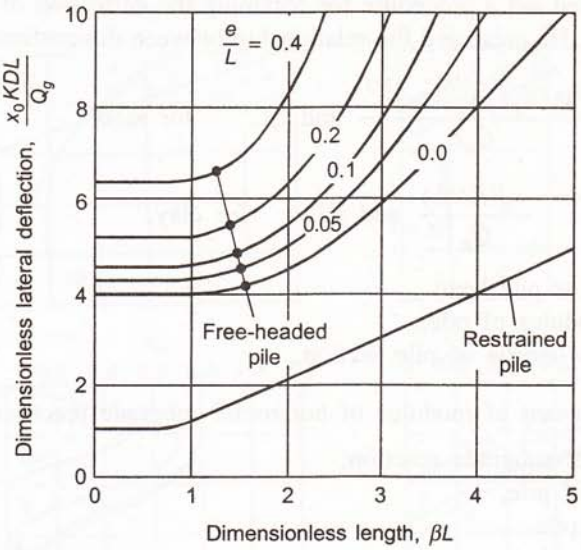


**Fig. 9.35** Deflection of pile head under working load: Cohesive soil (Broms, 1966).

## 9.15.5 I.S. Code Method

(I.S. 2911 (Part 1/Sec. 4)—1984, Amended in 1987)

In this method, a long pile is considered as a cantilever with fixity at some depth below the ground surface. The depth of fixity depends on the relative stiffness of pile and soil, Fig. 9.36.

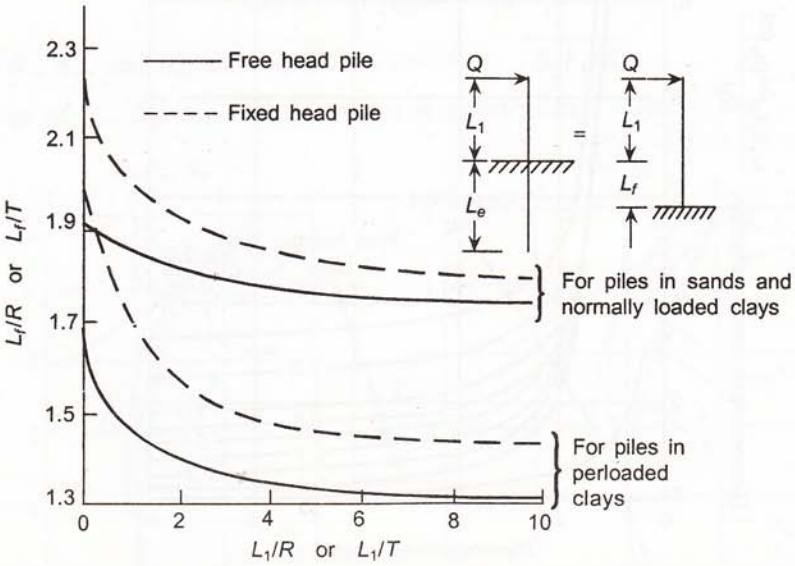


**Fig. 9.36** Analysis of lateral load: IS code method.

Considering the pile as an equivalent cantilever, the pile load deflection, $y$ is obtained as

$$\left.\begin{aligned} y &= \frac{Q(L_1 + L_f)^3}{3E_pI_p}, \quad \text{for free head pile} \\ &= \frac{Q(L_1 + L_f)^3}{12E_pI_p}, \quad \text{for fixed head pile} \end{aligned}\right\} \tag{9.45}$$

where $Q$ = lateral load and $L_1$ and $L_f$ are as shown in the figure.

The fixed end moment ($M_F$) of the equivalent cantilever is given by

$$\left.\begin{aligned} M_F &= Q(L_1 + L_f), \quad \text{for free head} \\ &= Q(L_1 + L_f), \quad \text{for fixed head} \end{aligned}\right\} \tag{9.46}$$

The actual moment is obtained by applying reduction factor, as depicted in Fig. 9.37, which is given by

$$M = m(M_F)$$

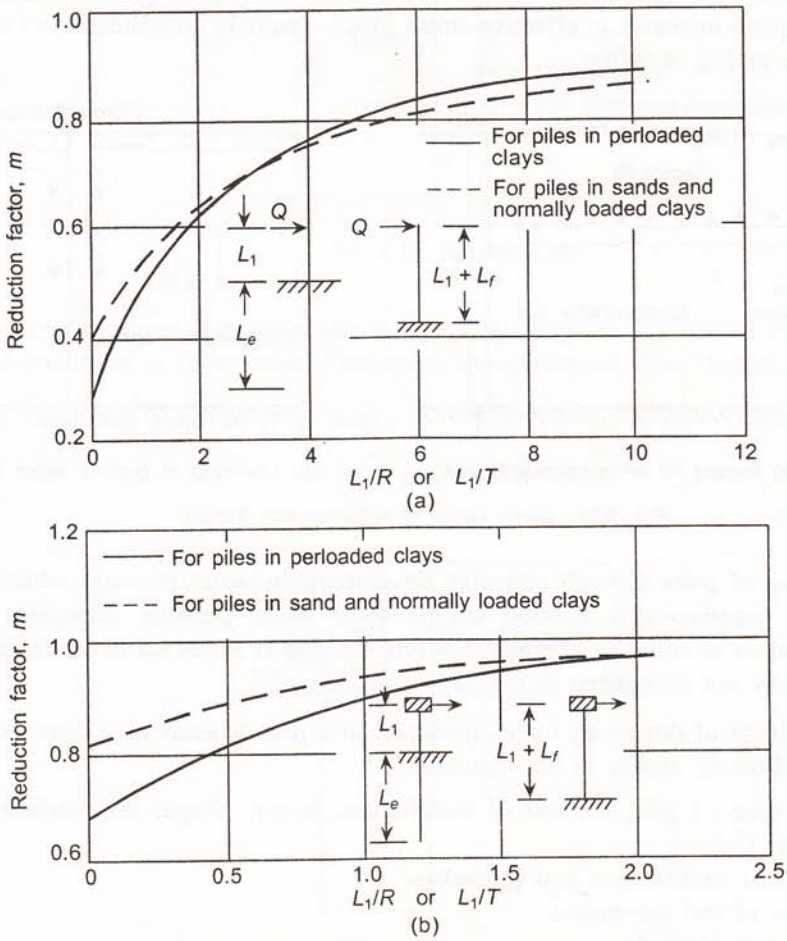


**Fig. 9.37** Correction factor for long piles (IS 2911).

## 9.16 NEGATIVE SKIN FRICTION

When a soil surrounding the pile shaft moves downward relative to the pile shaft, the friction between the soil and the pile tends to drag the pile downwards. The skin friction in that case increases the pile load instead of resisting it. This additional load on the pile is known as *negative skin friction* or *downdrag force*.

Negative skin friction may develop under any the following situations:

1. A pile is installed through a recently placed fill overlying soft compressible clay to a stiff bearing stratum. Alternatively, the fill might have been placed after the pile is installed through the soft compressible layer to the bearing stratum. The situation is illustrated in Fig. 9.38(a). As the soft clay layer consolidates, the fill as well as the soft clay layer move downward and exert a downdrag force on the pile. The magnitude of negative skin friction can be very high and may lead to failure of piles in the extreme case.
2. Negative skin friction may also occur due to lowering of ground water table and subsequent increases in effective stress which results in consolidation of soft clay as shown in Fig. 9.38(b).

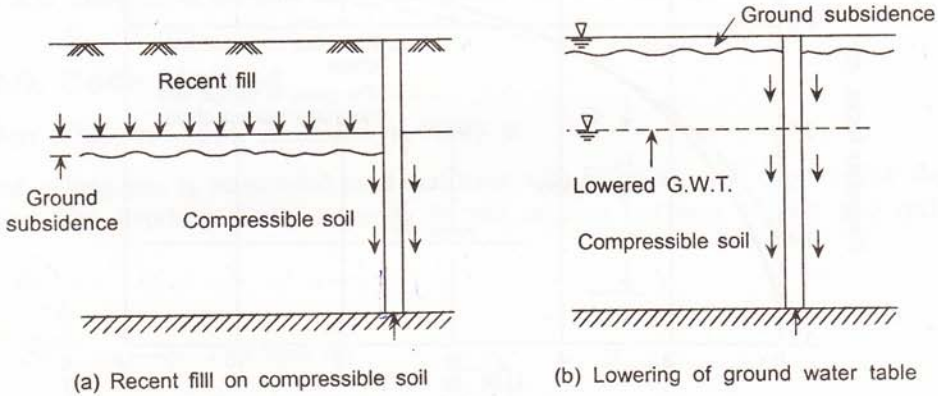


(a) Recent filll on compressible soil (b) Lowering of ground water table

**Fig. 9.38** Some cases of negative skin friction.

3. Driving of piles through soft clay develops pore water pressure which may also cause negative skin friction as the pore water pressure dissipates. But this dissipation is normally completed before the pile is subjected to structural load and generally not considered in design.

The magnitude of downdrag force developed in a pile depends on a number of factors of which the following appear to be important.

(a) The type of pile, method of installation, length, shape, and surface treatment (if any).
(b) The soil stratification and properties.
(c) Cause of soil movement.
(d) The time elapsed.

When a pile is subjected to external load in a soil which is undergoing consolidation under its own weight due to a fill, there is relative movement between the soil and the pile. If the elastic compression of the pile is neglected, the pile settles uniformly while the surrounding soil settlement is maximum at the top and minimum at the pile trip, visible in Fig. 9.39. Accordingly, a neutral point develops above which the soil moves more than the pile and below which the pile moves more than the soil. Obviously negative drag occurs on the length of the pile above the neutral point. In case of end bearing pile, the neutral point develops only at the pile trip and the negative drag occurs over the full length of the pile, as shown in Fig. 9.39.

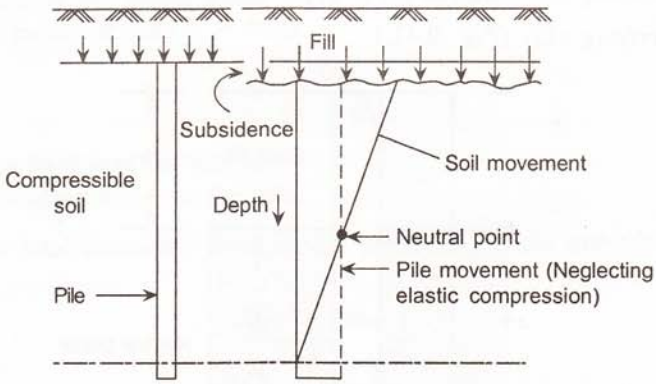


**Fig. 9.39** Neutral Point.

The unit negative drag on a pile at any depth may be determined in the same way as frictional resistance is determined. Two cases are considered, Das (1998), as follows:

(a) *Clay overlying sand fill (Fig. 9.40.)*

$$f_n = K'\gamma' z \tan \delta \tag{9.47}$$

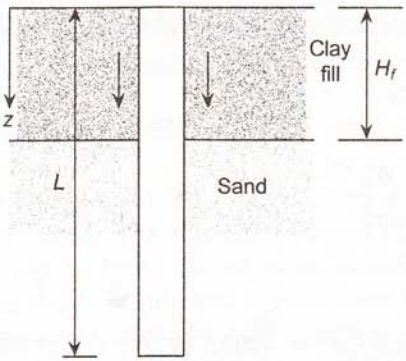


**Fig. 9.40** Negative skin friction in clay overlying sand fill.

where $K'$ = earth pressure coefficient (take $K' = K_o = 1 - \sin\phi'$),
$\gamma' z$ = effective vertical stress at depth $z$, and
$\delta$ = soil–pile friction angle: $0.5\phi'$–$0.7\phi'$.

Hence, total downdrag force on the pile

$$Q_u = \pi D \int_{z_1}^{z_2} K'\gamma' \tan\delta z\, dz$$

$$= \frac{\pi D}{2} K'\gamma'(z_2^2 - z_1^2)\tan\delta \tag{9.48}$$

(b) *Sand fill overlying clay (Fig. 9.41.)*

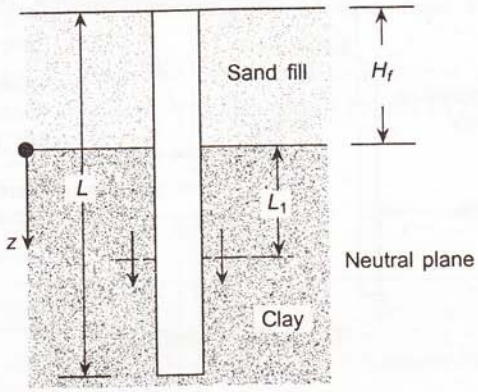


**Fig. 9.41** Negative skin friction in fill overlying clay.

For a height of fill, $H_f$ above the clay the depth of neutral point, $L_1$ may be obtained from the approximate relationship (Bowles, 1982)

$$L_1 = \frac{L - H_f}{L_1}\left(\frac{L - H_f}{2} + \frac{\gamma'_f - H_f}{\gamma'}\right) - \frac{2\gamma' H_f}{\gamma'} \tag{9.49}$$

where $\gamma'_f$ and $\gamma'$ are the effective unit weights of the fill and the underlying clay respectively.

The negative drag is given by

$$f_n = K'\sigma'_v \tan\delta$$

where $K' = K_o = 1 - \sin\phi'$,
$\sigma'_v = \gamma'_f H_f + \gamma' z$, and
$\delta = (0.5 - 0.7)\phi'$

$$\therefore \quad Q_u = \int_0^{L_1} \pi D f_n dz = \int_0^{L_1} \pi D K'(\gamma_f H_f + \gamma' z)\tan\delta\, dz$$

$$= (\pi D K'\gamma_f H_f \tan\delta)\, L_1 + \frac{\pi D L_1^2 K'\gamma' \tan\delta}{2} \tag{9.50}$$

A semi-empirical method of estimating the negative drag based on the one described by Terzaghi and Peck (1967) has been suggested by Nayak (1967). It can be undertaken through the following steps:

1. Estimate the length of pile over which negative skin friction develops.
2. Estimate the positive skin friction over that length.
3. Multiply the value obtained in (2) by a factor to obtain dragdown. This factor depends on the cause of soil movement and may be taken as a value varying over 0.6–0.8.
4. Estimate the ultimate pile capacity, $Q_{up}$ as consisting of point bearing and shaft resistance over the length *where there is no negative skin friction.*
5. Calculate factor of safety, $F$ from

$$F = \frac{Q_{up}}{(Q + Q_{ns})} \tag{9.51}$$

where $Q$ = structural load on pile and
$Q_{ns}$ = downdrag force on the pile.

In a pile group, the total downdrag force on the group, $Q_{ng}$ is the minimum of the following values.

$$Q_{ng} = NQ_{ns} \tag{9.52}$$

and

$$Q_{ng} = \gamma L_n P \tag{9.53}$$

the weight of soil enclosed with the pile groups,

where $N$ = no. of piles in the group,
$\gamma$ = unit weight of soil,
$L_n$ = length over which negative friction develops, and
$P$ = perimeter of the group.

Poulos and Davis (1980) have described a method based on elastic theory, with allowance for pile–soil slip, to estimate downdrag force. In this method, the dependence of downdrag on the settlement of the soil can be included, rather than assuming that sufficient soil movement occurs to mobilize the full adhesion along the pile shaft. Based on a study of the various parameters responsible for negative skin friction, the authors have presented charts which can be used very conveniently to calculate downdrag force.

## 9.17 TESTING OF PILES

Recent trends in foundation design follow the use of large diameter, high capacity piles for supporting heavy structural loads. Till the early sixties, driven piles of diameter upto 500 mm were normally in use in India. These piles would have safe load capacity upto 100 tonnes depending on the depth of pile and subsoil condition. With the coming of bored cast-in-situ systems, large diameter piles are now common and typical 1500 mm diameter piles with safe capacity of 500 tonnes or more have frequently been used in recent years. This obviously necessitates a strict quality control in the installation of the pile so that each pile carries the design load with certainty.

### 9.17.1 Purpose of Pile Testing

In bored cast-in-situ piles, a vertical hole is made into the soil by augering and the same is stabilized by casing or drilling mud. A reinforcement cage is inserted and the hole is filled with concrete by the tremie method. The entire operation being directed from the ground, uncertainties remain as to the condition of the soil at the pile tip and the integrity of the concrete in the pile shaft. The purpose of pile testing is, therefore, to determine

(a) whether the pile tip has reached firm stratum or it rests on loose soil at the bottom of the hole,
(b) whether the concreting of the pile shaft has been done properly and without any discontinuity, and
(c) whether the load carrying capacity of the pile has been correctly assessed.

There is no readily available method of checking the condition of the soil at the pile tip prior to concreting. Normally, at the end of boring, reverse circulation is done to remove all debris from the bottom of the hole and the depth is finally obtained from the length of the tremie pipe and the depth of boring. Even then, uncertainities remain about the possible existence of any thin layer of loose soil at the pile tip.

### 9.17.2 Causes of Defect in Piles

Defects in pile shaft normally occur in the form of unfilled voids which cause discontinuity in the pile shaft. Major causes of such defects have been listed by Tomlinson (1981) as

(a) Encrustation of hardened concrete on the inside of the casing which may cause the concrete to be lifted as the casing is withdrawn.
(b) The falling concrete which may arch across the casing or between the casing and the reinforcement.
(c) Falling concrete may get jammed between the reinforcing bars and not move towards the borehole wall.
(d) Clay lumps may fall into the hole as the concrete is placed.
(e) Soft or loose soil may squeeze into the pile shaft from the bottom of the lining.

Most of these defects can be minimized, if not eliminated, by having the inside of the casing properly cleaned, using a high slump concrete and by avoiding conjestion of reinforcing bars. Also, proper care needs to be taken in lifting the casing while concreting, particularly in unstable soils.

### 9.17.3 Integrity Testing

Often excavations for pile caps show defective construction near the pile head. Similar defects may be there at greater depth also. Therefore, integrity testing is done to check the soundness of the pile shaft after installation. The following methods of integrity testing of piles are generally available (Weltman, 1980; Robertson, 1982)

(a) Excavation surrounding the pile shaft
(b) Exploratory boring through the pile shaft
(c) Acoustic tests
(d) Radiometric tests
(e) Dynamic response of pile
(f) Load test

*Excavation around the pile shaft* is only possible for shallow depths. It is hardly conceivable that a deep pile can be fully exposed for visual inspection. However, short piles of limited length or pile near the ground surface can be examined thoroughly.

*Drilling/boring through the pile shaft* is possible through large diameter piles. Cores of concrete can be examined for soundness and they can be tested to determine their compressive strength. Even a TV Camera may be lowered into the hole to look for cavities and honeycombs.

*Various radiometric and acoustic tests* are also done in drilled holes. Pairs of ducts are made in the pile shaft at the time of concreting and suitable scanning devices are introduced to scan the concrete between the ducts. However, these require specialized equipment. Sonic integrity testing is one such test which is gaining popularity.

*Seismic and dynamic response tests* are extensively done because of their simplicity and adaptability. No hole is required to be made in the pile shaft. In the seismic method, a weight is dropped on the pile head and the time for return of the seismic wave after reflection from the toe is measured. In the dynamic response method, an electrodynamic vibrator is mounted on the pile head to apply a constant amplitude stress wave at the pile top and the response of the pile is seen through an oscillograph or digital indicator. Various types of pile diagnostic systems/pile driving analyzers are now commercially available to facilitate such testing.

*Load test* is the most direct method of determining the capacity of the pile. While other methods of integrity testing determine primarily the soundness of the concrete, the load test gives an integrated method of determining both the soundness of the concrete and the response of the soil under load. It also permits an evaluation of the load carrying capacity of the pile on the basis of soil response. The next section discusses load test on piles in a much greater depth.

## 9.18 LOAD TEST ON PILES

Initial and routine load tests are commonly undertaken in all piling work in India. The basic purpose of an *initial load test* is to obtain the failure load of a pile and then to determine the design load by applying a factor of safety. However, for larger diameter piles, this means applying a very heavy load on the pile to take it to failure. *Routine tests* are carried out on working piles to serve as a proof test to ensure that the behaviour of pile is satisfactory. This test is carried out on a limited number of working piles as a measure of quality control.

## 9.18.1 Test Procedure

The test load is applied on the pile by jacking against a reaction frame which is either loaded with kentledge or supported on anchor piles. The hydraulic jack is provided with a remote controlled pump and the pressure gauge gives a measure of the load applied. For more accurate measurement of load, a load cell or a proving ring may be used. The distance of the reaction frame supports from the pile should be at least five times the diameter of the pile. The displacement of the pile head is measured by dial gauges (3 or 4 nos.) suspended from datum bars resting on unyielding supports, sufficiently away from the pile, and reaction frame supports. A pile test arrangement is shown in Fig. 9.42.

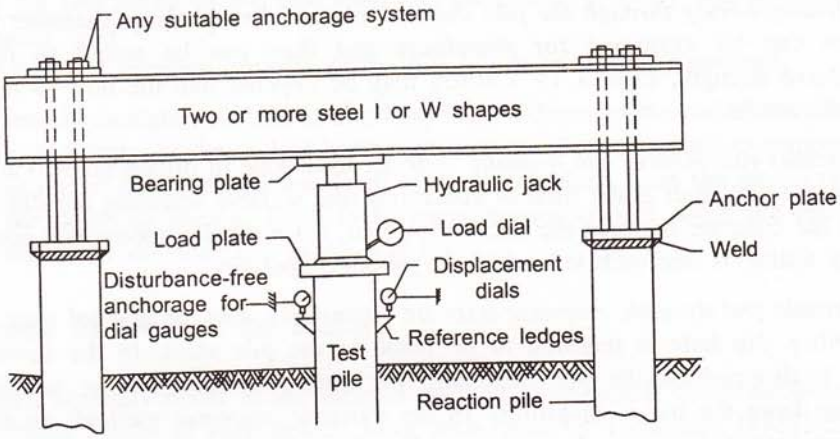


**Fig. 9.42** Load test on pile.

## 9.18.2 Maintained Load Test

This is the usual method of test to obtain a load settlement curve, which may be used for estimating the ultimate load as well as settlement under working load. The load is applied in suitable increments (say 20% of the estimated working load) and settlement observation under each load is made as a function of time. Each load is maintained till the settlement becomes negligible. According to I.S. 2911—1985, each load should be maintained for two hours or till the rate of settlement becomes 0.2 mm/hour, whichever is earlier. For initial load test, the loading is continued till the settlement of pile head equals one tenth of the pile diameter, or the load is three times the estimated safe load, whichever is earlier. In case of routine load test, the load is continued upto one and half times the working load. The load is then released in equal steps to zero, and settlement observations are made at each stage.

The result of load test is presented in the form of a load-settlement curve for both loading and unloading, as illustrated in Fig. 9.43. The ultimate load is obtained as the one among any of the following approaches:

(a) The load corresponding to the point of intersection of the tangents of upper and lower portion of the curve.

(b) The load corresponding to a break point when the load settlement curve is drawn on a log–log plot.

(c) The load at which the settlement of the pile head is equal to 10% of the pile diameter.

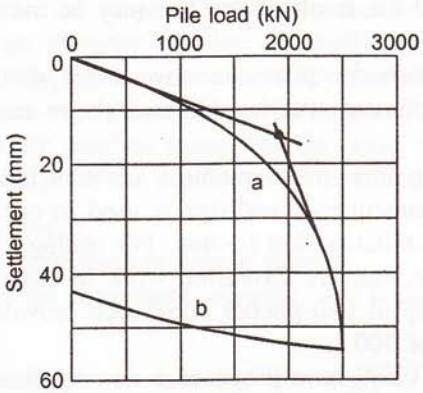


**Fig. 9.43** Load versus settlement relationship from pile test.

According to IS 2911—1985, the safe load from initial load test is taken as the least of the following:

(a) Two third of the load at which gross settlement is 12 mm or

(b) 50% of the final load at which gross settlement becomes 1/10th of the pile diameter.

The ultimate load obtained by these methods for the pile test data, as depicted through Fig. 9.43, is shown in Table 9.5.

**Table 9.5** Pile capacity from load test (Fig. 9.43)

| *Method* | *Ultimate load* (kN) | *Safe load* (kN) *FS* = 2 |
|---|---|---|
| Double tangent (on arithmetic plot) | 1900 | 950 |
| Double tangent (on log–log plot) | 1320 | 660 |
| Settlement 10% pile diameter | 2300 | 1150 |
| *I. S. 1985* | | |
| 2/3 gross load at 12 mm settlement | 1300 | 870 |
| 50% of load at settlement of 10% pile diameter | 2300 | 1150 |

In routine load test, the pile is considered to be safe if the gross settlement under 1.5 times the working load is not greater than 12 mm.

Maintained load test is very time consuming. Also, some amount of consolidation and creep may take place during the test. So, it may be difficult to correlate the test results with undrained shear strength data obtained from laboratory tests.

## 9.18.3 Constant Rate of Penetration (CRP) Test

This is a short duration test in which the load is applied at a constant rate of strain till the pile fails. The rate of strain depends on the type of soil. A common rate is 0.75 mm/min for

friction piles in clay, and 1.5 mm/min for end bearing piles in sand. The duration for the test corresponds to the time required for failure in a laboratory undrained shear test. So, the two tests have a common basis and the result of one test may be interpreted on the basis of the other.

The criteria for large diameter piles are now under review by Bureau of Indian Standards. Obviously, the settlement criteria indicated above may hardly be applicable to large diameter piles.

For testing large diameter piles, major problem arises in building up a huge kentledge to take the desired reaction. Sometimes, kentledge is used in conjunction with anchor piles which provides reaction by mobilizing skin friction. For testing 1000 mm diameter × 20 m long bored piles for the Metro Railway Extension work in Calcutta with a design load of 230 t, the reaction was made up of four anchor piles, each providing a reaction load of 70 t and a dead weight kentledge of 300 t.

Birmingham and James (1989) have proposed a new approach to load testing for high capacity piles. This is a quasi-static method of test using a statnamic apparatus. A reaction mass is placed over a pressure chamber on top of the test pile. Fuel is burnt within the pressure chamber to create large pressures to drive the reaction mass upwards at high velocity. The reaction force acts equally downwards on the pile top. A schematic diagram of the system and the details of the test chamber are shown in Fig. 9.44. The force–time history of the mass allows a linearly increasing load on the pile of greater than 600 t. The duration of the pulse is upto 80 ms which is an order of magnitude higher than that associated with the conventional drop hammer blow. The acceleration imparted to the pile is less than 1 g as compared to 50–100 g for dynamic loading. This emulates the stress condition within a pile during static loading.

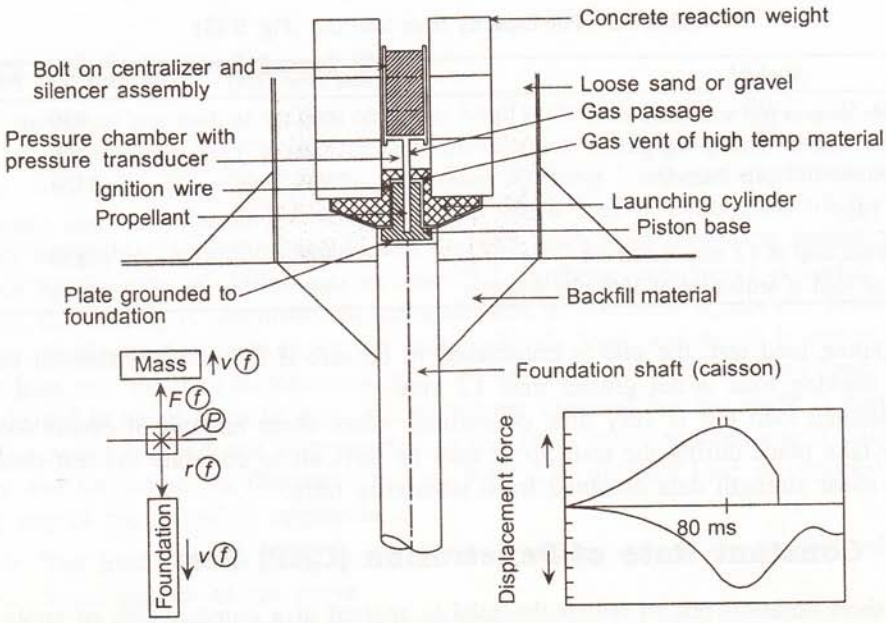


**Fig. 9.44** Statnamic test apparatus.

## 9.18.4 Pile Driving Analyzer

Measurement of stress waves in piles has led to the development of a new and versatile equipment for testing the integrity of piles and predicting pile capacity. Different types of pile driving analyzers (PDA) are now commercially available. These are essentially based on the propagation of stress waves down and up the length of the pile while the boundary values applied at the pile top are used as inputs for the wave equation analysis. The commonly available pile driving analyzers are capable of determining the

(a) pile bearing capacity,
(b) maximum compressible and tensile stresses,
(c) maximum pile top movement, velocity, and acceleration and
(d) pile integrity.

For interpretation of data, a wave equation analysis programme is developed and fed into the system. For example, PWDWAP (Tan et al., 1987) uses a model of the pile as discrete line elements and the soil as a system of elasto-plastic springs and viscous dashpots. The programme uses an implicit Newmark integration analysis and displays the measured and predicted responses on a computer screen and presents the data in convenient worksheet format. Tan et al. (1987) present five case histories of piles in residual soil and one in alluvium formation. The pile capacities that predicted the Hiley's formula were compared with the results of PDA and load tests data (refer Table 9.6).

**Table 9.6** Summary of pile capacities (Tan et al., 1987)

| *S.No.* | *Size of pile* (mm) | *Length* (m) | *Design load* (m) | *Ultimate Load* | | |
|---|---|---|---|---|---|---|
| | | | | *Hiley formula* (t) | *PDA* (t) | *Load test* (t) |
| | Residual Soil | | | | | |
| 1. | Conc. 280 × 280 | 25.1 | 93 | 220 | 272 | 268 |
| 2. | Conc. 325 × 325 | 25.6 | 115 | 355 | 360 | 380 |
| 3. | Steel 356 × 368 | 40.8 | 120 | 368 | 310 | 390 |
| 4. | Steel 356 × 368 | 29.4 | 120 | 352 | 250 | 283 |
| 5. | Steel 356 × 368 | 28.0 | 120 | 427 | 400 | 390 |
| | Alluvium | | | | | |
| 6. | Steel 356 × 368 | 11.0 | 110 | 252 | 372 | 330 |

A field test with PDA is shown in Fig. 9.45. Major defects such as cracks, soil incursions, necking, and changes in cross section are easily detected using this test. For complete pile driving analysis, two specially designed combined acceleration and strain transducers are mounted on the side of the pile near the pile top. During driving of piles, signals obtained through the mounted transducers are passed on to the signal conditioning subsystem for processing and finally to the computer. The processed signal for each blow is stored in a hard disc memory and displayed on the computer screen. After pile driving, a full record of all relevant parameters are available with respect to the number of blows as well as depth. Typical test data obtained for structurally sound piles and piles with discontinuity are shown in Fig. 9.45.

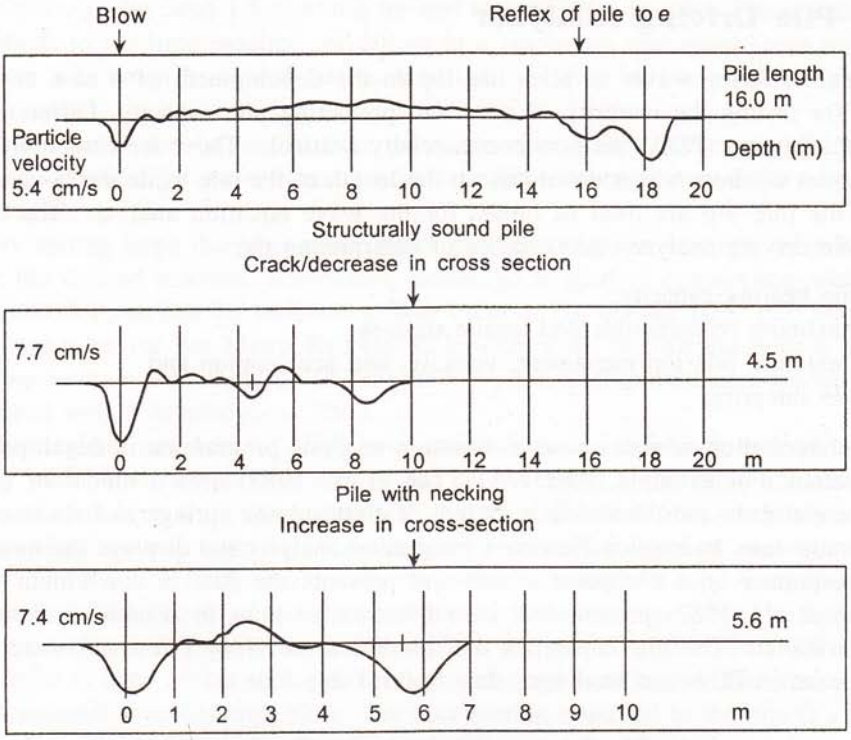


**Fig. 9.45** PDA results cast-in-situ concrete piles.

## Example 9.1

A closed ended steel pipe pile, 30 cm in diameter and 20 m long is driven to a sand deposit with cut off at ground level. The depth-wise variation of $N$ and $\phi$ values is given in Fig. 9.46. The water table is 3 m below ground level. Compute the ultimate load capacity of the pile based on soil support, using

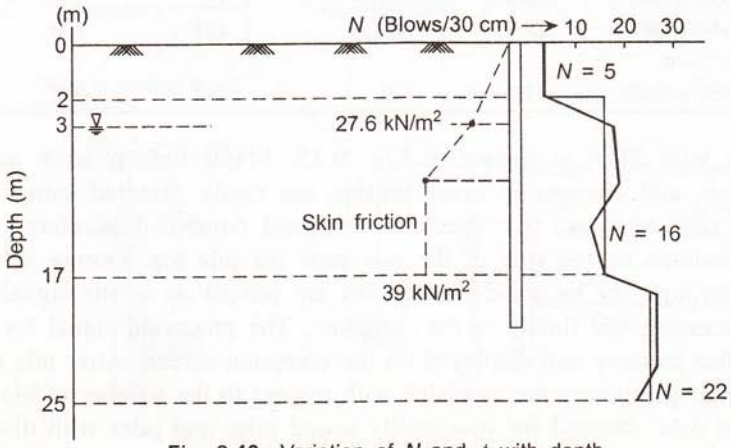


**Fig. 9.46** Variation of $N$ and $\phi$ with depth.

(i) $N$ value.

(ii) Overburden pressure considering critical depth.

Take effective unit, $\gamma' = 1.73$ t/m$^3$ above water table, and 0.73 t/m$^3$ below water table.

***Solution***

(i) Using $N$ value

Average $N$ along pile shaft, $N_{av} = [(5 \times 2) + (16 \times 15) + (22 \times 3.6)]/20.6 = 15.98 \simeq 16$ (upto $2D$ below tip)

$N$ value below tip = 22

Using Eq. (9.19)

$$Q_u = 4NA_p + \frac{N_{av}}{6} A_f$$

$$= 4 \times 22 \times 0.785 \times (0.3)^2 + (16/6)\ 3.14 \times 0.3 \times 20$$

$$= 62.22 + 50.24 = 112.41 \simeq 112 \text{ t} = 1120 \text{ kN}$$

(ii) Considering critical depth for overburden

For medium sand, $z_c/D = 20$, $z_c = 6$ m, $N_q = 45$, using Berezantzev's curve, Fig. 9.12.

For driven steel pile, take $K_s = 1.5$, $\phi_{av} = 0.7\phi'$

$$0\text{–}3 \text{ m:} \quad \phi_{av} = 0.7\phi' \times 28° = 19.50°$$

$$3\text{–}20 \text{ m:} \quad \phi_{av} = 0.7\phi' \times 32° = 22.5°$$

Also, $Q_u = \sum A_s f_s + A_p q_p$

$$f_{s_1} = K_s \gamma D_f \tan 19.5° = 1.5 \times 17.3 \times 3 \times \tan 19.50° = 27.6 \text{ kN/m}^2$$

$$f_{s_2} = K_s \gamma' D_f \tan 22.5°$$

$$= 1.5(17.3 \times 3 + 7.3 \times 1.5) \tan 22.5°$$

$$= 39.0 \text{ t/m}^2$$

$$\therefore \sum A_s f_s = \pi \times 0.3\left[\frac{3 \times 27.6}{2} + 3\left(\frac{27.6 + 39}{2}\right) + (14 \times 39)\right]$$

$$= \pi \times 0.3(41.4 + 99.9 + 546)$$

$$= 647 \text{ kN}$$

and $$A_p q_p = \frac{\pi \times 0.3^2}{4}(\gamma' D_f N_q)$$

$$= \frac{\pi \times 0.3^2}{4}(17.3 \times 3 + 7.3 \times 17) \times 45$$

$$= 559 \text{ kN}$$

$$Q_u = 647 + 559 = 1206 \text{ kN}$$

**Example 9.2**

Determine the safe load of a group of 9 driven cast-in-situ piles, 40 cm in diameter, 15 m long, installed in a cohesive deposit, as shown in Fig. 9.47. The cut off level is 1.5 m below ground level and the spacing of piles 1.2 m.

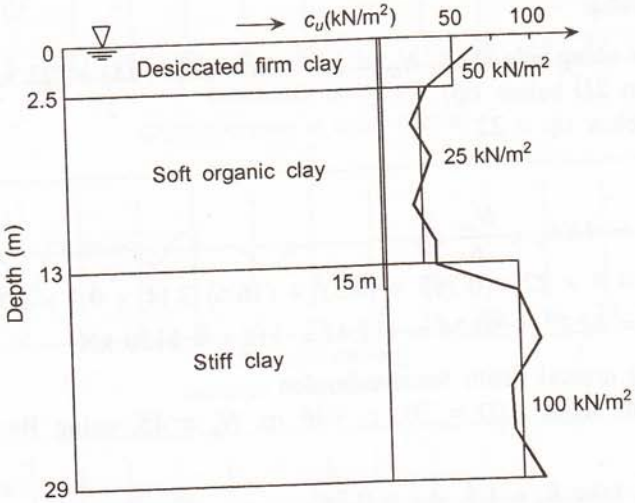


**Fig. 9.47** Group of piles in a cohesive deposit.

***Solution***

*Individual pile action*

Capacity of a single pile: $Q_u = Q_f + Q_p$

Taking adhesion factors as follows:

| $c_u$ (kN/m²) | $\alpha$ |
|---|---|
| 50 | 0.9 |
| 25 | 1.0 |
| 100 | 0.45 |

$$Q_f = 3.14 \times 0.4(0.9 \times 50 \times 1 + 1.0 \times 25 \times 10.5 + 0.45 \times 100 \times 3.5)$$

$$= 584.2 \text{ kN}$$

$$Q_p = 0.785 \times (0.4)^2 \times 9 \times 100 = 113 \text{ kN} \quad (\text{where } N_c = 9.0)$$

$$\therefore \quad Q_u = 584 + 113 = 697$$

$$\therefore \quad Q_{all} = 697/2.5 = 280 \text{ kN}$$

Safe capacity of 9 piles = 9 × 280 = 2520 kN

*Block action* (Fig. 9.48)

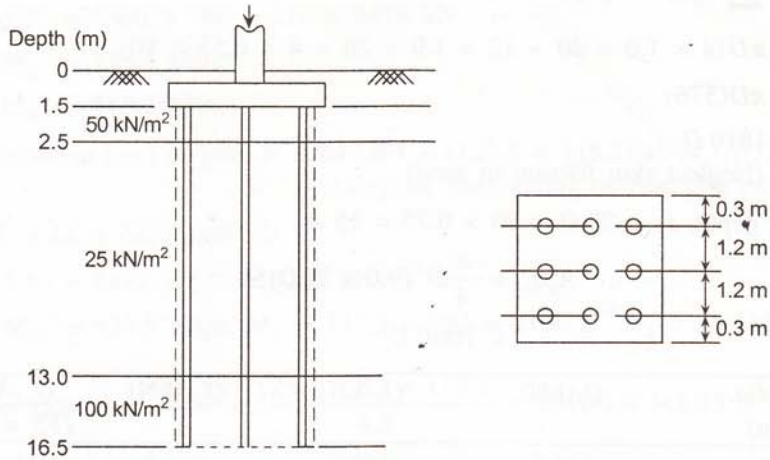


**Fig. 9.48** Block action.

$$Q_{ult} = 2(2.4 + 2.4)(50 \times 1 + 25 \times 10.5 + 100 \times 3.5) + (2.4 \times 2.4 \times 9 \times 100)$$
$$= 6360 + 5184$$
$$= 11{,}544 \text{ kN}$$

$$Q_{all} = \frac{11{,}544}{2.5} = 4600 \text{ kN, which is greater than } 2520 \text{ kN}$$

Hence, safe capacity of pile group = 2520 kN.

**Example 9.3**

A multistoreyed building is to be constructed at a site whose subsoil profile and properties are shown in Fig. 9.49. It has been decided to support the building on pile foundation, with cut-off level at 2 m below G.L. Compute the safe load of 25 m long bored piles of 650 mm, 750 mm, and 1 m diameter. Assume ground water table at ground level and average unit weight, $\gamma = 19$ kN/m$^3$.

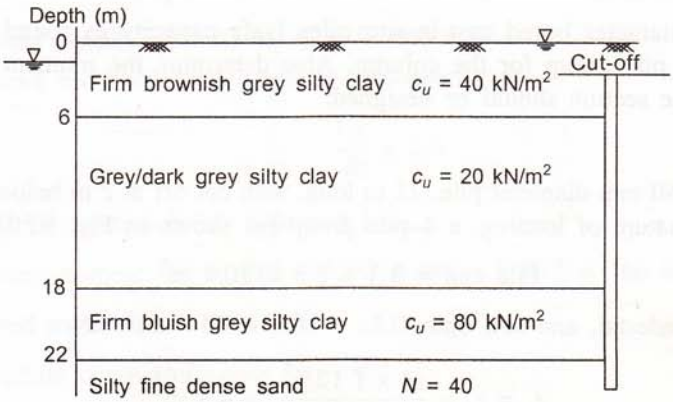


**Fig. 9.49** Subsoil profile for Example 9.3.

$$Q_{ult} = \sum A_f f_s + A_p q_p$$

$$\sum A_f = \pi D(4 \times 1.0 \times 40 + 12 \times 1.0 \times 20 + 4 \times 0.55 \times 80)$$

$$= \pi D(576)$$

$$= 1810\, D$$

(Neglect skin friction in sand)

Taking critical depth, $z_c = 20\,D = 20 \times 0.75 = 15$ m

$$A_p q_p = \frac{\pi}{4} D^2 (9.0 \times 20D)50$$

$$= 7060\, D^3$$

| *Pile dia.* (mm) | $Q_f$(kN) | $Q_p$(kN) | $Q_{ult}$(kN) | $Q_{all}$(kN) *(FS = 2.5)* |
|---|---|---|---|---|
| 600 | 1086 | 1524 | 2610 | 1050 |
| 750 | 1357 | 2978 | 4330 | 1730 |
| 1000 | 1810 | 7060 | 8870 | 3550 |

[*Note:* There is some uncertainty over the choice of critical depth in piles that penetrate through cohesive soil into sand. If the critical depth is not considered and full overburden is taken, end bearing in sand will increase appreciably.]

Therefore, 750 mm diameter piles with $Q_{all} = 1700$ kN are used.

**Example 9.4**

A typical column of the multistoreyed building in Example 9.3 is subjected to the following loads at ground level.

| *Vertical load V* (kN) | | | $M_{xx}$ (kNm) | | $M_{yy}$ (kNm) | | *Base shear* $H_x$(kN) | $H_y$(kN) |
|---|---|---|---|---|---|---|---|---|
| DL | LL | SL | DL + LL | SL | DL + LL | SL | SL | SL |
| 5500 | 760 | 657 | 123.5 | — | 115.2 | 985 | 380 | — |

Using 750 mm diameter bored cast-in-situ piles (safe capacity as found in Example 9.3), design a suitable pile group for the column. Also determine the moment due to horizontal load for which the section should be designed.

***Solution***

Safe bearing of 750 mm diameter pile, 22 m long, with cut-off at 2 m below G.L. is 1700 kN. Considering the nature of loading, a 4–pile group (as shown in Fig. 9.50) is chosen.

$$\text{Pile cap} = 3.3 \times 3.3 = 10.9 \text{ m}^2$$

Weight of cap, pedestal, and soil upto G.L. $\approx 10.9 \times 20 = 218$ kN

$$z_x = z_y = \frac{(4 \times 1.125)^2}{1.125} = 4.5 \text{ m}^3$$

(a) *DL + LL Condition*

$\Sigma V = 5500 + 760 + 218 = 6478$ kN

$M_{xx} = 123.5$ kNm

$M_{yy} = 115.2$ kNm

∴ Maximum load in pile, $P = 647.8/4 + (123.5 + 115.2)/45 = 1672.5$ kN > 1670 kN.
(Marginal overloading on one pile may be accepted.)

(b) *DL + LL + SL Condition*

$\Sigma V = 6478 + 657 = 7135$ kN

$M_{xx} = 123.5$ kNm, $M_{yy} = 115.2 + 985 = 1100.2$, $H_x = 380$ kN

Load per pile, $P = \dfrac{7135}{4} + \dfrac{123.5 + 45 + 110.2}{4.5} = 1845$ kN ($<1.25 \times 1700 = 2125$ kN)

(c) Horizontal load

$$H \text{ per Pile} = \frac{380}{4} = 95 \text{ kN}$$

Maximum Moment on Pile Section

(i) Using IS Code (IS 2911, Part I, Sec 4, 1984 with Amendment in 1987)

Stiffness Factor, $R = \sqrt[4]{\left(\dfrac{E_p I_p}{K_2}\right)}$

$E_p = 2 \times 10^6$ t/m$^2$

$I_p = (\pi/64) \times (0.75)^4 = 0.015$ m$^4$

$K_2 = 48.8$ from code

$$R = \sqrt[4]{\left(\frac{2 \times 10^6 \times \pi \times (0.75)^4}{64 \times 48.8}\right)} = 504 \text{ cm} = 5.04 \text{ m}$$

Embedded length, $L_e = 20$ m, $L_1 = 0$, and $L_1/R = 0$

Using the curve for fixed headed pile in preloaded clay,

$$\frac{L_f}{R} = 1.6$$

∴ Depth of fixity, $L_f = 1.6 \times 5.04 = 8.1$ m

Cantilever moment, $M_f = H(0 + L_f)/2 = (95 \times 8.1)/2 = 466$ kNm.

Corrected moment, $M = mM_f$

Using appropriate curve from code, $m = 0.7$

∴ Design moment $= 0.7 \times 466 = 326$ kNm.

**Example 9.5**

Compute the long term settlement of the pile group considered in Example 9.2.

The load on the pile cap is assumed to spread at a slope of 4 horizontal to 1 vertical upto the level of 2/3 pile length from the top, and then at slope of 2 vertical to 1 horizontal to a depth of 12 m below that level, which is about 1.5 times the width of equivalent imaginary footing.

***Solution***

Two points *A* and *B* are considered at the mid point of the relevant strata beneath the imaginary footing. Water table is assumed to be at G.L.

At A, $p_o = 12.25 \times 9 = 110 \text{ kN/m}^2$

$\Delta p = 2520/(8.2)^2 = 37.4 \text{ kN/m}^2$

$\delta_1 = 0.10 \times 150 \times \log_{10} [(110 + 37.4)/110)] = 1.9 \text{ cm}$

At B, $p_o = 19 \times 9 = 171 \text{ kN/m}^2$

$\Delta p = 2520/(12.2 \times 12.2)^2 = 10.2 \text{ kN/m}^2$

$\delta_2 = 0.08 \times 1200 \times \log_{10} [(171 + 10.4)/171)] = 2.46 \text{ cm}$

$\therefore$ Total settlement = 1.9 + 2.46 = 4.36 cm

**Example 9.6**

RCC bored piles, 1000 mm diameter × 20 m long are proposed to be used for a flyover passing over a canal bed with predominantly river channel deposits, as depicted in Fig. 9.50. DMC method of boring is adopted and steel liners would be used to a depth of at least 15 m below G.L. Design the safe pile capacity.

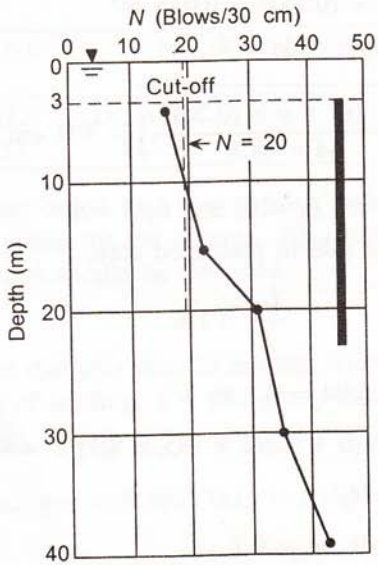


**Fig. 9.50** RCC bored piles for Example 9.6.

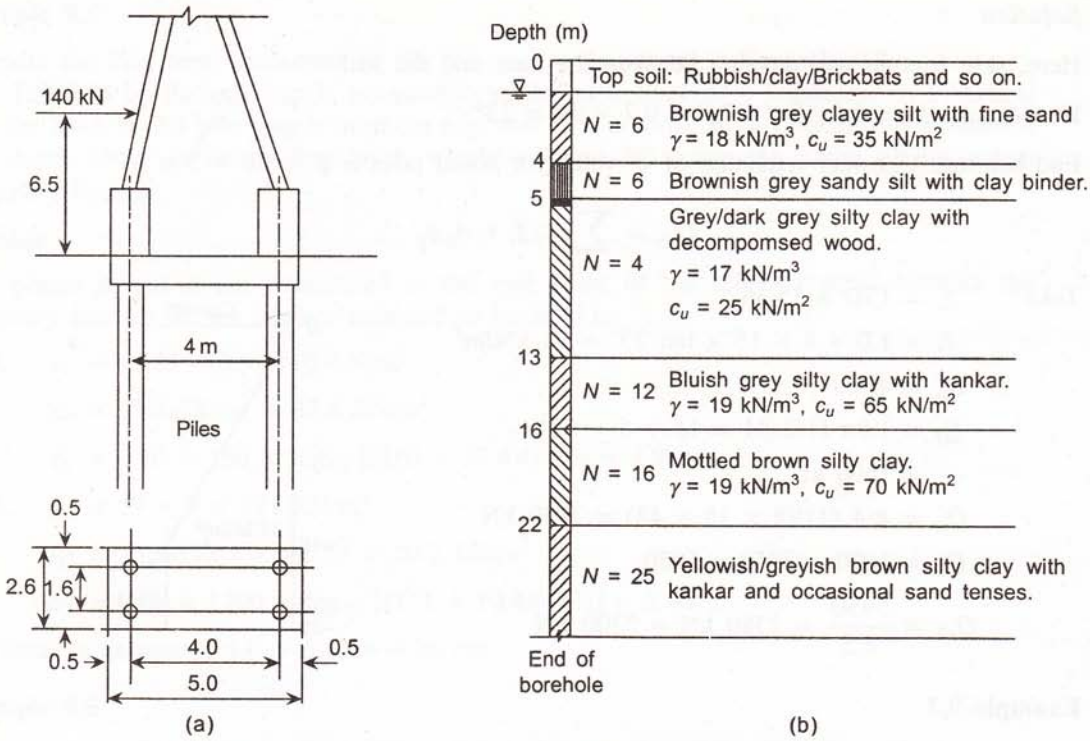


**Fig. 9.51** (a) Main trestle columns and (b) subsoil type for Example 9.8.

***Solution***

*Pile capacity*

Pile diameter = 500 mm

Depth = 18 m/24 m

Cut-off level = 1 m below ground level

Pile tip at 18 m below ground level

$$Q_{\text{ult}} \text{ per pile} = \sum A_f f_s + A_p q_p$$

$$= 0.5\pi(4 \times 35 \times 1.0 + 8 \times 25 \times 1.0 + 3 \times 65 \times 0.7 + 2 \times 70 \times 0.6) + \pi/4(0.5)^2\ (9 \times 70)$$

$$= 0.5\pi\ (140 + 200 + 136 + 84) + (0.2 \times 630)$$

$$= 879 + 126 = 1005 \text{ kN}$$

$$Q_{\text{all}} \text{ per pile} = \frac{1005}{3(FS)} = 333 \text{ kN} \approx 300 \text{ kN}$$

$$\text{Uplift per pile} = \frac{879}{3} = 293 \text{ kN} \approx 250 \text{ kN}$$

*Main trestle foundation*

**Case I**

Loading: vertical

$$DL = 240 \text{ kN}$$
$$LL = 520 \text{ kN}$$

Self weight of cap: 100 kN

Total 860 kN

Lateral service wind = 17.5 kN

$$Q \text{ per pile} = \frac{860}{4} = 215 \text{ kN}$$
$$I_{xx} = 4 \times 2^2 = 16 \text{ m}^4$$
$$z_{xx} = \frac{16}{2} = 18 \text{ m}^3$$

$$\therefore \text{ Maximum load on pile } = \frac{860}{4} + \frac{17.5 \times 6.5}{8}$$
$$= 215 + 14 = 229 \text{ kN} < 300 \text{ kN} \quad \text{which is OK.}$$

Also, $229 - 14 = 215 \text{ kN} < 300 \text{ kN}$ which is OK.

**Case II**

Loading: vertical

$$DL = 240 \text{ kN}$$

Pile cap: 100 kN

Total 340 kN

Lateral: Storm = 140 kN

$$\text{Maximum Compression in pile} = \frac{340}{4} + \frac{140 \times 6.5}{8} = 85 + 113$$
$$= 198 \text{ kN} < 300 \text{ kN, thus, accepted.}$$

$$\text{Maximum Uplift in pile} = \frac{340}{4} - \frac{140 \times 6.5}{8} = 85 - 113$$
$$= -28 \text{ kN} < 250 \text{ kN, thus, accepted.}$$

Hence, pile groups are safe for both cases.

*Pile design*

Consider storm load at 6.5 m above G.L. and vertical load (impact) at 0.6 m above G.L.

$c_u = 35 \text{ kN/m}^2$

$K$ = Coefficient of subgrade reaction = 600 kN/m$^3$

Stiffness factor, $T = \sqrt[5]{\dfrac{EI}{K}}$

$$= \sqrt[5]{\frac{2 \times 10^6 \times \pi/64(0.5)^4}{60}}$$

$$= \sqrt[5]{102.2} = 2.52 \text{ m}$$

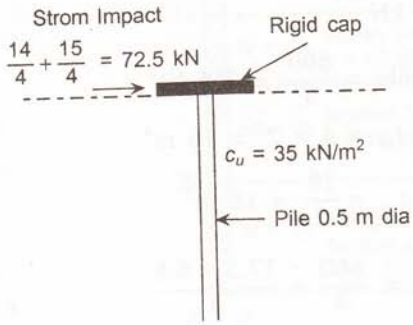


As pile depth = 18 m > 4*T*. Hence, it is a long elastic pile and we use Brom's method.

$$\frac{H_u}{c_u B^2} = \frac{35}{35 \times (0.5)^2} = 4.0$$

Also, $e/B = 0$

$\therefore$ $\dfrac{M_u}{c_u B^3} = 7$, which gives

$$M_u = 7 \times 35 \times (0.5)^3$$
$$= 30.6 \text{ kNm}$$

## REFERENCES

Berezantzev, V.G., V. Khristoforov, and V. Golubkov (1961), *Load Bearing Capacity and Deformation of Piled Foundations,* Proc. 5th Int. Conf. on SMFE, Vol. 2, pp. 11–15.

Birmingham, P. and M. James (1989), *An Innovative Approach to Load Testing of High Capacity Piles*, Proceedings of the International Conference on Piling and Deep Foundations, London, Balkema, Roterdam, 1989.

Bishop, A.W. (1966), Sixth Rankine Lecture: The Strength of Soils as Engineering Materials, *Geotechnique,* Vol. 16, pp. 89–130.

Bowles, J.E. (1968), *Foundation Analysis and Design*, McGraw-Hill Inc., New York.

Bowles, J.E. (1974), *Analytical and Computer Methods in Foundation Engineering*, McGraw-Hill, New York.

Broms, B.B. and J.O. Silberman (1964), *Skin Friction Resistance for Piles in Cohesionless Soils*, Sols-Soils, pp. 10–33.

Broms, B.B. (1966), *Methods of Calculating the Ultimate Bearing Capacity of Piles—a summary*. Sols-Soils, pp. 18–19: 21–32.

Broms, B.B. and L. Hill (1973), *Pile Foundations for Kuwait Towers*, Proc. 8th Int. Conf. on SMFE, Moscow, Vol. 2–1, pp. 33–38.

Burland, J.B. (1973), *Shaft Friction of Piles in Clay—a simple fundamental approach*, Ground Engineering, Vol. 6, No. 3, pp. 30–42.

Cooke, R.W. and G. Price (1973), *Strains and Displacements Around Friction Piles,* Proc. 8th Int. Conf. on SMFE, Moscow, Vol. 2–1, pp. 53–60.

Das, B.M. (1998), *Principles of Foundation Engineering*, PWS Publishing, California, USA.

Davisson, M.T. and H.L. Gill (1963), Laterally Loaded Piles in a Layered Soil System, *Journal of the Soil Mechanics and Foundations Division,* American Society of Civil Engineers, Vol. 89, No. SM3, pp. 63–94.

De Beer, E.E. (1970), Experimental Determination of the Shape Factors and Bearing Capacity Factors of Sand, *Geotechnique,* Vol. 20, No. 4, pp. 387–411.

Flaate, K. (1972), Effects of Pile Driving in Clays, *Canadian Geotechnical Journal,* Vol. 9, No. 1.

Hanna, T.H. and R.H.S. Tan (1973), The Behavior of Long Piles Under Compressive Loads in Sand, *Canadian Geotechnical Journal,* Vol. 10, No. 3: pp. 311–340.

Janbu, N. (1953), *An Energy Analysis of Pile Driving with the Use of Dimensionless Parameters*, Norwegian Geotechnical Institute, Oslo, Publication No. 3.

IS 2911 (1979)—*Code of Practice for Design of Pile Foundations*, Bureau of Indian Standards, New Delhi.

Kerisel, J. (1961), *Foundations Profondes en Milieu Sableux*, Proc. 5th Int. Conf. on SMFE, Vol. 2: pp. 73–83.

Marsland, A. (1971), *Shear Strength of Fissured Clay, Stress-Strain Behavior of Soils,* T.G. Foulis, pp. 59–68.

McClelland, B. (1974), Design of Deep Penetration Piles for Ocean Structures, *Journal of the Geotechnical Engineering Division,* American Society of Civil Engineers, Vol. 100, No. GT7, pp. 709–747.

Meyerhof, G.G. (1959), Compaction of Sands and Bearing Capacity of Piles, ASCE, *Journal of Soil Mechanics and Foundation Division,* SM6, pp. 1–29.

Meyerhof, G.G. and L.J. Murdock (1953), An Investigation of the Bearing Capacity of Some Bored and Driven Piles in London Clay, *Geotechnique,* Vol. 3: p. 267.

Meyerhof, G.G. (1976), Bearing Capacity and Settlement of Pile Foundations, *Journal, Geotechnical Engineering Division,* ASCE, Vol. 88, SM4: pp. 32–67.

Nordlund, R.L. (1969), Bearing Capacity of Piles in Cohesionless Soil, *Journal of Soil Mechanics and Foundation,* ASCE, Vol. 89, No. SM3, pp. 1–35.

Poulos, H.G. and E.H. Davis (1980), *Pile Foundations Analysis and Design*, John Wiley and Sons, New York.

Radhakrishnan, H.S. and J.I. Adams (1973), Long-term Uplift Capacity of Augured Footings in Fissured Clays, *Canadian Geotechnical Journal,* Vol. 10, No. 4, pp. 647–652.

Rees, L.C. and H. Matlock (1956), *Non-dimensional Solutions for Laterally Loaded Piles with Soil Modulus Assumed Proportional to Depth*, 8th Texas Conf. on SMFE, Special Publication No. 29, University of Texas.

Schultze, E. and G. Sherif (1973), *Prediction of Settlement from Evaluated Settlement Observations for Sand*, Proc. 8th Int. Conf. on SMFE, Moscow, Vol. 1, p. 225.

Skempton, A.W. (1948), *The $\phi = 0$ Analysis of Stability and its Theoretical Basis*, Proc. 2nd Int. Conf. on SMFE, Rotterdam, Vol. 2.

Skempton, A.W. (1951), *The Bearing Capacity of Clays*, Building Research Congress, England.

Skempton, A.W. (1959), Cast in-situ Bored Piles in London Clay, *Geotechnique,* Vol. 9, No. 4, pp. 153–173.

Skempton, A.W. and P. La Rochelle (1955), The Bradwell Ship: A short term failure in London Clay, *Geotechnique,* Vol. 15, No. 3.

Skempton, A.W. and R.D. Northey (1952), The Sensitivity of Clays, *Geotechnique,* Vol. 3, No. 1, pp. 40–51.

Smith, E.A.L. (1960), Pile Driving Analysis by the Wave Equation, *Journal on Soil Mechanics and Foundation Division,* ASCE, Vol. 86, SM4: pp. 35–61.

Sliwinski, Z. and W.G.K. Fleming (1974), *Practical Considerations Affecting the Performance of Diaphragm Walls,* Proc. Conference on diaphragm walls and anchors, ICE, London, pp. 1–10.

Terzaghi, K. (1942), *Discussion on the Progress Report of the Committee on the Bearing Value of Pile Foundations*, Proc. ASCE, Vol. 68: pp. 311–323.

Terzaghi, K. (1943), *Theoretical Soil Mechanics*, John Wiley and Sons Ltd., p. 510.

Terzaghi, K. (1955), Evaluation of Coefficient of Subgrade Reaction, *Geotechnique,* Vol. 5: p. 297.

Terzaghi, K. and R.B. Peck (1967), *Soil Mechanics in Engineering Practice*, 2nd ed., John Wiley and Sons, New York.

Thorburn, S. and R.S.L. MacVicar (1970), Discussion, Conf. on Behaviour of Piles, ICE, London, p. 54.

Tomlinson, M.J. (1965), *Foundation Design and Construction*, 2nd ed., Pitman, London.

Tomlinson, M.J. (1977), *Pile Design and Construction Practices*, 1st ed., Viewpoint Publications, London.

Tomlinson, M.J. (1981), *Pile Design and Construction Practices*, 4th ed., E and F N Spon, London.

Touma, F.T. and L.C. Reese (1974), Behaviour of Bored Piles in Sand, *Journal on Geotechnical Engineering Division,* ASCE, Vol. 100, No. GT7: pp. 749–761.

Vargas, M. (1948), *Building Settlement Observations in Sao Paulo*, Proc. 2nd Int. Conf. on SMFE, Rotterdam, Vol. 4, p. 13.

Vesic, A.S. (1967), *A Study of Bearing Capacity of Deep Foundations*, Final Report, Project B-189, School of Civil Engineering, Georgia Institute of Technology, Atlanta.

Vesic, A.S. (1975), *Principles of Pile Foundation Design*, Duke University, School of Engineering, Soil Mechanics, Series No. 38.

Vesic, A.S. (1970), Tests in Instrumented Piles—Ogeechee River Site, *Journal of the Soil Mechanics and Foundations Division,* American Society of Civil Engineers, Vol. 96, No. SM2, pp. 561–584.

Vijayvergiya, V.N. and J.A. Focht, Jr. (1972), *A New Way to Predict Capacity of Piles in Clay*, Offshore Technology Conference Paper 1718, Fourth Offshore Technology Conference, Houston.

Whitaker, T. (1976), *The Design of Pile Foundations*, 2nd ed., Pergamon Press, London.

# 10 Well Foundations

## 10.1 INTRODUCTION

The conventional foundations discussed in the previous chapters are applicable to low and medium rise buildings. Depending on the subsoil condition at a given site, an optimum foundation design is to be achieved for the given structure. For multistorey buildings, say upto 20 storeys high, pile foundations with or without basement are generally adopted. For even heavier structural load—for bridge pier and abutments for example,—the vertical load may go upto a few thousand tonnes and major horizontal forces due to wind, current, and so on may apply. Conventional pile foundations are not suitable in such cases because of the limited capacity of piles to resist lateral forces. Large size foundations, often quite deep, are required for this type of loading. The behaviour of these foundations under large lateral forces are determined by conditions which are somewhat different from conventional foundations. Such foundations may undergo rigid body movement under the external forces and the lateral earth pressure on the embedded portion of the foundation. These foundations are commonly known as caissons and well foundations.

## 10.2 CLASSIFICATION

*Wells or caissons* are large size prismatic or cylindrical shells which are built deep into the ground to support heavy loads. Depending on the method of installation the caissons may be of three types, namely (i) open caisson or well, (ii) box caisson or floating caisson, and (iii) pneumatic caisson. The types of caissons or well foundations are depicted in Fig. 10.1. The top and bottom of *open caissons* are kept open and installed into the ground by excavation of soil within the shaft so that it may sink into the ground either under its own weight or by addition of surcharge load. The *box caisson* is a shell open at the top and closed at the bottom, built first on the solid ground and then towed to the site where it is sunk to a prepared foundation base. The *pneumatic caisson* has a working chamber at the bottom which is kept dry by maintaining a high air pressure to prevent water from entering into the chamber, thus, facilitating sinking of the caisson.

Although caissons are often used to support heavy structures including high rise buildings, they constitute by far the most common type of foundations for major bridges on

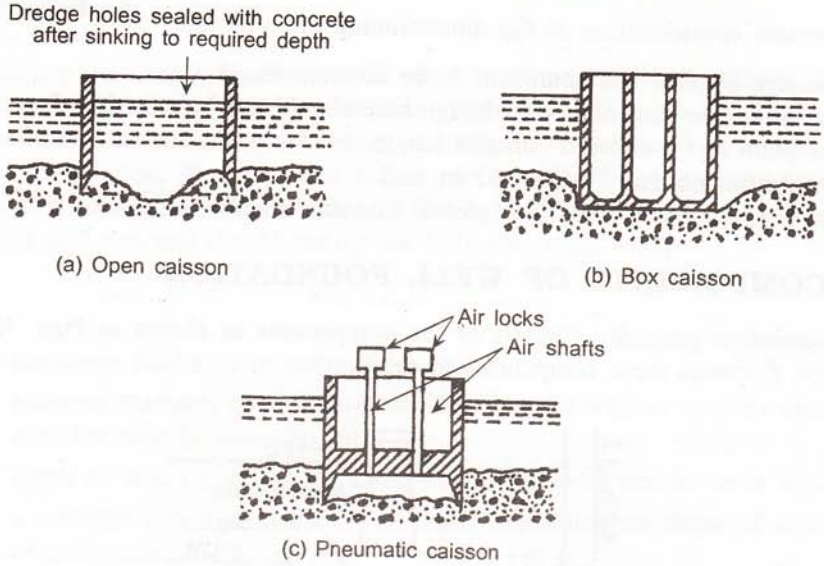


**Fig. 10.1** Types of well foundations.

rivers with erodable bed. Mostly open caissons or well foundations are used in India. This is because the well can be installed to sufficient depth below the maximum depth of scour, and a single well is capable of supporting large axial and lateral loads.

## 10.3 PHYSICAL CHARACTERISTICS—SHAPE AND SIZE

Taking into consideration the ease in sinking and construction, the most favoured shape of well, except for a very large size, is *circular*. The circular shape is equally strong in all directions, and presents a uniform surface to any direction of river current. Such wells are more suited for distribution of force uniformly over circumference during sinking, and are generally economical. Other alternatives are *double-D* and *dumb-bell* shapes. Typical cross-sections of wells of these shapes are shown in Fig. 10.2.

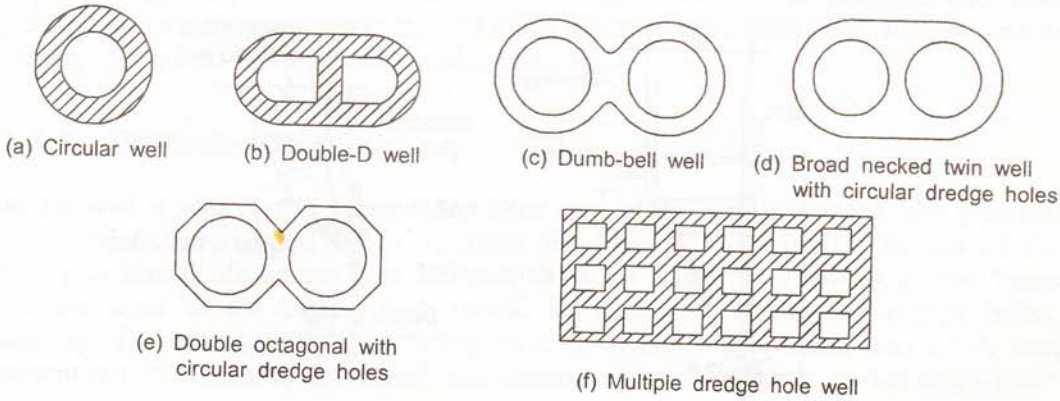


**Fig. 10.2** Typical cross-sections of well foundations.

Some important considerations in the dimensioning of wells are:

(a) the size of piers and abutments to be accommodated,
(b) the minimum dimensions of dredge hole should not be less than 2 m,
(c) for plain and reinforced concrete single circular wells, the external diameter of well should not normally exceed 12 m, and
(d) for brick masonry well, the external diameter should not exceed 6 m.

## 10.4 COMPONENTS OF WELL FOUNDATION

A well foundation generally consists of the components as shown in Figs. 10.3 and 10.4. This section discusses these components in detail.

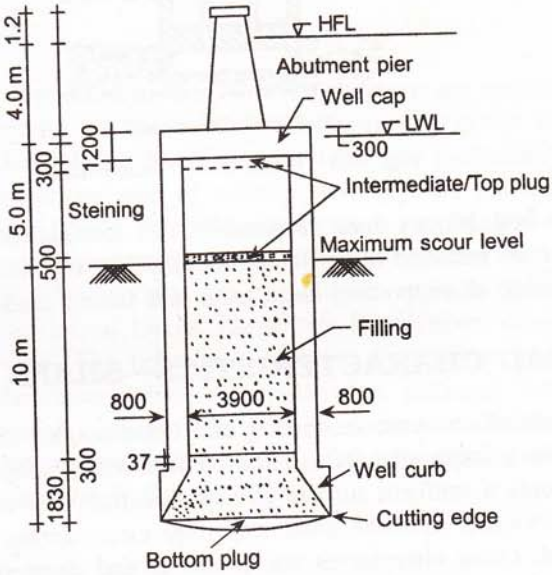


**Fig. 10.3** Components of well foundation.

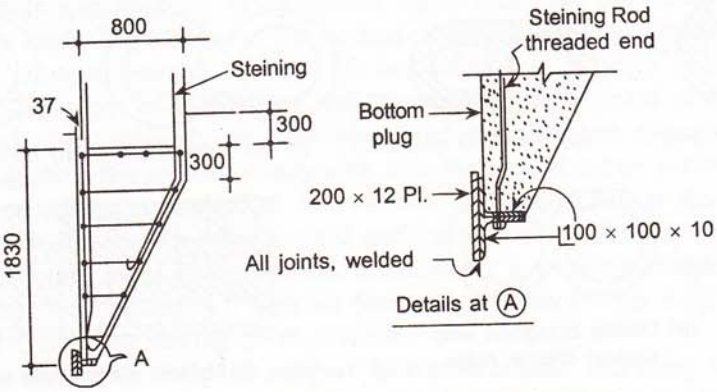


**Fig. 10.4** Typical details of well curb and cutting edge.

### 10.4.1 Steining

The *well steining* is the main body of the well which transfers load to the subsoil. It also acts as a coffer dam during sinking, and provides the weight for sinking. In addition to the usual design forces at service condition, the steining is likely to be subjected to certain additional loading during installation. The thickness and reinforcement of well steining are generally determined as per recommendations of IRC 78–1983. The thickness of well steining should not be less than 500 mm and should satisfy the following relationship

$$h = kd\sqrt{L} \tag{10.1}$$

where $h$ = minimum thickness of steining (in m),

$d$ = external diameter of circular/dumb-bell shaped well or smaller dimension in plan for twin D wells (in m),

$L$ = depth of well (in m) below LWL or ground level whichever is higher, and

$k$ = a constant varying from 0.030 to 0.068 depending on shape of well and type of soil strata.

### 10.4.2 Well Curb

The wedge shaped part of the well steining at the lower end is called *well curb*. It facilitates the process of sinking. To satisfy the requirement of minimum resistance during sinking and the strength to transmit superimposed load from steining to bottom plug, the shape and outline dimensions should be as per Fig. 10.3. The concrete grade should not be lower than M20 and minimum reinforcement of 72 kg/cu m should be provided.

### 10.4.3 Cutting Edge

The lower most portion of the well curb is the *cutting edge*. This should be strong enough to facilitate sinking through the type of soil strata expected to be encountered during sinking and should be properly anchored to well curbs. Cutting edge should be fabricated from steel angles and plates weighing not less than 40 kg/m length of the cutting edge. Heavier section (80 kg/m) is required for hard and bouldery soil strata.

### 10.4.4 Bottom Plug

After the well is sunk to the required depth, the base of the well is plugged with concrete. This is called *bottom plug* which transmits the load to the subsoil. The top of the bottom plug should not be less than 300 mm above the top of well curb. A suitable sump below the level of the cutting edge should be made and cleaned thoroughly before concreting. The concrete mix used in bottom plug should not be leaner than 1:2:4, with minimum cement content of 330 kg/m$^3$, and should be placed by tremie or skip boxes under water.

### 10.4.5 Dredge Hole

The well is sunk by excavating soil from within the well. The hole so formed is called *dredge hole* which is later filled fully or partly by sand or excavated soil. The extent of filling is decided by the function it is required to do. Filling is used to increase the stability of the well against overturning. Where it is not possible to attain a positive sump for bottom plug (specially in sandy strata), complete filling of well is desirable. In case of soft/normally consolidated clay, the allowable bearing pressure can be considerably increased by keeping the well empty.

### 10.4.6 Intermediate/Top Plug

Intermediate plugs over the fill should be of thickness 500 mm of 1:3:6 concrete. When the well is filled upto the top, a top plug of thickness 300 mm of 1:3:6 concrete is generally provided. The top plug provides contact between the well cap and the sand filling, and helps in transferring the load through the sand filling.

### 10.4.7 Well Cap

Wells are provided with a properly designed RCC well cap, with its bottom surface preferably at LWL.

## 10.5 SINKING OF WELLS

Wells are sunk to the desired depth by excavating the soil from the dredge hole by means of manual labour, mechanical winch and grab. Divers' help and/or pneumatic sinking may be adopted in difficult situations. As far as possible, the wells shall be sunk plumb without any tilt and shift. However, a tilt of 1 in 80 and a shift of 150 mm is considered allowable and the same has to be considered in the design of well foundations.

## 10.6 PHYSICAL CHARACTERISTICS—DEPTH

The depth of a well foundation must be such that the following requirements are met:

- In erodable soil, there is a minimum grip length of one third the maximum anticipated depth of scour below high flood level (HFL),
- In non-erodable strata, there is adequate seating and embedment on sound rock soil, and
- The base pressure is within permissible limits.

### 10.6.1 Scour Depth

For natural streams in cohesionless soil, the scour depth may be determined from Lacey's formula. Accordingly,

the normal depth of scour, $d$ (in metres), below the highest flood level is given by

$$d = 1.34\left(\frac{q^2}{f}\right)^{1/3} \tag{10.2}$$

where $q$ = discharge (in $m^3/s$) through width of the channel obtained by dividing the design discharge by linear waterway between abutments/guidebanks and

$f$ = Lacey's silt factor which is related to the mean diameter of soil grains forming the bed, by the empirical formula, $f = 1.76\sqrt{m}$. Here, $m$ is the weighted mean diameter in mm. The value of $f$ generally varies from 0.6 to 1.50. The method of determination of $m$ is described in IRC 5–1998.

For preliminary design, the normal depth of scour below HFL may be obtained from

$$d = 0.473\left(\frac{Q^2}{f}\right)^{1/3} \tag{10.3}$$

where $Q$ = maximum flood discharge in $m^3/s$.

The maximum depth of scour below the highest flood level (HFL) is given by,

$$D_{max} = 2d \text{ in the vicinity of piers}$$

$$\left.\begin{aligned} &= 1.27d\,(\text{scour restrained}) \\ &= 2d\,(\text{scour all round}) \end{aligned}\right\} \text{near abutment}$$

If the river bed is not readily susceptable to scouring effect of floods, the fomula for scour depth (Eq. (10.2)) shall not apply. In such cases, the maximum depth of scour shall be assessed from actual observation and experience.

## 10.7 ALLOWABLE BEARING PRESSURE

The base of a well is normally located at some depth below the maximum depth of scour. During exceptionally heavy flood, the depth of scour in sandy soil may increase, thereby, reducing the grip length. Also for some depth below the maximum scour level, there may be some gap between the well surface and the soil because of tilt under fluctuating lateral load. Hence, skin friction is normally ignored in calculating bearing capacity of wells installed in sand.

For wells embedded in sand, the depth of foundation is generally sufficient ($D/B \geq 2$) to prevent base failure. Hence, settlement is normally the guiding factor. The allowable bearing pressure for a permissible settlement may be calculated from the following (Eq. (10.4)), for footings on sand as suggested by Teng (1962).

$$q_a = 0.14C_b(N - 3)\left(\frac{\overset{B}{\cancel{D}} + 0.3}{2B}\right)^2 R'_w C_d s_a \tag{10.4}$$

where $q_a$ = allowable net soil pressure in t/m$^2$,
$C_b$ = correction factor (Peck and Bazzaraf, 1969)
= 2.0 for gravelly soil,
= 1.5 for coarse to medium sand, and
= 1.0 for fine and silty sand,
$N$ = standard penetration resistance corrected for overburden and dilatancy,
$B$ = diameter or equivalent width of well in m,
$R'_w$ = water table correction factor
= 0.5 for water level at or above the base of well,
$D$ = depth of well from maximum scour level in m, and
$C_d$ = depth correction factor.

Alternatively, safe bearing pressure may be obtained from the ultimate net bearing capacity of footings as per IS: 6403–1971. A factor of safety, say 2.5, may be applied and the weight of soil (removed by excavation) is added to get the gross bearing capacity.

For wells founded in overconsolidated clay and clay shale, scour is much less and effective depth of embedment is usually much more. So, skin friction may be considered over a part of embedded length with due allowance for possible gap due to tilt. However, the general practice is to ignore the skin friction and calculate allowable bearing pressure from bearing capacity and settlement analysis by treating the well as a deep footing and using relevant equations discussed in Chapters 6 and 7.

In case of rock, the allowable bearing pressure may be estimated from crushing strength of rock or from judgement based on core recovery and R & D.

## 10.8 FORCES ACTING ON WELL FOUNDATION

A well foundation for a bridge pier is subjected to the following forces:

(a) dead load (weight of pier/abutment, weight of the well and relevant weight of bridge structure),
(b) live load (all superimposed, vertical load including traffic load),
(c) wind force,
(d) forces due to water currents,
(e) forces due to tractive effect of vehicles, braking force and/or those caused by restraint to movement of bearings,
(f) centrifugal forces in case the well is located on a curve,
(g) buoyancy,
(h) earth pressure,
(i) temperature stress, and
(j) seismic forces

Normally, three combinations of the forces are considered for stability analysis, which are grouped as

1. N case : All forces except temperature and seismic forces.
2. (N + T) case : All forces including temperature except seismic forces.
3. (N + T + S) case : All forces including temperature and seismic forces.

The permissible stresses may be increased by 15% for (N + T) case, and by 50% for (N + T + S) case. Also when wind or earthquake forces are considered, the allowable bearing pressure may be increased by 25%.

With the knowledge of the magnitude, direction, and points of application of all the forces and for the worst combination of forces, the resultant vertical force $W$ and resultant horizontal forces $P$ across the pier and $Q$ along the pier, are determined. The horizontal force acting in the direction of the transverse axis of the pier, that is, perpendicular to the flow, is more critical for stability. The forces must satisfy the following conditions of equilibrium:

$$\sum V = 0 \tag{10.5}$$

i.e., total downward force = base reaction + friction on the sides of the well

$$\sum H = 0 \tag{10.6}$$

i.e., net lateral earth pressure including friction at the base should be zero.

$$\sum M = 0 \tag{10.7}$$

i.e., the algebraic sum of moments at base due to net lateral earth pressure, friction on sides and base reaction should be zero.

## 10.9 LATERAL STABILITY

### 10.9.1 Analysis Based on Bulkhead Concept

The simplest approach to analyzing the lateral stability of a well foundation is based on Terzaghi's analysis of a free, rigid bulkhead (Terzaghi, 1943). The force system on a bulk-head with an embedment $D$, subjected to a horizontal force $q$, at the top, is shown in Fig. 10.5(a). The bulkhead tends to rotate about a point O, at a depth $d$ from the ground surface. At failure, the soil reaches a state of plastic equilibrium and the resistance offered by the soil can be approximated by the pressure diagram shown in Fig. 10.5(b), for cohesionless soil.

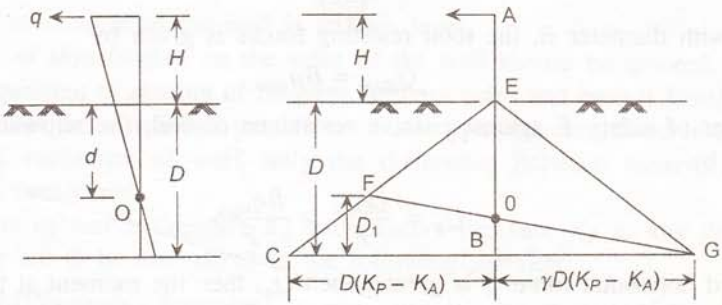


(a) Forces on a free rigid bulkhead

(b) Earth pressure on a free rigid bulkhead

**Fig. 10.5** Stability of well: rigid bulkhead method.

Resultant pressure per unit length of bulkhead, $q_{max} = \Delta CEB - \Delta GEF$. The analysis is based on the assumption that the bulkhead is light, there is no friction at the base and the sides, and earth pressure can be calculated by Rankine's theory. This can be applied to a well foundation if the moments on account of base reaction and side friction are neglected.

A heavy well under a lateral load will rotate about its base, and the force diagram will be as shown in Fig. 10.6. For soil below scour level, submerged unit weight $\gamma'$ is considered.

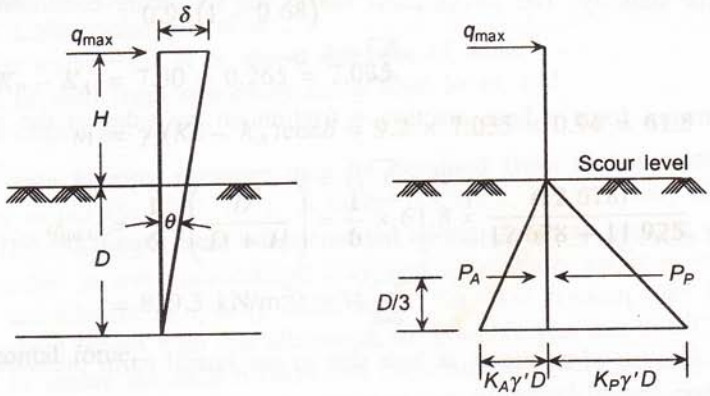


**Fig. 10.6** Force and deflection diagrams of a well for rotation about base.

By calculating moment about the base,

$$q_{max}(H + D) + \frac{1}{2} DK_A\gamma' D \frac{D}{3} = K_P\gamma' D \frac{D}{2}\frac{D}{3} \tag{10.8}$$

$$\Rightarrow \quad q_{max} = \frac{1}{6}\gamma'(K_P - K_A)\frac{D^3}{H + D} \tag{10.9}$$

If there is unscoured soil of thickness $Z$ above the maximum scour level, then its effect on active earth pressure is considered. As a result,

$$q_{max} = \frac{1}{6}\gamma'(K_P - K_A)\frac{D^2(D + Z)}{H + D} \tag{10.10}$$

For a well with diameter $B$, the total resisting forces is given by

$$Q_{max} = Bq_{max} \tag{10.11}$$

With a factor of safety $F$ against passive resistance of soil, the allowable horizontal force $Q_a$ is given by

$$Q_a = \frac{Q_{max}}{F} = \frac{Bq_{max}}{F} \tag{10.12}$$

If the applied horizontal force $Q$ is greater then $Q_a$, then the moment at the base, $M_B$ due to unbalanced horizontal force $(Q - Q_a)$ is given by

$$M_B = (Q - Q_a)(H + D) \tag{10.13}$$

Thus, the foundation pressure (maximum $f_{max}$ or minimum $f_{min}$) at the base is given by

$$f = \frac{W}{A} \pm \frac{M_B}{Z_B} \tag{10.14}$$

where $W$ = net direct vertical load on the base taking into account buoyancy and skin friction,

$A$ = area of the base of the well, and

$Z_B$ = section modulus of the well base.

The above analysis is based on the assumptions that

- bulkhead is weightless,
- there is no contribution of base reactions
- there is no wall friction

## 10.9.2 IRC Method

Correct evaluation of passive relief is a very important factor in the design of a well foundation, because it governs the depth to which the well is to be sunk. Views differ regarding the assumptions and methods, to be adopted for working out its values. The main points to be addressed while deciding for the method are:

(a) whether the rotation of the foundation takes place only at the base or at points above or below the base,

(b) whether the skin friction on the sides can be considered in the calculation of well resistance, and

(c) what fraction of applied moment is resisted by soil resistance on the sides and base resistance.

To have a uniform practice in design, IRC Bridge Sub-committee in its Bombay meeting held in 1963, suggested the procedure for calculation of ultimate soil resistance below scour level. This is known as *Bombay method.*

**Bombay method**

This method is based on the following assumptions:

(a) The point of rotation of the well is at base level.

(b) The effect of skin friction on the sides of the well should be ignored.

(c) Until the question of sharing of moment between sides and base is finally resolved, only the relief from resultant passive resistance is to be considered in the design.

(d) For lateral resistance of well, only the difference between passive and active pressure is considered.

(e) Coefficients of active pressure $K_A$ and passive pressure $K_P$ at any depth below scour level are to be considered in the following manner:

For cohesionless soil (Coulomb's formulae)

$$K_A = \frac{\cos^2\phi}{\cos\delta\left(1 + \sqrt{\frac{\sin(\phi+\delta)\sin\phi}{\cos\delta}}\right)^2} \tag{10.15}$$

$$K_P = \frac{\cos^2 \phi}{\cos\delta\left(1 - \sqrt{\frac{\sin(\phi + \delta)\sin\phi}{\cos\delta}}\right)^2} \tag{10.16}$$

For cohesive soil (Rankine's formulae)

$$K_A = \frac{\gamma Z}{N_\phi} - \frac{2C}{\sqrt{N_\phi}} \tag{10.17}$$

$$K_P = \frac{\gamma Z}{N_\phi} + \frac{2C}{\sqrt{N_\phi}} \tag{10.18}$$

where $\phi$ = angle of internal friction of soil,

$\delta$ = angle of wall friction (to be taken as 2/3 $\phi$, limited to 22.5°),

$C$ = cohesion,

$N_\phi = \tan^2(45 + \phi/2)$,

$\gamma$ = submerged unit weight of soil, and

$Z$ = depth below design scour level.

The total soil resistance is obtained as algebric sum of the areas of the force diagram due to active and passive pressure.

The factors of safety for determining the net permissible soil resistance mobilized below maximum scour level are

| | Load combination (excluding seismic/wind) | For load combination (including seismic/wind) |
|---|---|---|
| Noncohesive soil | 2 | 1.6 |
| Cohesive soil | 3 | 2.4 |

**IRC: 45–1972**

The method is based on model and prototype studies. It has been observed that,

- sharing of the moment between sides and base continuously changes with increasing deformation of soil and
- elastic theory gives soil pressure at the sides and the base under design load. To determine the actual factor of safety, it would be necessary to calculate the ultimate soil resistance.

Following considerations are made in formulating the design procedure:

(a) *At elastic stage*

(i) point of rotation is at base level,

(ii) skin friction at base and side is taken into account, and

(iii) sharing of moments between the base and side need to be accounted for on the basis of respective coefficients of subgrade reaction.

(b) *At ultimate stage*

(i) the ultimate pressure distribution at front and back is calculated considering the point of rotation at $0.2D$ above base level,

(ii) the base resisting moment is the moment of the frictional force along the surface of rupture, and

(iii) the frictional force due to passive pressure on the front and back results in a resisting moment.

## Method based on elastic theory

*Assumptions*

(a) This method assumes that the soil surrounding the well and under the base is perfectly elastic, homogeneous, and obeys Hooke's law,

(b) the lateral deflections are small and the unit soil reaction $p$ increases with lateral deflection $Z$ as expressed by $p = K_H Z$, where $K_H$ is the coefficient of horizontal subgrade reaction at base,

(c) in cohesionless soils, $K_H$ increases linearly with depth, and

(d) the well behaves as a rigid body and is acted upon by a unidirectional horizontal force $H$ and moment $M$ at scour level.

*Calculation*

**Step 1**

Having determined the minimum grip length, the applied loads ($W$ and $H$) and moment $M$ under normal load combinations without wind and seismic loads are calculated. In this case $W$ is the total downward load acting at the base of well; $H$ is external horizontal force acting on the well at scour level; and $M$ is the total applied moment about the base of the well, including those due to tilts and shifts.

**Step 2**

Using the well dimensions, geometrical properties are calculated as:

Moment of inertia of base about an axis passing through CG and perpendicular to horizontal resultant forces,

$$I_B = \frac{\pi}{64} B^4 \tag{10.19}$$

where $B$ = well diameter.

Moment of inertia about the horizontal axis passing through the CG of the projected area in elevation of the soil mass offering resistance,

$$I_v = \frac{LD^3}{12} \tag{10.20}$$

where $L$ = projected width of well in contact with soil offering passive resistance, multiplied by appropriate shape factor (0.9 for circular well and 1.0 for square or rectangular well) and

$D$ = depth of well below scour level.

$$I = I_B + mI_v\,(1 + 2\mu'\alpha) \tag{10.21}$$

where $m$ = ratio of horizontal to vertical coefficient of subgrade reaction = $\dfrac{K_H}{K_V}$

$\mu'$ = coefficient of friction between the sides and soil

= $\tan\delta$ ($\delta$ is the angle of wall friction)

$\alpha$ = $B/2D$ for rectangular well and $B/\pi D$ for circular well

**Step 3**

Ensure that
$$H > M/r\,(1 + \mu\mu') - \mu w \tag{10.22}$$
and
$$H > M/r\,(1 - \mu\mu') + \mu w \tag{10.23}$$
so that the point of rotation of the well lies at the base.

Here, $r = (D/2)(I/mI_v)$ and

$\mu$ = coefficient of friction between the base and the soil

= $\tan\phi$ ($\phi$ is angle of internal friction of soil).

**Step 4**

Check that the soil on the sides remains elastic. This can be ensured by keeping

$$\frac{mM}{I} > \gamma(K_P - K_A) \tag{10.24}$$

where $\gamma$ = effective unit weight of soil.

$K_A$ and $K_P$ = earth pressure coefficients according to Coulomb's theory. Take angle of wall friction $\delta$ as $(2/3)\phi$ but limited to 22.5°.

**Step 5**

Check the base pressures ensuring that the maximum compressive pressure is less than bearing capacity of soil and that the minimum pressure is not tensile.

$$\sigma_1, \sigma_2 = \frac{W - \mu' P}{A} \pm \frac{MB}{2I} \tag{10.25}$$

where $\sigma_1$ and $\sigma_2$ are maximum and minimum base pressures, respectively, as depicted in Fig. 10.7,

$A$ = area of the base of well,

$P$ = $M/r$, is the total horizontal reaction from the side, and

$B$ = width of base of well in the plane of bending.

**Step 6**

Check minimum and maximum base pressures so that $\sigma_2 < 0$, that is, no tension and $\sigma_1 >$ allowable bearing capacity of soil.

**Step 7**

If any or all of the conditions in Steps 3, 4 and 6 do not satisfy, redesign the well accordingly.

**Step 8**

Repeat the same steps for combination with wind/seismic separately.

Derivation of the theoretical relationships can be obtained from IRC: 45–1972. The pressure distribution and deflection diagrams of a well used in the derivation are presented in Fig. 10.7.

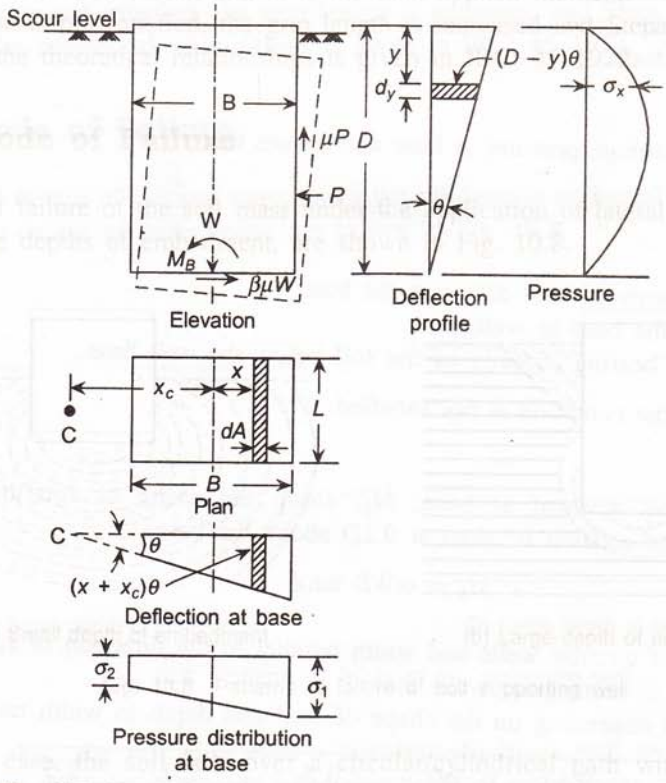


**Fig. 10.7** Pressure and deflection diagrams of a well for elastic case.

## Method based on ultimate soil resistance

The applied loads are increased by multiplying with suitable load factors and the ultimate resistance is reduced by appropriate strength factors. The two are then compared.

**Step 1**

Compute the applied load for different combinations of loading using appropriate load factors as

(a) $1.1W_D + 1.6W_L$

(b) $1.1W_D + W_B + 1.4(W_L + P_c + P_e)$

(c) $1.1W_D + W_B + 1.4(P_c + P_e + P_w \text{ or } P_s)$
(d) $1.1W_D + W_B + 1.25(W_L + P_c + P_e + P_w \text{ or } P_s)$

where,

$W_D$ = dead load,
$W_L$ = live load including braking force and so on,
$W_B$ = buoyancy,
$P_c$ = water current force,
$P_e$ = earth pressure,
$P_w$ = wind forces, and
$P_s$ = seismic force.

**Step 2**

Check for maximum average pressure at base and ensure that

$$\frac{W}{A} \ngtr \frac{q_{ult}}{2} \tag{10.26}$$

where,

$W$ = total downword load acting at the base,
$A$ = area of the base or well, and
$q_{ult}$ = ultimate bearing capacity of the soil below the well base.

Increase base area if the condition is not satisfied.

**Step 3**

Calculate the resisting moment at base, $M_b$, along the plane of rotation (as already mentioned, the point of rotation is taken at $0.2D$ above the base)

$$M_b = \alpha WB \tan\phi \tag{10.27}$$

where,

$B$ = diameter of circular wells and width parallel to the direction of forces in case of square or rectangular wells and
$\alpha$ = a constant depending on the shape of well and depth to width ratio $D/B$.

| $D/B$ | 0.5 | 1.0 | 1.5 | 2.0 | 2.5 |
|---|---|---|---|---|---|
| $\alpha$ | 0.41 | 0.45 | 0.50 | 0.56 | 0.64 |

The values are for square/rectangular well. For circular wells, the values of $\alpha$ are to be multiplied by 0.6.

**Step 4**

Compute the ultimate moment of resistance on the side of well due to passive soil resistance, $M_s$ and due to frictional resistance on side, $M_f$.

For rectangular wells,

$$M_s = 0.10\gamma' D^3 (K_P - K_A) L \tag{10.28}$$

$$M_f = 0.18\gamma' (K_P - K_A) LBD^2 \sin\delta \tag{10.29}$$

For circular wells,

$$M_f = 0.11\gamma'(K_P - K_A)B^2D^2\sin\delta \tag{10.30}$$

**Step 5**

Compute the total resisting moment,

$$M_r = M_b + M_s + M_f \tag{10.31}$$

and ensure that $0.7\ M_r \not< 1\ m$

where 0.7 is a reduction factor, and $m$ is the total applied moment.
If this condition is not satisfied, the grip length is increased and Steps 1 to 5 are repeated. Derivation of the theoretical relationships is given in IRC: 45–1972.

## 10.9.3 Mode of Failure

The patterns of failure of the soil mass under the application of lateral forces to wells, with small and large depths of embedment, are shown in Fig. 10.8.

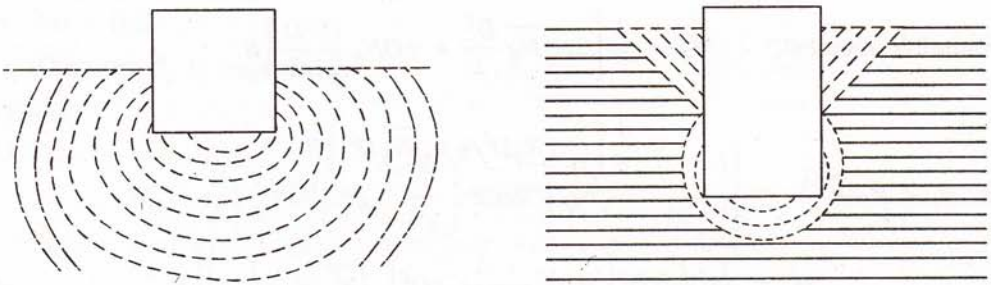

(a) Small depth of embedment (b) Large depth of embedment

**Fig. 10.8** Patterns of failure of soil supporting well.

In either case, the soil fails over a circular/cylindrical path with centre of rotation somewhere above the base. For wells with large depth of embedment, the plastic flow at the side follows the same concept as that of a rigid bulkhead.

## 10.9.4 Recommendations of IRC: 78–1983

Guidelines for calculation of passive pressure on abutment wells in any type of soil, and on wells in cohesive soils are given in IRC: 78–1983. The basic assumptions and procedure of design are in agreement with "Bombay method" except that the effect of skin friction is allowed to be considered in calculating resistance against moment and direct load.

The expressions of permissible resisting moments for pier and abutment wells in cohesive soil are presented under this subsection.

**Case 1:** Pier well (Fig. 10.9)

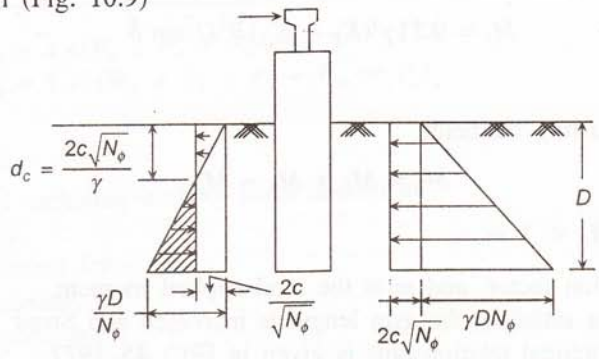


**Fig. 10.9** Active and passive pressure diagram for pier well in cohesive soil.

Depth of tension crack, $d_c = \dfrac{2c\sqrt{N_\phi}}{\gamma} \geq D$

where $D$ = depth below scour line,
$c$ = cohesion
$\gamma$ = unit weight of soil

Permissible moment, $$M_p = \frac{1}{F}\left(2c\sqrt{N_\phi}\frac{D^2}{2} + \gamma D N_\phi \frac{D}{2}\frac{D}{3}\right)B$$

$$= \frac{1}{F}\left(\frac{1}{6}\gamma N_\phi D^3 + c\sqrt{N_\phi}D^2\right)B \tag{10.32}$$

For $d_c < \cancel{H}\ D$

$$M_p = \frac{1}{F}\left[\frac{1}{6}\gamma D^3\left(N_\phi - \frac{1}{N_\phi}\right) + cD^2\left(\sqrt{N_\phi} + \frac{1}{\sqrt{N_\phi}}\right)\right]B \tag{10.33}$$

**Case 2:** Abutment well (Fig. 10.10)
Tension crack extends down to a depth $d_c$ where net $P_a = 0$

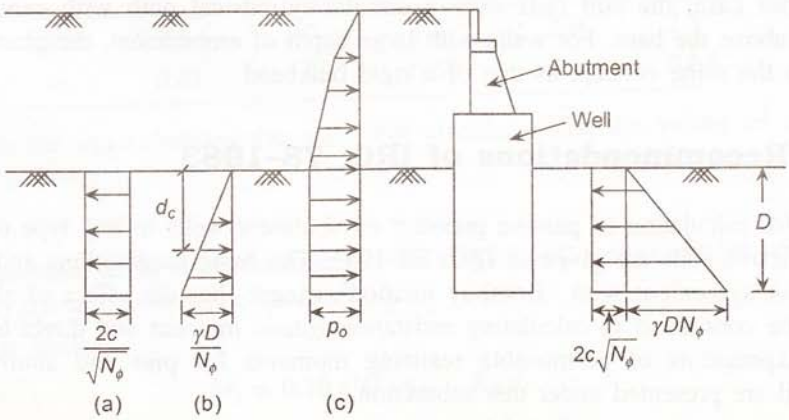


**Fig. 10.10** Active and passive pressures on abutment well in cohesive soil.

That is, (b) + (c) = (a)

or,
$$p_o + \frac{\gamma d_c}{N_\phi} = \frac{2c}{\sqrt{N_\phi}}$$

or,
$$d_c = \frac{2c\sqrt{N_\phi}}{\gamma} - p_o\frac{N_\phi}{\gamma} \qquad (10.34)$$

For $d_c \geq D$

then $P_a = 0$, that is, same as in case 1 of pier well.

For $d_c < D$, that is, (a) > (b) but < (b) + (c)

$P_a$ exists below $d_c$.

At base,

$$M_p = \frac{1}{F}\left[\frac{1}{6}\gamma D^3\left(N_\phi - \frac{1}{N_\phi}\right) + c\cancel{H^2}\left(\sqrt{N_\phi} + \frac{1}{\sqrt{N_\phi}}\right)\right]B - p_o\frac{D^2}{2}B \qquad (10.35)$$

For (a) < (b)

Then net $P_a$ is trapezoidal.

At base,

$$M_p = \frac{B}{F}\left[\frac{1}{6}\gamma D^3\left(N_\phi - \frac{1}{N_\phi}\right) + cD^2\left(\sqrt{N_\phi} + \frac{1}{\sqrt{N_\phi}}\right)\right] - p_o\frac{D^2}{2}B \qquad (10.36)$$

## 10.10 WELL SINKING

The sinking of a well foundation is done by excavating the soil within the dredged hole. This can be done manually or by mechanical dredger. A mechanical dredger consists of prongs with hard steel teeth which are pushed into the soil. When the dredger is pulled up, the prongs close to form a bucket full of excavated soil. The mechanical dredger should be adapted to suit the soil condition.

With increasing depth of well during well sinking, the friction on the sides of the well increases. If the weight of the steining is not adequate to overcome the friction, suitable kentledge may be placed on a platform to increase the load on the steining. Air and water jets are also used to minimize friction. Compressed air is used when well sinking is done below water level to counter the water pressure inside the well.

**Example 10.1**

A bridge 120 m long, is to be constructed over a river having $Q_{max}$ = 2418 m³/s, *HFL* = 81.17 m; *LWL* = 73.00 m and existing bed level = 72.00 m. The subsoil consists of

loose silty sand layer ($N_{corr}$ = 10), 3.5 m thick, underlain by a thick stratum of medium to coarse sand ($N_{corr}$ = 24). Determine the founding level and allowable bearing capacity of a 4.5 m diameter abutment well. The weighted mean diameter of the bed material upto relevant depth is 0.275 mm, and permissible settlement is 45 mm.

***Solution***

$m = 0.275$ mm

Silt factor, $f = 1.76\sqrt{m} = 0.923$

Discharge intensity, $q = \dfrac{2418}{120} = 20.15 \text{ m}^3/\text{s/m}$

Normal scour depth, $d = 1.34\left(\dfrac{q^2}{f}\right)^{1/3} = 1.34\left(\dfrac{(20.15)^2}{0.923}\right)^{1/3} = 10.17 \text{ m}$

Maximum scour depth (near abutment) = 1.27 × 10.17 = 12.92 m

∴ Scour level below *HFL* = 81.17 − 12.92 = 68.25 m

Grip length = $\dfrac{1}{3} \times 12.92 = 4.30$ m

∴ Required bottom level of well = 68.25 − 4.30 = 64.95 m

Depth below existing bed level = 72.00 − 64.95 = 7.05 m

The embedment in dense sand layer = 7.05 − 3.5 = 3.55 m

For better embedment in dense sand, provide grip length which is 1.5 times well diameter = 6.75 m

Thus, founding level provided = 68.25 − 6.75 = 61.50 m

Allowable bearing pressure, $q_a$ can be calculated using Eq. (10.4) as

$$q_a = 0.14 \times 1.5(24 - 3)\left(\frac{4.5 + 0.3}{2 \times 4.5}\right)^2 0.5 \times 45$$

$$= 555 \text{ kN/m}^2$$

**Example 10.2**

The subsoil at the typical pier location of a major bridge consists of medium to coarse sand ($N_{corr}$ = 11) upto a depth of 6 m from bed level (RL + 9.20 m). This is underlain by 9 m thick layer of very stiff to hard sandy silty clay ($N_{corr}$ > 30), overlying highly weathered rock ($RQD \approx 0$).

Using Lacey's formula calculate the maximum scour depth and determine the founding level of the well. Also, estimate the allowable net bearing pressure if the diameter of the well is 6 m.

Given: Maximum flood discharge = 10,465 $m^3/s$

Length of bridge = 382.5 m; *HFL* = 13.00 m; silt factor, $f = 1.053$; submerged unit weight of soil and rock = 10 $kN/m^3$; $c' = 0$; and $\phi' = 35°$ for weathered rock.

***Solution***

$$\text{Discharge intensity, } q = \frac{10{,}465}{382.5} = 27.36 \text{ m}^3/\text{s/m}.$$

$$\text{Normal scour depth, } d = 1.34\left(\frac{q^2}{f}\right)^{1/3} = 1.34\left(\frac{(27.36)^2}{1.053}\right)^{1/3}$$

$$= 11.70 \text{ m}$$

Maximum scour depth = 2 × 11.70 = 23.40 m

∴ Computed maximum scour level = 13.00 – 23.40 = – 10.40 m (RL)

But as stiff clay overlying weathered rock exists at 6 m below bed level (+9.20 m), the above calculation of scour depth is not applicable.

Now take maximum scour level = 9.2 – 6.0 = 3.20 m

Below this level there is 9 m thick clay followed by weathered rock. For restricting settlement, it is preferable to take bottom of well 3 m into the rock.

∴ Provide founding Level = 3.2 – (9 + 3) = – 8.8 m

For bearing capacity:

$B = 6$ m, $D_f = 12$ m, $\gamma' = 10$ $kN/m^3$, $c' = 0$, and $\phi' = 35°$ for weathered rock

Now $q_{ult} = \gamma' D_f (N_q - 1) s_q d_q + 0.5\gamma' B N_\gamma s_\gamma d_\gamma w' + \gamma D_f$

For $\phi = 35°$

$N_q = 32$, $N_\gamma = 33$,

$s_q = 1.2$, $s_\gamma = 0.6$

$$d_q = d_\gamma = 1 + 0.1\left(\frac{3}{6}\right)\tan\left(45 + \frac{35}{2}\right)^\circ$$

$$\approx 1$$

or $q_{ult} = (10 \times 12\ (32 - 1) \times 1.2 \times 1) + (0.5 \times 10 \times 6 \times 33 \times 0.6 \times 1 \times 0.5) + (10 \times 12)$

$= 4460 + 297 + 120$

$\approx 4870$ $kN/m^2$

$$\therefore \quad q_{safe} = \frac{4870}{3} \approx 1620 \text{ kN/m}^2$$

As the well is founded on weathered rock, settlement will be negligible.
Hence, allowable bearing pressure = 1620 kN/m$^2$

**Example 10.3**

Using IRC methods, check the adequacy of design of the pier well of a bridge (Fig. 10.11(a)). Use the following data on loads and soil properties:

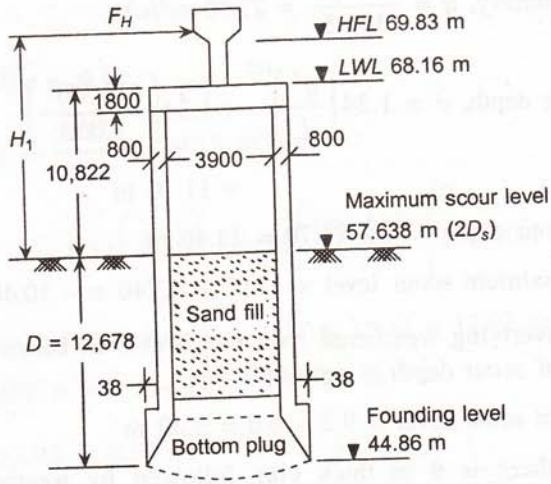


**Fig. 10.11(a)** Pier well design for Example 10.3.

Loading:

Vertical Load:

$DL$ = 12,400 kN

$LL$ = 1390 kN

∴ Total load = $DL + LL$ = 13,790 kN

Above well cap—8100 kN

Below well cap—5690 kN

Total 13,790 kN

Total horizontal force, $F_H$ = 1755 kN

Moment at base = 43,180 kNm

Consider Tilt: 1 in 60

Shift : 0.15 m

*Soil Properties:*

$N_{corr}$ = 20; $\phi$ = 33°; $\gamma$ = 19.2 kN/m$^3$; $\delta$ = 20°

Soil type: Coarse to medium sand

Consider permissible settlement of 1.5% of well diameter.

*Solution*

$$e = \frac{4318}{175.5} = 24.603 \text{ m}$$

$$D = 12.678 \text{ m}$$

Also, $e = H_1 + D$

$\therefore \quad H_1 = 11.925$ m

Moment due to tilt and shift

For load above well cap: $8100\left(0.15 + \frac{23.5}{60}\right) = 4390$ kNm

For load below well cap: $5690\left(\frac{23.5}{120}\right) = 1110$ kNm

Total $= 5500$ kNm

Total moment at base = 43,180 + 5500 = 48,680 kNm

Total vertical load = 8100 + 5690 = 13,790 kNm

Bombay method (Fig. 10.11(b))

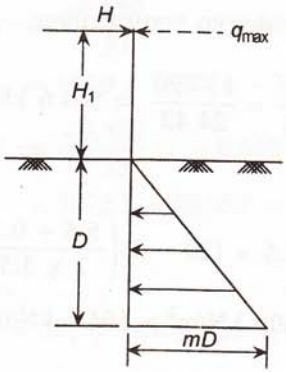


**Fig. 10.11(b)** Bombay method.

$$K_A = \frac{\cos^2\phi}{\cos\delta\left(1 + \sqrt{\frac{\sin(\phi+\delta)\sin\phi}{\cos\delta}}\right)^2}$$

$$= \frac{0.703}{0.94\left(1 + \sqrt{\frac{0.799 \times 0.545}{0.94}}\right)^2}$$

$$= 0.265$$

$$K_P = \frac{\cos^2\phi}{\cos\delta\left(1 - \sqrt{\frac{\sin(\phi + \delta)\sin\phi}{\cos\delta}}\right)^2}$$

$$= \frac{0.703}{0.94(1 - 0.68)^2} = 7.30$$

$$K_P - K_A = 7.30 - 0.265 = 7.035$$

$$m = \gamma'(K_P - K_A)\cos\delta = 9.2 \times 7.035 \times 0.94 = 61.8$$

$$q_{\max} = \frac{1}{6}m\left(\frac{D^3}{D + H}\right) = \frac{1}{6} \times 61.8 \times \frac{(12.678)^3}{12.678 + 11.925}$$

$$= 839.3 \text{ kN/m}^2$$

Allowable horizontal force,

$$Q_{\max} = \frac{q_{\max} B}{FS} = \frac{839.3 \times 5.5}{1.6} = 2885 \text{ kN} > 1755 \text{ kN (applied force)}$$

Hence, base pressure ($f_{\max}$) is only due to vertical force.

$$f_{\max} = \frac{W}{A} = \frac{13,790}{24.42} = 564.6 \text{ kN/m}^2$$

Allowable bearing capacity, $q_a$

Using Eq. (10.4), $q_a = 0.14 \times 1.5 \times (20 - 3)\left(\frac{5.5 + 0.3}{2 \times 5.5}\right)^2 0.5 \times 2 \times 82.5$

$$= 81.9 \approx 800 \text{ kN/m}^2 > 564.6 \text{ kN/m}^2$$

Hence, this is acceptable.

$N = 20,$

$C_{b1} = 1.5$

$R_W = 0.5$

$B = 5.5$

$C_d = 2$

$S_a = 1.5$ % of 5500 = 82.5 mm

Method Based on IRC: 45 (elastic)

**Step 1** $W = 13,790$ kN, $M = 48,680$ kNm, $H = 1755$ kN

**Step 2** $D_B = 5500 + 2 \times 38 = 5576$ mm

$$I_B = \frac{\pi}{64}(5.576)^4 = 47.43 \text{ m}^4$$

$$I_v = \frac{LD^3}{12} = \frac{0.9 \times 5.5 \times (12.678)^3}{12} = 840.574 \text{ m}^4$$

$$\mu' = \tan\delta = \tan 20° = 0.364$$

$$\mu = \tan\phi = \tan 33° = 0.649$$

$$\alpha = \frac{B}{\pi D} = \frac{5.5}{3.14 \times 12.678} = 0.138$$

$$m = \frac{K_h}{K_v} = 1$$

$$I = I_B + mI_v(1 + 2\mu'\alpha)$$

$$= 47.43 + 1 \times 840.574\,(1 + 2 \times 0.364 \times 0.138) = 972.45 \text{ m}^4$$

**Step 3**

$$r = \frac{D}{2}\left(\frac{I}{mI_v}\right) = \left(\frac{12.678}{2}\right)\left(\frac{972.45}{1 \times 840.574}\right) = 7.33$$

$$\frac{M}{r}(1 + \mu\mu') - \mu W = \frac{48{,}680}{7.33}(1 + 0.649 \times 0.364) - 0.649 \times 13{,}790$$

$$= 8210 - 8950 = -740 \text{ kN} < H$$

$$\frac{M}{r}(1 - \mu\mu') + \mu W = \frac{48{,}680}{7.33}(1 - 0.649 \times 0.364) + 0.649 \times 13{,}790$$

$$= 5072.3 + 8950.7 = 14{,}023 \text{ kN} > H$$

**Step 4**

$$\frac{mM}{I} = \frac{1 \times 48{,}680}{972.45} = 50;\ \gamma'(K_P - K_A) = 9.2 \times 7.035 = 64.7$$

with seismic, $1.25\gamma'(K_P - K_A) = 1.25 \times 64.7 = 80.88 < 50$

**Step 5**

$$\sigma_1, \sigma_2 = \frac{W - \mu' p}{A} \pm \frac{MB}{2i}$$

$$= \frac{13{,}790 - 0.364 \times 6641}{24.42} \pm \frac{48{,}680 \times 5.5}{2 \times 972.45}$$

$$= 465.8 \pm 137.7$$

$= 603.5,\ 328.1$ kN/m$^2$ < 800 kN/m$^2$. Hence, it is acceptable.

Method based on IRC: 45 (Ultimate)